HELICOPTER BLADE-TIP STABILITY IN FORWARD FLIGHT

A THESIS

Presented to

The Faculty of the Division of Graduate

Studies and Research

by

Keith Waldo Shipman

In Partial Fulfillment

of the Requirements for the Degree

Doctor of Philosophy

in the School of Aerospace Engineering

Georgia Institute of Technology

June, 1971

HELICOPTER BLADE-TIP STABILITY IN FORWARD FLIGHT

Approved:

Chairman

Date approved by Chairman: 8/5/71

A method for determining rotor blade flutter in forward flight is presented, developed, and applied in this thesis. The unsteady effects of the layers of the helical wake below the rotor are accounted for. Since the blade tangential velocity and, consequently, the aerodynamic damping vary with azimuth, the vorticity shed due to blade oscillations incipient to flutter will be contained within a region on either side of a critical azimuth position. Assuming this region to be small allows the wake system to be two-dimensionalized. The lift deficiency function developed from the new theory is simplified for limiting cases and compared with earlier results obtained for fixed wings and helicopters in hover. It is found to be consistent with earlier results when simplified. The theory is then applied to bending-torsion flutter for the tip segment of a rotor blade. The previously shed wakes are found to be destabilizing. The flutter velocity becomes constant at higher advance ratios.

ACKNOWLEDGMENTS

To Dr. Edward R. Wood, who suggested the problem and supplied the special guidance and ideas that carried it through, I express my greatest appreciation. Special thanks go to Dr. G. Alvin Pierce and Dr. Robin B. Gray who provided much of the physical insight necessary for setting up the mathematical model and to Dr. Michael P. Stallybrass whose aide on several aspects of the mathematics was most helpful. To Dr. David J. McGill and all of the above I express my appreciation for reading this thesis and their critiques on it.

The financial assistance of the National Aeronautics and Space Administration Traineeship, institution funds from Georgia Tech, and the Ford Foundation made my graduate studies possible. For their support and the efforts of Dr. Arnold L. Ducoffe in arranging it I express my great appreciation.

To Mrs. Jacqueline Van Hook I express my appreciation for her skill and extra efforts in typing the final draft of this thesis.

My deepest appreciation goes to my wife Rogene for her encouragement and patience during the completion of my graduate program and this thesis.

TABLE OF CONTENTS

TABLE OF CONTENTS (Continued)

LIST OF TABLES

LIST OF ILLUSTRATIONS

LIST OF ILLUSTRATIONS (Continued)

NOMENCLATURE

Roman Symbols

$A(y)$	a generalized amplitude function used in Appendix B.
a	non-dimensional distance from midchord to elastic axis, positive aft
b	number of blades
$C(k)$	Theodorsen's lift deficiency function, given in equation (2)
$\hat{C}(p+ik)$	Jones' lift deficiency function
$C'(k,m,h)$	Loewy's lift deficiency function, given in equation (3)
$C_1(k,\mu,\lambda)$	present lift deficiency function, defined in equation (35)
C_D	drag coefficient
C_L	lift coefficient
C_T	thrust coefficient $(T/\pi\rho\Omega^2 R'^4)$
C_W	weight coefficient $(W/\pi\rho\Omega^2 R'^4)$
c'	semi-chord length
D	drag of fuselage
$f(y)$	decay function centered about $y = 0$
f', f''	first and second derivatives of decay function
ΔF_1	defined in equation (28)
ΔF_2	$(\Delta F_2 = \Delta F_3 - \Delta F_1)$ terms arising due to the decay function
ΔF_3	defined in equation (23)
ΔF_4	defined in equation (32)
ΔF_5	defined in equation (38)
$G(k,s,h)$	a denominator common to many equations, defined in equation (22)

g	damping coefficient
$H_n^{(1)}(k)$	Hankel function of first kind and order n
$H_n^{(2)}(k)$	Hankel function of second kind and order n
h	non-dimensional vertical distance between shed wakes
h'	deflection of blade segment
h'_o	amplitude of blade deflection ($h' = h'_o e^{i\omega t}$)
Im	abbreviation for "imaginary part of"
I_n n=1,2,...,6	integrals used in the description of the approximate integration that was used, defined by equations (B-1) through (B-4)
$J_n(k)$	Bessel function of the first kind and order n
K_j	residue of the jth pole, used in Appendix C
K_h	flexural spring stiffness
K_α	torsional spring stiffness
k	reduced frequency $[\omega c'/\Omega R'(1+\mu)]$
L	lift
L_h	non-dimensional lift due to deflection when the elastic axis is at the quarter chord, given in equation (51)
L'_h	non-dimensional deflection coefficient for lift, given in equation (51)
L_α	non-dimensional lift due to rotation, when the elastic axis is at the quarter chord, given in equation (53)
L'_α	non-dimensional rotation coefficient for lift, given in equation (52)
M_d	moment term arising due to decay, defined by equation (55)
$M_{1/4}$	aerodynamic moment about the quarter chord
$M_{1/2}$	aerodynamic moment about the midchord
M_{ea}	aerodynamic moment about the elastic axis

M'_h	non-dimensional deflection coefficient for the moment about the elastic axis, given in equation (61)
M_h	non-dimensional moment due to deflection when the elastic axis is at the quarter chord, given in equation (56)
M'_α	non-dimensional rotation coefficient for the moment about the elastic axis, given in equation (62)
M_α	non-dimensional moment due to deflection when the elastic axis is at the quarter chord, given in equation (56)
m	mass distribution of blade; also frequency ratio, $m = \omega/\Omega$ (Loewy)
p	pressure
Δp	pressure difference across the airfoil
R'	blade radius
R	non-dimensional blade radius (R'/c')
Re	abbreviation for "real part of"
r'	radius position for arbitrary blade station
r_α	radius of gyration about the elastic axis, r_α^2 = mass moment of inertia/mc'^2
S'	area of auxiliary lifting surface
S	non-dimensional area of lifting surface $(S'/\pi R'^2)$
S'_F	cross-sectional area of fuselage
S_F	non-dimensional area of fuselage $(S'_F/\pi R'^2)$
s	non-dimensional distance between centers of successive shed wakes $(\mu 2\pi R'/bc')$
T	thrust
T_{aux}	auxiliary thrust
t	time
U	tip velocity divided by semi-chord length
V	hub velocity of helicopter

V_{FL}	flutter speed
V_t	tangential speed ($\Omega R' + V \sin \psi$)
v_a	downwash along airfoil
v_i	induced velocity
W	weight of aircraft
$\hat{W}(kh,m)$	wake weighting function of Loewy
$W(k,s,h)$	portion of present wake weighting function when the wakes do not build-up and decay
ΔW	contribution of decay to wake weighting function, defined by equation (18)
x, x^*	non-dimensional distance from midchord on the airfoil
x_α	non-dimensional distance from the elastic axis to the center of gravity
$Y_n(k)$	Bessel function of second kind and order n
y	dummy variable of integration, measured from midchord
z'	absolute deflection along the airfoil $[h' + c'(x-a)\alpha]$

Greek Symbols

α	rotation of airfoil, positive for nose up
α_o	amplitude of rotation ($\alpha = \alpha_o e^{i\omega t}$)
α_T	tilt of tip path plane, positive forward
β	intermediate integration limit, used in Appendix D
γ_a	local bound vorticity
γ_n	shed vorticity in the nth wake
Γ'_a	total bound vorticity, defined in equation (9)
$\bar{\Gamma}_a$	magnitude of total bound vorticity, given in equation (21)
ζ	complex binomial coefficient, defined in equation (64)
η	complex binomial coefficient, defined in equation (65)

μ	mass ratio ($\pi\rho c'^2/m$)
λ	inflow ratio [$(V \sin \alpha_T + v_i)/\Omega R'$]
μ	advance ratio ($V \cos \alpha_T/\Omega R'$)
ξ	non-dimensional distance from midchord
ξ_n	non-dimensional distance from center of nth wake
ρ	air density
φ	phase angle; also velocity potential
ψ	azimuth angle measured from downstream position
$\Delta\psi_{FL}$	half of the angle in which the tip encounters negative damping
ω	oscillation frequency
ω_h	natural bending frequency
ω_α	natural torsional frequency
Ω	blade rotation speed
$\Omega_1(x,\xi)$	a function appearing in the pressure equations, given in equation (29)
$\Omega_2(x,y)$	a function appearing in the pressure equations, given in equation (27)

Subscripts

cg	center of gravity
ea	elastic axis
h	bending
FL	flutter
L	lower
U	upper
α	torsion

Superscripts

$(')$	dimensional
$(\bar{})$	independent of time
$(^{(n)})$	nth derivative

SUMMARY

A method for determining rotor blade flutter in forward flight is presented in this thesis. Incompressible unsteady aerodynamic theory is applied where shed vorticity both in and below the plane of the rotor is accounted for. This is made possible by noting that the aerodynamic damping acting on the blade varies with velocity. Since the tangential velocity of any blade segment varies with azimuth, so will the aerodynamic damping. Thus it is assumed at the onset of flutter that oscillations will begin to build up prior to the blade reaching a critical azimuth position, then decay as the blade moves beyond this point. This buildup and decay means that the vorticity shed due to the oscillations will be contained within a double azimuth region on either side of the critical azimuth position. Assuming this region to be small allows the wake system to be two-dimensionalized.

The lift deficiency function resulting from the two-dimensional wake model is compared with earlier results obtained for a helicopter in hover and fixed wings. It is shown that in limiting cases the present work is consistent with earlier flutter theories.

The theory is applied to bending-torsion flutter for the tip segment of a rotor blade. The results followed the normal trends of having the flutter velocity decrease as the center of gravity was moved aft and of having the flutter velocity increase as blade stiffness increased. The previously shed wakes are destabilizing so that they reduce the flutter velocity. The buildup and decay produces wakes that are

essentially centers of vorticity. Thus their position with respect to the reference blade will be sensitive to the advance ratio which determines their horizontal spacing and to the inflow ratio which determines the vertical spacing. The variation of flutter speed with advance ratio and inflow ratio was tested and it was found to change according to the geometry of the wake system. As the wakes were brought closer by reducing the advance ratio and/or inflow ratio, the flutter speed decreased. With buildup and decay of the wakes the flutter velocity will not change when the advance ratio goes above a certain point (an advance ratio of about 0.3 in the cases considered here) since the previously shed wakes become too far removed to have any effect any longer.

A possible application for design considerations is presented. If the pilot is allowed to change the blade speed, as in the case of compound helicopters in which auxiliary wings could provide lift at higher airspeeds, then the chart that is obtained by this method shows the stable region in which the combination of the helicopter's airspeed and rotor tip speed does not exceed the flutter speed.

CHAPTER I

INTRODUCTION

This thesis is directed at improving forward flight blade flutter analysis. The method presented is based upon extending Loewy's (1) theory for a hovering rotor to forward flight. If the magnitude of rotor downwash velocities is such that wakes shed from preceding blades remain relatively near the rotor disk, then neither fixed-wing quasi-steady nor unsteady aerodynamics can be reliably used for predicting blade flutter. This influence of the layers of shed vorticity was accounted for by Loewy (1) and J. P. Jones (2) who considered the rotor to be operating in hover or vertical flight. By applying Loewy's (1) lift deficiency function to a flutter analysis for a hovering rotor, Hammond (3) found that the effect of reducing the spacing of the wake layers, thus bringing them closer to the rotor, was destabilizing. That is, the most critical flutter condition appeared to be at very low inflow values.

In this thesis a method is given which accounts for the unsteady contribution of a simplified wake model for the forward flight condition. Currently to meet forward flight blade flutter requirements the rotorcraft manufacturer must rely on: (1) the fixed-wing unsteady aerodynamic flutter analysis of Theodorsen (4), which does not account for the unsteady contribution of the wake below the rotor; and (2) rotor whirl tests at normal and overspeed conditions which, while providing information in regard to blade flutter, do not accurately simulate either blade

dynamics or unsteady aerodynamics in forward flight. Accounting for the contribution of the rotor's wake in forward flight could be especially important for the case of a compound helicopter. Here, in high-speed flight the rotor may be partially or fully unloaded and set at zero angle of attack. This would result in wakes near the rotor due to very low or zero induced flow with no inflow contribution from the forward flight velocity component.

Rotor blade harmonic airloads in forward flight have been analyzed by Miller (5) and Ichikawa (6). Miller (5) used lifting surface theory for the wakes shed near the blade and lifting line theory for the more distant wakes. The lifting surface equations for forward flight were reduced to lifting line equations by Ichikawa (6). The flow was assumed to be incompressible by both Miller (5) and Ichikawa (6).

Previous approaches to the problem of determining flutter for a helicopter in forward flight have relied on quasi-steady aerodynamics or fixed-wing flutter coefficients for their determination of aerodynamic loads. A discussion of the assumptions underlying the use of steady-state aerodynamics in aeroelastic rotor studies is given by Drees (7).

Brooks and Sylvester (8) tested the effect of forward speed on the flutter of a dynamically scaled model rotor. Qualitative agreement between theory and experiment with respect to major parameters was found by Gates, Piziali, and DuWaldt (9). The calculations made for a model rotor set on a small rotorcraft test apparatus were conservative.

Using the Myklestad method of structural vibrations along with oscillatory aerodynamic forces derived from Theodorsen's (4) work, Leone (10) obtained graphical results for forced modes in high speed

level flight. Daughaday, DuWaldt, and Gates (11) obtained aerodynamic damping factors which were derived from both forced response and decay data and compared these factors with those computed using quasistatic and non-stationary aerodynamic coefficients. Improved agreement was obtained by empirical reductions of the bound vorticity.

Stammers (12,13) developed a method for determining bending-torsion flutter with particular reference to the case of forward flight where the equations of motion contain periodic coefficients. Quasi-steady aerodynamics were assumed. Under normal conditions, flutter was heavily damped and forward flight had a beneficial effect on the stability. Niebanck (14) tested a dynamically scaled articulated rotor model with the center of gravity located at the 25%, 30%, and 35% chord positions. Simulated advance ratios of 0.29 to 1.91 were run and classical flutter was encountered by the advancing blade. Discrete azimuth theories were used to calculate the onset of flutter and they showed good qualitative agreement with the test data. Fixed wing two-dimensional compressible-flow flutter coefficients such as those obtained by Garrick (15) were used for the aerodynamic forces.

Extension of the work of Theodorsen (4) and Loewy (1) to forward flight for a rotor blade in the general case presents a formidable mathematical problem. Here, the effect of a shed skewed helical wake would have to be considered and the contribution of each element of that wake on each segment of the blade at each azimuth position accounted for. However, closer examination of this problem reveals that it is possible to make several rational assumptions that make the problem tractable. Based upon these assumptions a wake mathematical model is

defined. The problem then is to determine the pressure difference across the airfoil due to the vorticity shed in the wakes, and consequently to determine the unsteady lift and moment acting on the airfoil.

By relating to the earlier works of Theodorsen (4) and Loewy (1) it is shown that the theory presented is consistent with their work for limiting conditions. For example, when forward flight speed is made to approach zero (hover) and the build-up and decay of the wakes is reduced to zero (constant strength vorticity), then the lift deficiency function becomes that of Loewy (1). Further, if wake spacing below the rotor is made very large and constant strength vorticity is maintained as before, then the results are shown to approach those of the fixed-wing theory of Theodorsen (4).

The forward flight theory is applied to a simplified numerical example which considers bending-torsion flutter for the tip segment of a rotor blade. Numerical results are presented and discussed. The influence of several parameters on flutter speed is explored, including wake build-up and decay, advance ratio, and chordwise location of the blade center of gravity.

CHAPTER II

THEORETICAL ANALYSIS

This chapter begins with a background which includes the wake models used in the unsteady aerodynamic theory for a fixed wing and for a helicopter rotor in hover. The lift deficiency functions obtained from these models are briefly presented. The second section describes the approach used for setting up the wake model used for the work done in this thesis. The last section presents the mathematical development for the unsteady lift and moment that were used in the flutter analysis that was run.

Background

The classical solution for fixed wing flutter is that of Theodorsen (4) who considered a wing oscillating in simple harmonic motion as shown in Figure 1. The wake, as shown in Figure 2, was of sinusoidal strength with constant amplitude and lay in the plane of the airfoil. For a wing oscillating at a frequency of ω, the lift is given by

$$L = \pi\rho\omega^2 c'^3\left\{L_h \cdot \frac{h'}{c'} + \left[L_\alpha - \left(\frac{1}{2} + a\right)L_h\right]\alpha\right\} \qquad (1)$$

where c' is the semi-chord length and ac' is the location of the elastic axis, measured from the midchord. If the elastic axis is at the quarter chord then a = - 1/2 and so the non-dimensional lift due to deflection in equation (1) would be

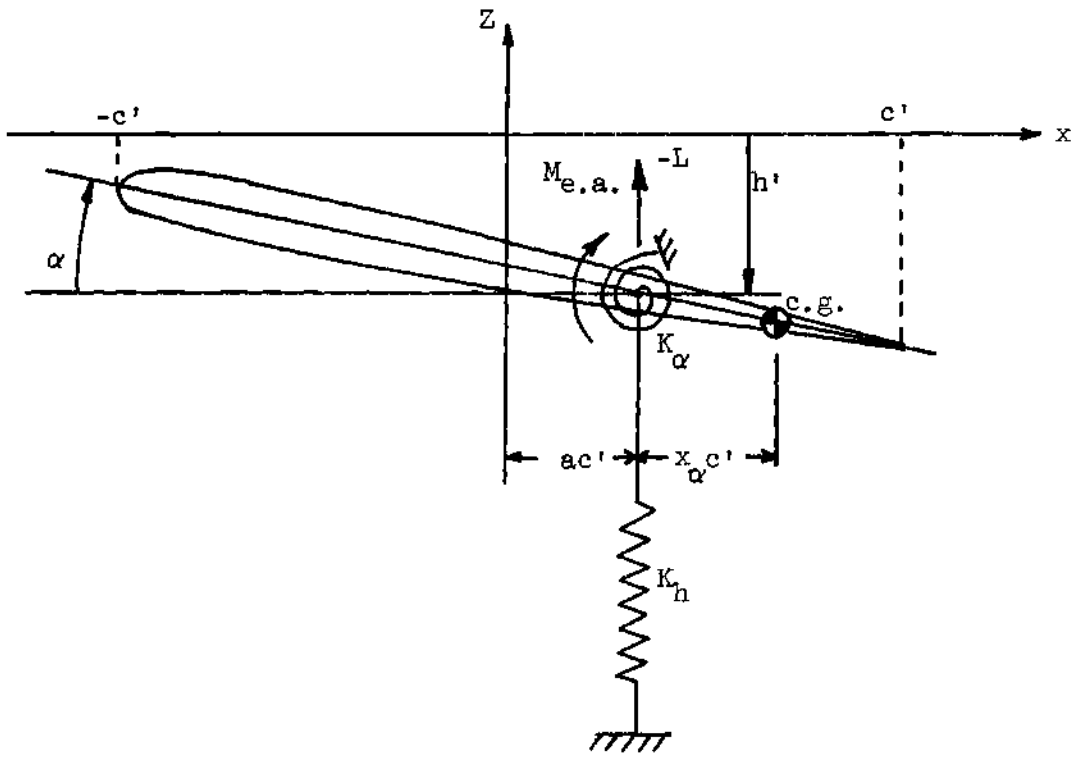

Figure 1. Bending-Torsion Flutter Model Showing Notation Used in Flutter Analysis.

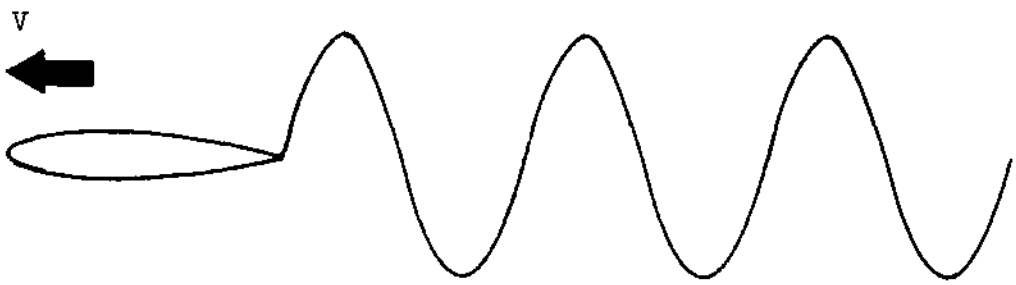

Figure 2. Wake with Constant Strength Amplitude Shed From Wing.

$$L_h = 1 - \frac{2i}{k} C(k)$$

and the non-dimensional lift due to rotation would be

$$L_\alpha = \frac{1}{2} - \frac{2i}{k}\left[\frac{1}{2} + (1 - i/k)C(k)\right]$$

where $k = \omega c'/V$ is the reduced frequency.

Theodorsen's (4) lift deficiency function, $C(k)$, is expressed as

$$C(k) = \frac{H_1^{(2)}(k)}{H_1^{(2)}(k) + i\, H_o^{(2)}(k)} \qquad (2)$$

where $H_n^{(2)}(k)$ is the Hankel function of the second kind and is given in terms of Bessel functions as

$$H_n^{(2)}(k) = J_n(k) - i\, Y_n(k) \ .$$

The lift relation of Equation (1) was confirmed by Schwarz (16) in 1940. Schwarz applied Söhngen's (17) inversion formula and was able to determine the vorticity, and hence the pressure distribution and lift on an airfoil, in terms of general motion.

W. P. Jones (18) later extended this concept by allowing the strength of the airfoil's motion to grow or decay exponentially. This meant that the amplitude of motion could be written as

$$A = a\, e^{pt}\, e^{i\omega t} \ .$$

With p positive, the motion will grow with time and the distribution of shed vorticity would be as shown in Figure 3(a). For decaying motion,

that is p negative, the vorticity distribution would appear as shown in Figure 3(b).

The lift deficiency function determined by Jones (18) is expressed as

$$\hat{C}(p+ik) = \frac{K_1(p+ik)}{K_o(p+ik) + K_1(p+ik)}$$

where K_o and K_1 are modified Hankel functions. As the build-up approached zero Jones (18) found that

$$\lim_{p \to 0+} \hat{C}(p+ik) = C(k) ,$$

where $C(k)$ is Theodorsen's lift deficiency function. In contrast, when the decay approached zero,

$$\lim_{p \to 0^-} C(p+ik) = \frac{H_1^{(1)}(k) + 2J_1(k)}{H_1^{(1)}(k) + iH_o^{(1)}(k) + 2[J_1(k) + iJ_o(k)]} .$$

Loewy (1) accounted for vortex sheets below the blade which had been shed by previous blade passes and obtained a lift deficiency function for a hovering rotor. This vortex strength model is shown in Figure 4. With a vibratory frequency of ω and a blade rotational frequency of Ω, Loewy's (1) lift deficiency function is given by

$$C'(k,m,h) = \frac{H_1^{(2)}(k) + 2J_1(k)\hat{W}(kh,m)}{H_1^{(2)}(k) + iH_o^{(2)}(k) + 2\hat{W}(kh,m)[J_1(k) + iJ_o(k)]} \quad (3)$$

where the effect of the wakes shed below the plane of the rotor appears

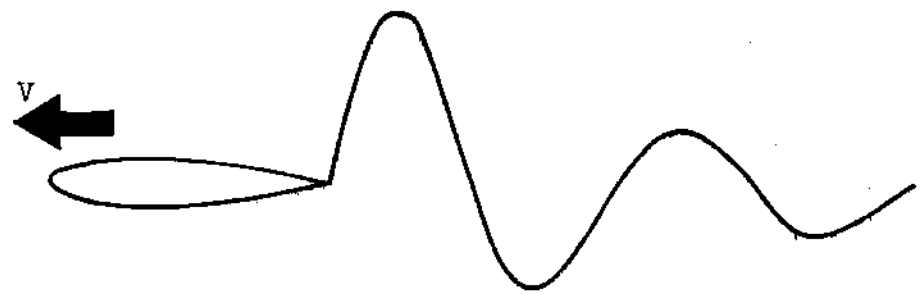

Figure 3a. Wake with Increasing Strength Amplitude Shed from Wing.

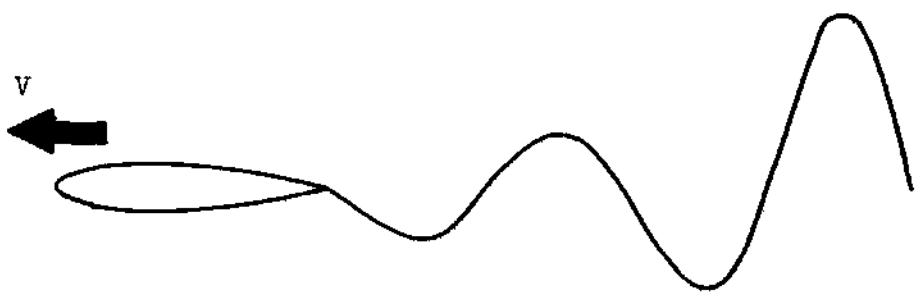

Figure 3b. Wake with Decreasing Strength Amplitude Shed from Wing.

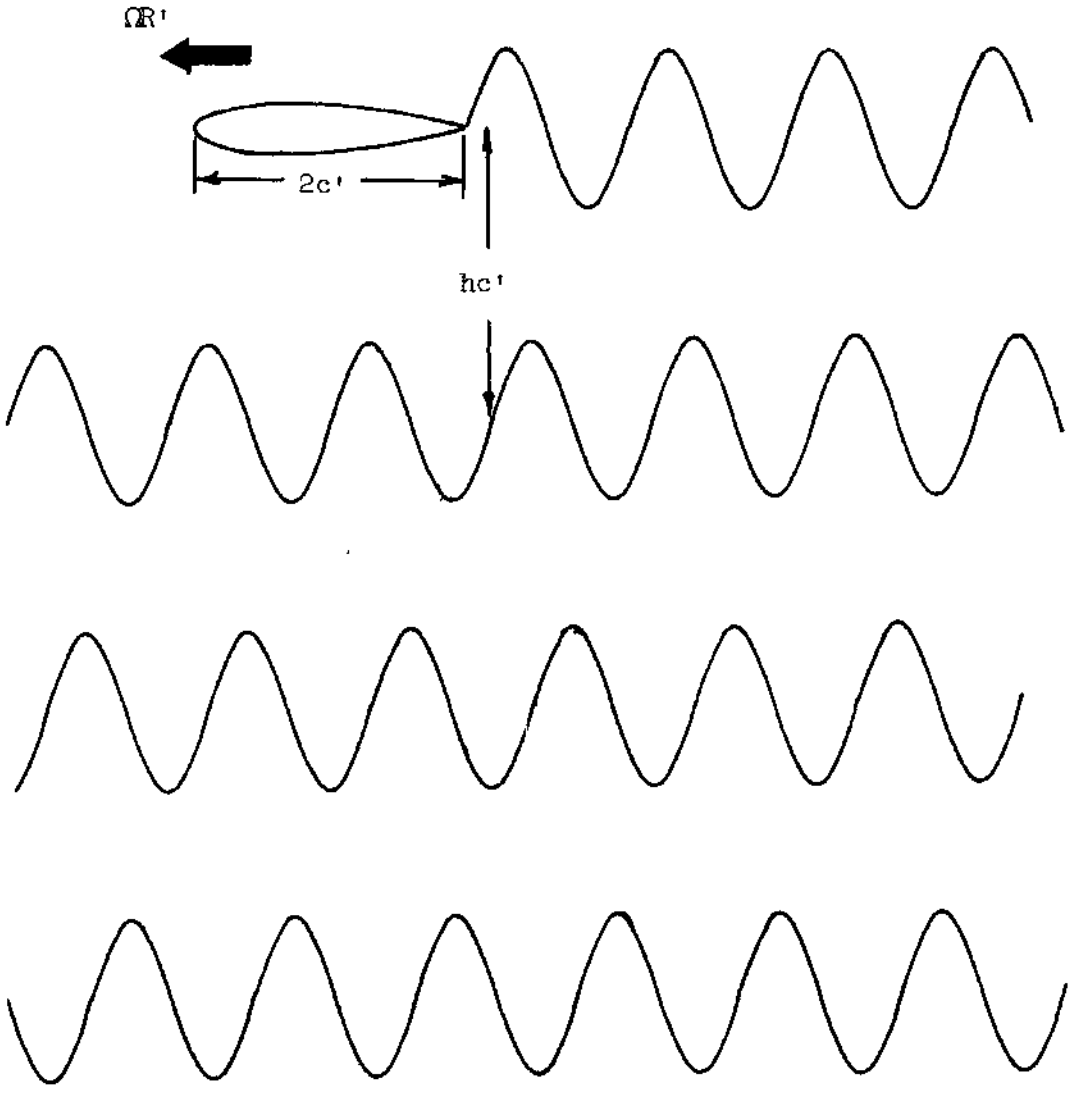

Figure 4. Wake Vortex System for Rotor Blade in Hover.

in the weighting function

$$\hat{W}(kh,m) = 1/(e^{kh}e^{i2\pi m/b}-1) \tag{4}$$

in which b is the number of blades and where the frequency ratio and non-dimensional wake spacing are given by

$$m = \omega/\Omega$$

$$h = \lambda\, 2\pi R'/bc'$$

and R' is the radius of the blade.

Method of Approach

The basic assumptions incorporated are as follows:

1. Two-dimensional, incompressible potential flow.

2. Respective layers of the wake are two-dimensionalized and treated as parallel horizontal sheets.

3. In forward flight, each blade of the rotor will respond in the same manner as every other blade.

4. The most critical azimuth positions of the blade in forward flight for the onset of flutter are at $\psi = 90^{\circ}$ and $\psi = 270^{\circ}$. This thesis is concerned with the 90° azimuth position, but extension of this work to the 270° case is straight forward.

5. At the onset of blade flutter oscillations will begin to build up prior to the blade reaching the critical azimuth position, and these oscillations will decay as the blade moves beyond the critical azimuth position. Each blade, then, behaves the same during its travel through the critical azimuth position.

A typical plot of the variation of aerodynamic damping with velocity, as might be obtained from fixed-wing flutter analysis, is shown in Figure 5. At a specified radial location r' on a rotor blade, the local tangential velocity is given by

$$V_t(r') = \Omega r' + V \sin \psi \ .$$

If the flutter speed for this blade segment is such that

$$V_{FL} < \Omega r' + V$$

then, as the blade passes through the 90° azimuth position, the blade segment at r' will experience velocities which will increase to the flutter speed and beyond, then return through the flutter boundary to lower airspeeds. If Figure 5 represents an effective flutter plot for the blade station at r', then one blade revolution would correspond to a point moving on the diagram as indicated by the arrows in Figure 5.

The blade tangential velocity will exceed the flutter speed whenever the rotor azimuth and radius positions are such that

$$V \sin \psi + \Omega r' > V_{FL} \ .$$

An example of this region is shown in Figure 6. All of the points within the shaded region of Figure 6 will experience negative damping. This negative damping will tend to cause blade motion to grow. In the region $\psi > \pi/2 + \Delta\psi_{FL}$, damping will be positive and will increase so that a blade instability would tend to die out.

The effect of this variation in damping on an outboard portion of

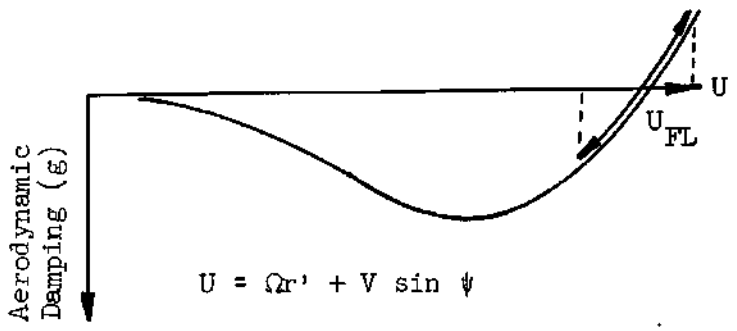

Figure 5. Typical Velocity-Damping Plot.

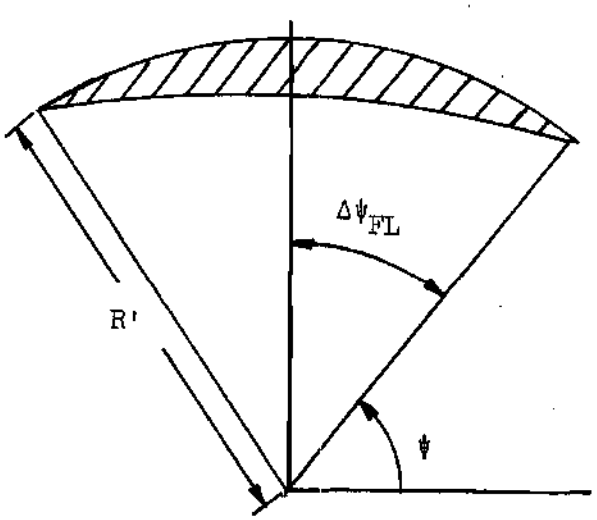

Figure 6. Unstable Region Encountered by Advancing Blades.

the advancing blade is such that as damping decreases with the blade approaching $\psi = 90^{\circ}$, the amplitude of oscillations will build up. Conversely as the blade advances beyond the $\psi = 90^{\circ} + \Delta\psi_{FL}$ position, damping will increase and there will be a corresponding decrease in blade vibratory amplitude. This build-up and decay of blade amplitude will result in a distribution of shed vorticity as shown in Figure 7. Here, the timewise variations in amplitude of blade vibrations have resulted in spacewise variations of shed vorticity.

Based on the foregoing, the bound vorticity on the airfoil can be expressed as the product of a function of chordwise position, a decay function, and a harmonic function of time. The bound vorticity is written as

$$\gamma_a = \bar{\gamma}_a(x) f(\xi_o) e^{i(\omega t + \varphi)} \tag{5}$$

where $f(\xi_o)$ is an assumed decay function centered about $\xi_o = 0$. The limiting case of constant-strength shed vorticity, such as considered by Theodorsen (4) and Loewy (1) for their analyses, is simply achieved by taking $f(\xi_o) = 1$.

The downwash which is induced by an element of vorticity which is located a distance s_1 behind and s_2 below the point of interest is found from the Biot-Savart law which states that

$$dv_a(x,t) = \frac{\gamma(s_1,t)\, s_1\, ds_1}{2\pi(s_1^2 + s_2^2)} . \tag{6}$$

When the inflow velocity through the rotor is small, the shed

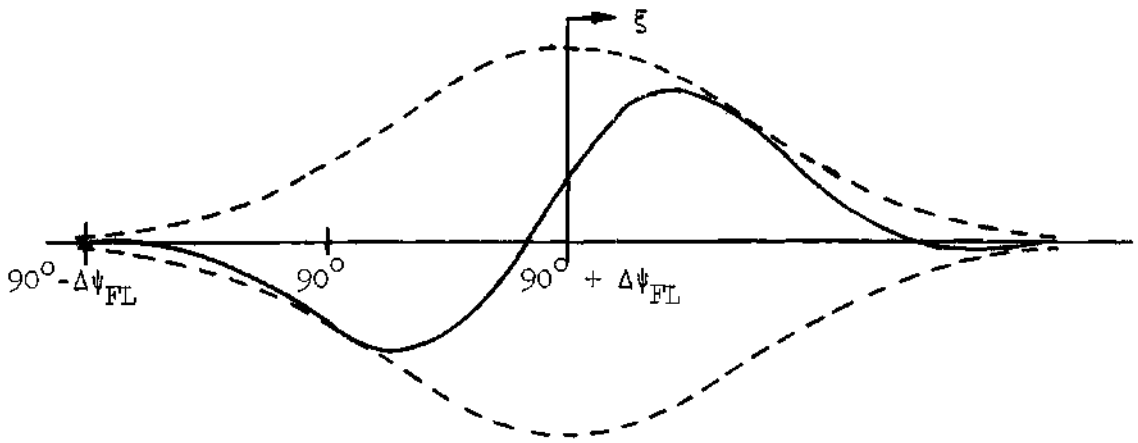

Figure 7. Proposed Model for the Shed Vorticity Distribution.

vorticity remains close to the rotor so that s_2 is small. In this case, as can be seen from equation (6) the wakes shed from each blade during several previous passes as well as the present pass must be considered. The vorticity shed by each blade as it passed $\psi = 90^\circ$ will be contained within a small double azimuth angle centered about $90^\circ + \Delta\psi_{FL}$ and this is shown by the solid lines in Figure 8. In this region the azimuth angle between a shed vortex filament and the reference blade may be ignored. Also, the tip does not move very far from the vertical plane shown in Figure 8 and so the tip path may be assumed to lie in this plane. The two-dimensionalized model resulting from the simplifications achieved by these restrictions is shown in Figure 9.

With the mathematical model defined, the problem is to determine the pressure difference across the airfoil due to the vorticity shed in the wakes, and consequently to determine the unsteady lift and moment acting on the airfoil.

Analytical Development

From the geometry shown in Figure 9 it can be seen that the vertical downwash produced at some point x on the blade by a vortex element at some point ξ_n in the nth wake is found, by the Biot-Savart law, to be

$$dv_{a_n}(x,t) = \frac{\gamma_n(\xi_n,t)(\xi_n + n\mu 2\pi R/b + Ut - x)d\xi_n}{2\pi[(\xi_n + n\mu 2\pi R/b + Ut - x)^2 + (n\lambda 2\pi R/b)^2]} \qquad (7)$$

where the following nondimensional quantities have been used:

$$\mu = V\cos\alpha_T/\Omega R' \qquad R = R'/c'$$

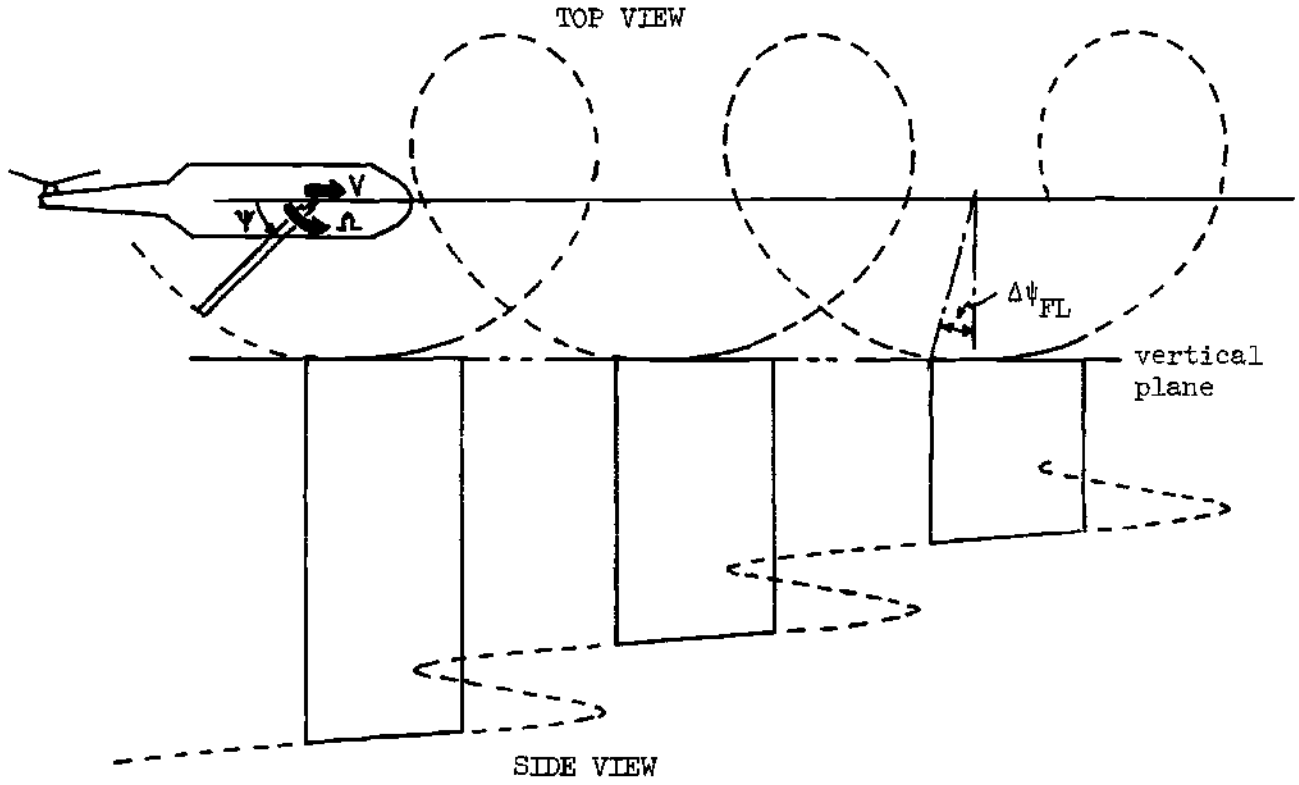

Figure 8. Skewed Helical Shape of the Wake Shed from a Helicopter in Forward Flight.

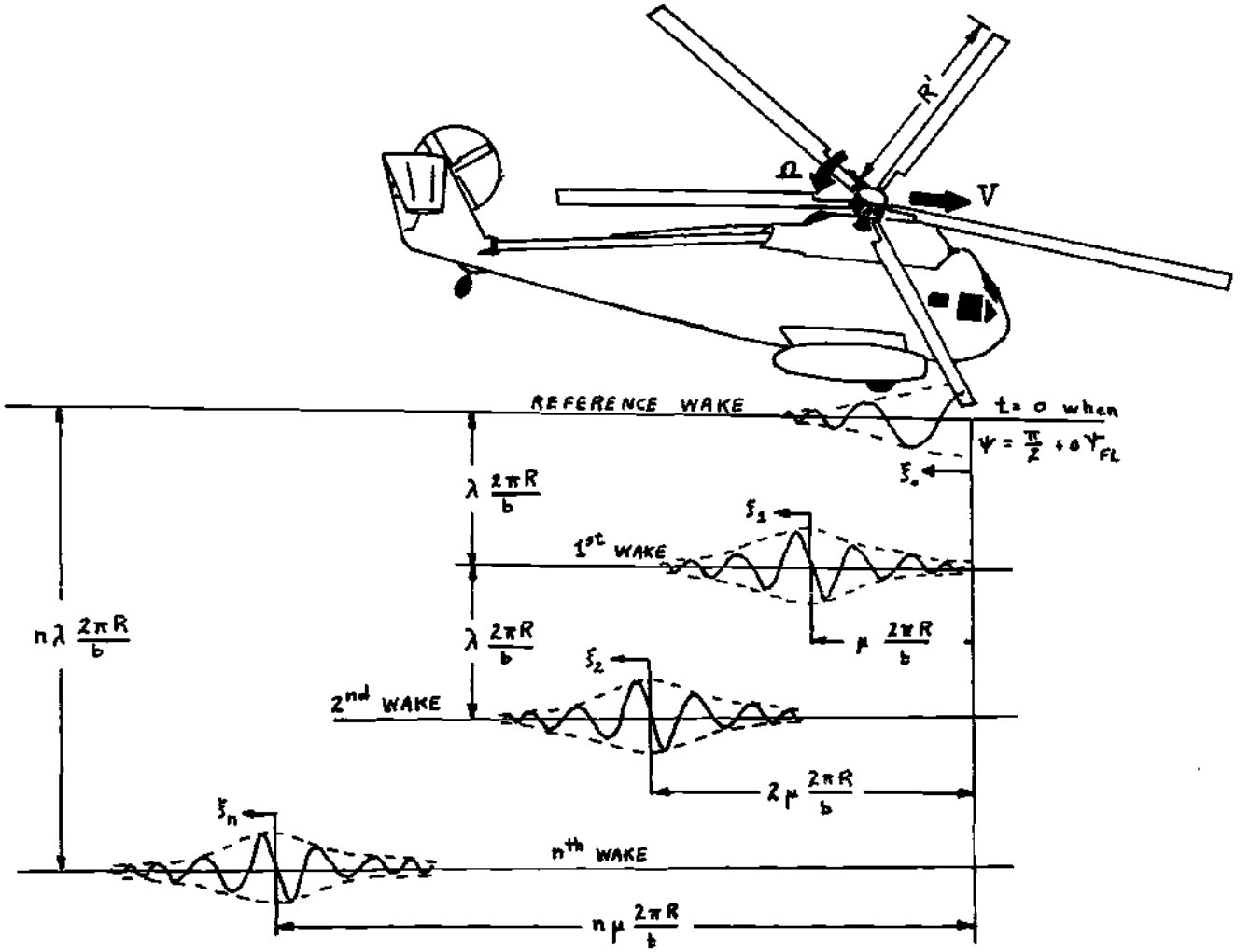

Figure 9. Two Dimensional Wake Model for Forward Flight As Described by Nondimensional Coordinates.

$$\lambda = (V \sin\alpha_T + v_i)/\Omega R'$$

and

$$U = \Omega R'(1 + \mu)/c' \quad .$$

Since the total downwash, $v_a(x,t)$, is the summation of the effect of the vorticity on the airfoil, γ_a, in the reference wake, γ_o, and all of the previous wakes, γ_n, it is apparent that

$$2\pi v_a(x,t) = \int_{-1}^{1} \frac{\gamma_a(\xi,t)d\xi}{\xi - x} + \int_{1}^{\infty} \frac{\gamma_o(\xi,t)d\xi}{\xi - x}$$

$$+ \sum_{n=1}^{\infty} \int_{-\infty}^{\infty} \frac{\gamma_n(\xi_n,t)(\xi_n + ns + Ut - x)d\xi_n}{(\xi_n + ns + Ut - x)^2 + n^2h^2} \qquad (8)$$

where

$$s = \mu 2\pi R/b$$

and

$$h = \lambda 2\pi R/b \quad .$$

In forward flight the blade will enter flutter only at $\psi = 90^\circ - \Delta\psi_{FL}$, if at all. Since conditions will be different at all of the other azimuth stations we can assume that each blade will behave the same. This means that the strength of the shed vorticity will have the same variation in each wake with respect to the origin of that wake. That is,

$$\bar{\gamma}_n(\xi_n) = \bar{\gamma}_o(\xi_o) \quad .$$

With each change of total circulation, Γ_a', vorticity is shed at

the trailing edge of the airfoil. This shed vorticity is given by

$$\gamma_o(c',t)d\xi' = -\frac{d\Gamma_a'}{dt}\,dt \quad .$$

Recalling the bound vorticity relation given in equation (5) and noting that $\xi_o = \xi - Ut$ gives

$$\Gamma_a' = \int_{-c'}^{c'} \gamma_a(x',t)dx'$$

$$= c' f(-Ut)e^{i(\omega t + \varphi)} \int_{-1}^{1} \bar{\gamma}_a(x)dx \quad . \tag{9}$$

It has been assumed here that the decay function, $f(\xi - Ut)$, does not vary much over the chord and so can be taken constant with respect to space, ξ, with its value being that which it has at the midchord ($\xi = 0$).

Now, let

$$\bar{\Gamma}_a' = c' \int_{-1}^{1} \bar{\gamma}_a(x)dx \quad . \tag{10}$$

Substituting equation (10) into equation (9) yields

$$\Gamma_a' = \bar{\Gamma}_a' f(-Ut)e^{i(\omega t + \varphi)} \quad .$$

With this definition it is obvious that

$$\gamma_o(c',t) = -\bar{\Gamma}_a'\left(-U\frac{df}{d\xi_o} + i\omega f\right)e^{i(\omega t+\varphi)}\frac{dt}{d\xi'} \quad .$$

But $d\xi'/dt = Uc'$ and so

$$\gamma_o(c',t) = -\frac{\omega}{U}\frac{\bar{\Gamma}'_a}{c'}\left(if - \frac{U}{\omega}\frac{df}{d\xi_o}\right)e^{i(\omega t+\varphi)}$$

$$= -ik\,\bar{\Gamma}_a\left(f - \frac{1}{ik}\frac{df}{d\xi_o}\right)e^{i(\omega t+\varphi-k)} \qquad (11)$$

where

$$\bar{\Gamma}_a = \frac{\bar{\Gamma}'_a}{c'}e^{ik} \qquad (12)$$

and

$$k = \omega c'/(\Omega R' + V\cos\alpha_T) = \omega/U\ . \qquad (13)$$

Since the shed vorticity does not change in strength with time, the vorticity which is a distance ξ' behind the midchord at time t will have the strength of the vorticity which was shed at the trailing edge at an earlier time $t - \Delta t$. It is obvious then that

$$\gamma_o(c',t - \Delta t) = \gamma_o(\xi',t)$$

where

$$\Delta t = \frac{\xi' - c'}{Uc'} = \frac{\xi-1}{U}\ .$$

Thus, substituting $t - \Delta t$ for t in equation (11) yields

$$\gamma_o(\xi,t) = -ik\,\bar{\Gamma}_a\left(f - \frac{1}{ik}\frac{df}{d\xi_o}\right)e^{i(\omega t + \varphi - k\xi)}\ . \qquad (14)$$

If we note that $\omega t - k\xi = -k\xi_o$ then it is apparent from the similarity of all wake elements that

$$\gamma_n(\xi_n,t) = -ik\bar{\Gamma}_a\left[f(\xi_n) - \frac{1}{ik}\frac{df}{d\xi_n}\right]e^{i(\varphi - k\xi_n)} \quad . \tag{15}$$

Substituting equations (14) and (15) as the shed vorticity relations into the downwash equation (8) yields

$$2\pi\, v_a(x,t) = \int_{-1}^{1} \frac{\bar{\gamma}_a(\xi) f(x-Ut)}{\xi - x}\, d\xi \cdot e^{i(\omega t+\varphi)}$$

$$- ik\,\bar{\Gamma}_a\, e^{i(\omega t+\varphi)} \int_{1}^{\infty} \left[f(\xi-Ut) - \frac{1}{ik}\frac{df}{d\xi_o}\right] \frac{e^{-ik\xi}}{\xi - x}\, d\xi \tag{16}$$

$$- ik\,\bar{\Gamma}_a\, e^{i\varphi} \sum_{n=1}^{\infty} \int_{-\infty}^{\infty} \frac{\left[f(\xi_n) - \frac{1}{ik}\frac{df}{d\xi_n}\right] e^{-ik\xi_n}(\xi_n + ns + Ut - x)}{(\xi_n + ns + Ut - x)^2 + n^2h^2}\, d\xi_n$$

Due to forward motion, and consequently to the decay function, time remains as an explicit variable in the downwash equation (16). It has been assumed from the start that the motion is strongest at $\psi = 90^\circ + \Delta\psi_{FL}$. In terms of stability this means that the airfoil is least stable at time $t = 0$ and this will be the only time to be considered.

If a coordinate change of

$$\xi_n + ns + Ut - x = nhy$$

is applied to the integral in the last term of equation (16) then the summation becomes

$$e^{i\omega t} \sum_{n=1}^{\infty} e^{ikns}\, e^{-ikx} \int_{-\infty}^{\infty} \frac{y\, e^{-iknhy}}{y^2+1}\, dy$$

$$+ e^{i\omega t} \sum_{n=1}^{\infty} e^{ikns}\, e^{-ikx} \int_{-\infty}^{\infty} \left[f(nhy-ns+x) - 1 - \frac{1}{ik}\frac{df}{dy} \right] \frac{y\, e^{-iknhy}}{y^2+1}\, dy$$

$$\triangleq - i\pi\, e^{i\omega t}\, e^{-ikx} \left[W(k,s,h) + \Delta W \right] . \qquad (17)$$

The function $W(k,s,h) + \Delta W$ just defined represents the effect of the previously shed wakes upon the downwash and is a function of reduced frequency, advance ratio, and inflow ratio. The variation of the decay function with x, as shown in the last equation, is eliminated by noting that x can vary only from -1 to 1. This means that x is small so that the decay function does not vary significantly with x. With the dependency on x thereby removed, the portion of the wake weighting function for no decay is found to be (see Appendix C)

$$W(k,s,h) = 1/(e^{kh}e^{-iks} - 1) .$$

The segment of the wake weighting function due to the introduction of the decay function is

$$-i\pi\Delta W = \sum_{n=1}^{\infty} e^{ikns} \int_{-\infty}^{\infty} \left[f(nhy-ns) - 1 - \frac{1}{ik}\frac{df}{dy} \right] \frac{y\, e^{-iknhy}}{y^2+1} dy . \qquad (18)$$

For time near zero the decay function f(x-Ut) is very near one since $-1 \le x \le 1$. Letting $v_a(x,t) = \bar{v}_a(x)e^{i(\omega t+\varphi)}$ then makes the downwash equation (16) become

$$2\pi\bar{v}_a(x) = \int_{-1}^{1} \frac{\bar{\gamma}_a(\xi)d\xi}{\xi-x} - ik\,\bar{\Gamma}_a \int_{1}^{\infty} \frac{\left[f(\xi_o) - \frac{1}{ik}\frac{df}{d\xi_o} \right] e^{-ik\xi_o}}{\xi_o - x}\, d\xi_o$$

$$- \pi k \bar{\Gamma}_a e^{-ikx} [W(k,s,h) + \Delta W] \qquad (19)$$

for time $t = 0$.

Through investigations for the solutions to certain integral equations Carleman (19) found that the unique solution of the equation

$$a(x) \hat{h}(x) - \beta \int_{-1}^{1} \frac{\hat{h}(\xi)}{\xi - x} d\xi = g(x) \qquad (\beta > 0),$$

within the class of continuous functions having an integrable singularity at the left-hand end of the segment $[-1,1]$ and bounded at the other end, can be written as

$$\hat{h}(x) = \frac{a(x)}{a^2(x)+\pi^2\beta^2} g(x) + \frac{\beta e^{\omega(x)}}{\sqrt{a^2(x)+\pi^2\beta^2}} \int_{-1}^{1} \frac{e^{-\omega(x)} g(\xi)}{\sqrt{a^2(x)+\pi^2\beta^2}} \frac{d\xi}{\xi - x}$$

where

$$\omega(x) = \int_{-1}^{1} \frac{\theta(\xi)}{\xi - x} d\xi, \quad 2\pi i \ \theta(x) = \ln \frac{a(x) + \beta\pi i}{a(x) - \beta\pi i} \quad (0 < \theta(x) < 1) .$$

If $a(x) \equiv 0$ and $\beta = \frac{1}{2\pi}$, so that $\theta(x) = \frac{1}{2}$ and

$$\omega(x) = \frac{1}{2} \ln \frac{1+x}{1-x} ,$$

we obtain

$$\hat{h}(x) = \frac{2}{\pi} \sqrt{\frac{1-x}{1+x}} \int_{-1}^{1} \sqrt{\frac{1+\xi}{1-\xi}} \frac{g(\xi)}{\xi - x} d\xi ,$$

which is Söhngen's (17) solution to the integral equation

$$g(x) = -\frac{1}{2\pi}\int_{-1}^{1} \frac{\hat{h}(\xi)}{\xi - x}\, d\xi \ .$$

The case under consideration in equation (19) is that $\hat{h}(x) = -\bar{\gamma}_a(x)$. The bound vorticity, $\bar{\gamma}_a(x)$, will be finite at the trailing edge and have an integrable singularity at the leading edge of the airfoil. These conditions are met by the above assumptions on the function $\hat{h}(x)$.

Applying Söhngen's (17) inversion to equation (19) yields the formula for the bound vorticity as a function of downwash:

$$\bar{\gamma}_a(x) = \frac{2}{\pi}\sqrt{\frac{1-x}{1+x}}\left\{\int_{-1}^{1}\sqrt{\frac{1+\xi}{1-\xi}}\,\frac{\bar{v}_a(\xi)}{x-\xi}\, d\xi\right.$$

$$+\frac{ik\bar{\Gamma}_a}{2\pi}\int_{-1}^{1}\sqrt{\frac{1+\xi}{1-\xi}}\,\frac{1}{x-\xi}\int_{1}^{\infty}\left[f(y) - \frac{1}{ik}\frac{df}{dy}\right]\frac{e^{-iky}}{y-\xi}\, dy\, d\xi$$

$$\left.+\frac{k\bar{\Gamma}_a}{2}(W+\Delta W)\int_{-1}^{1}\sqrt{\frac{1+\xi}{1-\xi}}\,\frac{e^{-ik\xi}}{x-\xi}\, d\xi\right\} \ .$$

Now the total downwash can be found by noting from the relations shown in equations (10) and (12) that

$$\bar{\Gamma}_a'/c' = \bar{\Gamma}_a\, e^{-ik} = \int_{-1}^{1} \bar{\gamma}_a(x)\, dx \ .$$

Thus, by integrating equation (20) over the chord, reversing the order

of integration and noting that

$$\int_{-1}^{1} \sqrt{\frac{1+\xi}{1-\xi}}\, e^{-ik\xi}\, d\xi = \pi[J_0(k) - i\, J_1(k)]$$

the total bound vorticity may be expressed as

$$\bar{\Gamma}_a = \frac{4G(k,s,h)}{ik\pi} \int_{-1}^{1} \sqrt{\frac{1+\xi}{1-\xi}}\; \bar{v}_a(\xi)d\xi \tag{21}$$

where

$$G(k,s,h) = 1/\{H_1^{(2)}(k) + i\, H_0^{(2)}(k) + \Delta F_3(k)$$

$$+ 2i(W + \Delta W)[J_0(k) - iJ_1(k)]\} \; . \tag{22}$$

The function $G(k,s,h)$ is introduced here for notational convenience and it involves Hankel functions, Bessel functions and the integral

$$\Delta F_3(k) = \frac{-2}{\pi} \int_1^{\infty} \left[f(y) - 1 - \frac{1}{ik}\frac{df}{dy}\right]\sqrt{\frac{y+1}{y-1}}\, e^{-iky}\, dy \; . \tag{23}$$

In order to determine the pressure difference across the airfoil in terms of the vorticity given in equation (20) we begin with Bernoulli's equation for unsteady motion using non-dimensional lengths

$$\frac{\partial \varphi}{\partial t} + U \cdot \frac{\partial \varphi}{\partial x} + \frac{p}{\rho} = F(t) \; .$$

The difference in velocity between the upper and lower surfaces of the airfoil is $\gamma_a(x,t)$. Thus,

$$\frac{\partial \varphi_U}{\partial x} - \frac{\partial \varphi_L}{\partial x} = c'\, \gamma_a(x,t)$$

and so

$$\varphi_U - \varphi_L = c' \int_{-1}^{x} \gamma_a(\xi,t)d\xi \ .$$

Applying these relations between the velocity potential and the bound vorticity we get

$$p_U - p_L \triangleq \Delta p = - \rho\left[uc'\gamma_a(x,t) + c'\int_{-1}^{x} \frac{\partial}{\partial t} \gamma_a(\xi,t)d\xi\right] .$$

Recalling the vorticity relation from equation (5) and the fact that $\xi_o = \xi - Ut$ makes this pressure equation become

$$\frac{-\Delta p}{\rho U c'} = \bar{\gamma}_a(x)f(x-Ut)e^{i(\omega t+\varphi)}$$

$$+ \frac{e^{i(\omega t+\varphi)}}{U} \int_{-1}^{x} \left[i\omega\, f(\xi_o) - U \frac{df}{d\xi_o}\right] \bar{\gamma}_a(\xi_o)d\xi_o \ .$$

For time t near zero this can be reduced, by letting

$$\Delta p = \Delta\bar{p}(x)\ e^{i(\omega t+\varphi)} \ ,$$

to

$$\frac{-\Delta\bar{p}}{\rho U c'} = \bar{\gamma}_a(x) + ik \int_{-1}^{x} \bar{\gamma}_a(\xi)d\xi - \int_{-1}^{x} \frac{df}{d\xi} \bar{\gamma}_a(\xi)d\xi \ .$$

The slope of the decay function will be very near zero over the chord of the airfoil. Thus the second integral in the previous pressure equation will by negligible. So,

$$\frac{-\Delta\bar{p}(x)}{\rho U c'} = \bar{\gamma}_a(x) + ik\int_{-1}^{x} \bar{\gamma}_a(\xi)d\xi \ . \tag{24}$$

The local bound vorticity is given by equation (20). Substituting equation (20) into equation (24) and performing the necessary operations, as shown in Appendix A, yields

$$-\frac{\Delta\bar{p}(x)}{\rho U c'} \cdot \frac{\pi}{2} = \int_{-1}^{1} \left[\sqrt{\frac{1-x}{1+x}} \sqrt{\frac{1+\xi}{1-\xi}} \frac{1}{x-\xi} - ik\Omega_1(x,\xi) \right] \bar{v}_a(\xi)d\xi$$

$$+ G(k,s,h)\left[iH_0^{(2)} + \Delta F_1 + 2i(W+\Delta W)J_0\right]\sqrt{\frac{1-x}{1+x}} \int_{-1}^{1} \sqrt{\frac{1+\xi}{1-\xi}}\, \bar{v}_a(\xi)d\xi$$

$$+ G(k,s,h)F_1(k,x) \int_{-1}^{1} \sqrt{\frac{1+\xi}{1-\xi}}\, \bar{v}_a(\xi)d\xi \tag{25}$$

which is the pressure in terms of the downwash. Equation (25) involves the integrals

$$F_1(k,x) = -\frac{2}{\pi}\int_1^{\infty} \left[\frac{df}{dy} - \frac{1}{ik}\frac{d^2f}{dy^2}\right] \Omega_2(x,y)e^{-iky}\, dy \tag{26}$$

where

$$\Omega_2(x,y) = 2\tan^{-1}\left[\sqrt{\frac{1-x}{1+x}}\sqrt{\frac{y+1}{y-1}}\right] - \pi \tag{27}$$

and

$$\Delta F_1(k) = \frac{-2}{\pi}\int_1^{\infty} \left[f(y) - 1 - \frac{1}{ik}\frac{df}{dy}\right] \frac{e^{-iky}}{\sqrt{y^2-1}}\, dy \tag{28}$$

and the function

$$\Omega_1(x,\xi) = \frac{1}{2} \ln \left[\frac{1 - x\xi + \sqrt{1-\xi^2}\sqrt{1-x^2}}{1 - x\xi - \sqrt{1-\xi^2}\sqrt{1-x^2}} \right] \quad . \tag{29}$$

The lift acting on the airfoil is obtained by integrating the pressure over the chord. That is,

$$L = c' \int_{-1}^{1} \Delta\bar{p}(x)dx \quad . \tag{30}$$

Integrating by parts and noting that

$$\frac{\partial\Omega_1(x,\xi)}{\partial x} = \sqrt{\frac{1-\xi}{1+\xi}}\sqrt{\frac{1+x}{1-x}} \left(\frac{1}{1+x} + \frac{1}{\xi-x} \right)$$

then it follows that

$$\int_{-1}^{1} \Omega_1(x,\xi)dx = \pi\sqrt{1-\xi^2} \quad . \tag{31}$$

With a function $\Delta F_4(k)$ defined as

$$\Delta F_4(k) = \frac{2}{\pi} \int_{1}^{\infty} (f'-f''/ik)(y - \sqrt{y^2-1})e^{-iky}\, dy \tag{32}$$

it can be shown that

$$\int_{-1}^{1} F_1(k,x)dx = \frac{1}{2}\pi^2\, \Delta F_4(k) \quad . \tag{33}$$

If the pressure equation (25) is substituted into the lift equation (30) and equations (31) and (33) are applied to the result, then

$$\frac{L}{2\rho U c'^2} = ik \int_{-1}^{1} \sqrt{1-x^2}\, \bar{v}_a(x)\, dx$$

$$+ C_1(k,\mu,\lambda) \int_{-1}^{1} \sqrt{\frac{1+x}{1-x}}\, \bar{v}_a(x)\, dx \qquad (34)$$

where $C_1(k,\mu,\lambda)$ is defined to be

$$C_1(k,\mu,\lambda) = G(k,s,h)\{H_1^{(2)}(k) + \Delta F_2(k) + \Delta F_4(k)$$

$$+ 2J_1(k)[W(k,s,h) + \Delta W]\} \qquad (35)$$

where

$$\Delta F_2(k) = \Delta F_3(k) - \Delta F_1(k) .$$

The moment about the midchord is

$$M_{\frac{1}{2}} = c'^2 \int_{-1}^{1} \Delta\bar{p}(x) x\, dx . \qquad (36)$$

Integration by parts yields

$$\int_{-1}^{1} \Omega_1(x,\xi) x\, dx = \frac{1}{2}\pi\xi\sqrt{1-\xi^2} \quad . \qquad (37)$$

Defining $\Delta F_5(k)$ to be

$$\Delta F_5(k) = \frac{2}{\pi} \int_{1}^{\infty} y(f'-f''/ik)\,(y - \sqrt{y^2-1})e^{-iky}\, dy \qquad (38)$$

gives the relation

$$\int_{-1}^{1} F_1(k,x)x\,dx = \frac{\pi^2}{8}\,\Delta F_5(k) \quad . \tag{39}$$

By substituting the pressure equation (25) into the moment equation (36) and applying equations (37) and (39), it can be shown that

$$\frac{M_{\frac{1}{2}}}{\rho\, Uc'^3} = -\int_{-1}^{1} (2 - ikx)\sqrt{1 - x^2}\,\bar{v}_a(x)\,dx$$

$$- C_1(k,\mu,\lambda)\int_{-1}^{1}\sqrt{\frac{1+x}{1-x}}\,\bar{v}_a(x)\,dx \tag{40}$$

$$+ \left\{G(k,s,h)\left[\Delta F_4(k) + \frac{1}{2}\,\Delta F_5(k)\right] + 1\right\}\int_{-1}^{1}\sqrt{\frac{1+x}{1-x}}\,\bar{v}_a(x)\,dx \quad .$$

The moment about the quarter chord is

$$M_{\frac{1}{4}} = M_{\frac{1}{2}} + \frac{1}{2}\,c'L \quad .$$

Thus, adding the lift equation (34) to the midchord moment equation (40) yields

$$\frac{M_{\frac{1}{4}}}{\rho\, Uc'^3} = -\int_{-1}^{1} (2-ik-ikx)\sqrt{1-x^2}\,\bar{v}_a(x)\,dx$$

$$+ \left\{G(k,s,h)\left[\Delta F_4(k) + \frac{1}{2}\Delta F_5(k)\right] + 1\right\}\int_{-1}^{1}\sqrt{\frac{1+x}{1-x}}\,\bar{v}_a(x)\,dx \quad . \tag{41}$$

Now consider a strip of a two-dimensional airfoil having a bending and a pitching freedom as shown in Figure 1. The bending h' is measured positive down at the elastic axis and the pitch α is measured positive

for nose-up rotation.

For an element of mass dm situated a distance xc' aft of the midchord, the inertia force is

$$-dm[\ddot{h}' + (x-a)c'\ddot{\alpha}] .$$

So the total inertia force is

$$-c'm\left[\frac{\ddot{h}'}{c'} + (x_{cg} - a)\ddot{\alpha}\right] .$$

The inertia force exerts a moment about the elastic axis which is

$$-\int(x-a)c'[\ddot{h}' + (x-a)c'\ddot{\alpha}]dm = -c'^2m\left[(x_{cg}-a)\frac{h'}{c'} + (I-2ax_{cg}+a^2)\ddot{\alpha}\right]$$

where Imc'^2 is the section's mass moment of inertia about the midchord.

Now let

$$x_\alpha = x_{cg}-a$$

and

$$r_\alpha^2 = I - 2ax_{cg} + a^2 .$$

With these definitions it is apparent that $x_\alpha mc'$ is the static mass unbalance about the elastic axis and $r_\alpha^2 mc'^2$ is the mass moment of inertia about the elastic axis.

With the displacements being resisted by springs of stiffness K_h and K_α and enforced by the aerodynamic lift and moment about the elastic axis, the equations of motion for the section are

$$mc'\left(\frac{\ddot{h}'}{c'} + x_\alpha \ddot{\alpha}\right) + K_h h' = -L$$

$$mc'^2\left(x_\alpha \frac{\ddot{h}'}{c'} + r_\alpha^2 \ddot{\alpha}\right) + K_\alpha \alpha = M_{e.a.} \quad . \tag{42}$$

The square of the uncoupled natural frequency in bending is

$$\omega_h^2 = K_h/m$$

and in rotation is

$$\omega_\alpha^2 = K_\alpha / r_\alpha^2 mc'^2 \quad .$$

Thus, in terms of natural frequencies of the system, the equations of motion (42) can be written as

$$\ddot{h}'/c' + x_\alpha \ddot{\alpha} + \omega_h^2 h'/c' = -L/mc'$$

$$x_\alpha \ddot{h}'/c' + r_\alpha^2(\ddot{\alpha} + \omega_\alpha^2 \alpha) = M_{ea}/mc'^2 \quad . \tag{43}$$

It has been observed that the energy dissipated by structural damping varies with the square of the amplitude of oscillations. The effect of damping is therefore represented by a shift of the phase angle of the elastic restoring force. That is, the restoring force $h'K_h$ can be replaced by $h'K_h(1+ig_h)$ where g_h is the damping coefficient for bending. Thus, ω_h^2 is replaced by $\omega_h^2(1+ig_h)$ and similarly ω_α^2 is replaced by $\omega_\alpha^2(1+ig_\alpha)$.

If simple harmonic motion is assumed so that

$$h' = h'_o \, e^{i\omega t}$$

and

$$\alpha = \alpha_o e^{i\omega t}$$

and if the lift is expressed as

$$L = -\pi\rho\omega^2 c'^3\left(L'_h \frac{h'_o}{c'} + L'_\alpha \alpha_o\right) \tag{44}$$

and the moment about the elastic axis as

$$M_{ea} = \pi\rho\omega^2 c'^4\left(M'_h \frac{h'_o}{c'} + M'_\alpha \alpha_o\right) \tag{45}$$

then the equations of motion (43) become

$$\left[(\omega_h/\omega)^2(1+ig_h) - 1 - \varkappa L'_h\right]\frac{h'_o}{c'} - (\varkappa L'_\alpha + x_\alpha)\alpha_o = 0$$

$$(x_\alpha + \varkappa M'_h)\frac{h'_o}{c'} + \left[r_\alpha^2 - (\omega_\alpha/\omega)^2(1+ig_\alpha)r_\alpha^2 + \varkappa M'_\alpha\right]\alpha_o = 0 \tag{46}$$

where $\varkappa$ is the mass ratio defined as $\varkappa = \pi\rho c'^2/m$.

If

$$g = g_h = g_\alpha$$

and

$$Z = (\omega_\alpha/\omega)^2 (1+ig) \tag{47}$$

then a nontrivial solution to equation (46) is possible only if

$$\begin{vmatrix} \left[Z - (1+\varkappa L'_h)(\omega_\alpha/\omega_h)^2\right] & \left[-(\varkappa L'_\alpha + x_\alpha)(\omega_\alpha/\omega_h)^2\right] \\ \left[-(x_\alpha + \varkappa M'_h)/r_\alpha^2\right] & \left[Z - 1 - \varkappa M'_\alpha/r_\alpha^2\right] \end{vmatrix} = 0 \quad . \tag{48}$$

In order to find the expressions for L_h', L_α', M_h' and M_α', the relation for the local downwash along the airfoil must be known so that it can be used in the lift equation (34) and moment equation (41). For small oscillations the displacement along the chord of the airfoil is

$$z' = h' + c'(x - a)\alpha \ .$$

The downwash on the airfoil must be

$$v_a(x,t) = Uc' \ \partial z'/\partial x' + \partial z'/\partial t \ .$$

Since $v_a(x,t) = \bar{v}_a(x)e^{i\omega t}$ the relation for the displacement z' immediately yields

$$\bar{v}_a(x) = iUc'k \left[\frac{h_o'}{c'} + (x-a-i/k)\alpha_o\right] . \tag{49}$$

Substituting the downwash equation (49) into the lift equation (34) yields

$$-L = \pi\rho c'^3\omega^2\{[1+2C_1(k,\mu,\lambda)/ik]h_o'/c'$$

$$+ [C_1(k,\mu,\lambda)/ik - (a+i/k)(1+2C_1/ik)]\alpha_o\} . \tag{50}$$

So, comparing the lift equations (50) and (44), shows that

$$L_h' = L_h = 1 + 2C_1(k,\mu,\lambda)/ik \tag{51}$$

and

$$L_\alpha' = L_\alpha - \left(\frac{1}{2} + a\right)L_h \tag{52}$$

where

$$L_\alpha = \frac{1}{2} - i[1+2C_1(k,\mu,\lambda)]/k - 2C_1(k,\mu,\lambda)/k^2 \quad . \tag{53}$$

Substituting the downwash equation (49) into the quarter chord moment equation (41) yields

$$M_{\frac{1}{4}} = \pi\rho c'^4\omega^2 \left\{\left[\frac{1}{2} + M_d\right]\frac{h_o'}{c'} + \left[\frac{1}{8} - \frac{a}{2} - \frac{i}{k} + \left(a - \frac{1}{2} + \frac{i}{k}\right)M_d\right]\alpha_o\right\} \tag{54}$$

where the term appearing due to the decay function is

$$M_d = \frac{i}{k} G(k,s,h) \left[\Delta F_4(k) + \frac{1}{2}\Delta F_5(k)\right] . \tag{55}$$

If we let

$$M_h = \frac{1}{2} + M_d \tag{56}$$

and

$$M_\alpha = 3/8 - i/k + (2a + i/k)\, M_d \tag{57}$$

then the quarter chord moment equation (54) becomes

$$M_{\frac{1}{4}} = \pi\rho c'^4\omega^2 \left\{M_h \frac{h_o'}{c'} + \left[M_\alpha - \left(\frac{1}{2} + a\right)M_h\right]\alpha_o\right\} . \tag{58}$$

The moment about the elastic axis is

$$M_{ea} = M_{\frac{1}{4}} + \left(\frac{1}{2} + a\right)c'L \quad . \tag{59}$$

It has been shown that

$$L = -\pi\rho\omega^2 c'^3 \left\{ L_h \frac{h'_o}{c'} + L_\alpha - \left(\frac{1}{2} + a\right) L_h \right] \alpha_o \right\} . \tag{60}$$

Substituting the lift equation (60) and the quarter chord moment equation (58) into the elastic axis moment equation (59) shows, by comparison with the elastic axis moment equation (45), that

$$M'_h = M_h - \left(\frac{1}{2} + a\right) L_h \tag{61}$$

and

$$M'_\alpha = M_\alpha - \left(\frac{1}{2} + a\right)(L_\alpha + M_h) + \left(\frac{1}{2} + a\right)^2 L_h . \tag{62}$$

Expanding the flutter determinant given in equation (48) yields

$$Z^2 - 2\zeta Z + \eta = 0 \tag{63}$$

where

$$2\zeta = (1 + \varkappa L'_h)(\omega_\alpha/\omega_h)^2 + 1 + \varkappa M'_\alpha/r_\alpha^2 \tag{64}$$

and

$$\eta = [(r_\alpha^2 + \varkappa M'_\alpha)(1 + \varkappa L'_h) - (L'_\alpha \varkappa + x_\alpha)(x_\alpha + \varkappa M'_h)](\omega_\alpha/\omega_h)^2/r_\alpha^2 . \tag{65}$$

The roots of equation (63) are

$$Z = \zeta \pm \sqrt{\zeta^2 - \eta} .$$

From equation (47) it is obvious that the two values obtained from each of the roots are

$$\omega_\alpha/\omega = \sqrt{\mathrm{Re}[Z]} \tag{66}$$

and

$$g = \mathrm{Im}\{Z\}/\mathrm{Re}\{Z\} \ . \tag{67}$$

For a given advance ratio and its associated inflow ratio, the flutter boundary is determined by varying the reduced frequency until the flutter determinant is zero with zero damping coefficient. A flutter analysis then is carried out as follows:

1. Given k, μ, and λ, compute the modified lift deficiency from equation (35). The methods for evaluating the terms due to the decay function are given in Appendix B.

2. Compute the lift coefficients from equations (51), (52) and (53) and the moment coefficients from equations (61) and (62), where M_h and M_α are obtained from equations (55), (56), and (57).

3. The blade characteristics such as mass ratio, $\varkappa = \pi\rho c'^2/m$, natural torsional to bending frequency ratio, ω_α/ω_h, and mass unbalance, x_α, are known. Thus step (2) completes the information necessary to calculate the binomial coefficients ζ, equation (64), and η, equation (65), for equation (63).

4. The roots for Z yield the damping coefficient from equation (67) and the oscillatory frequency from equation (66). The latter term yields the velocity for the velocity-damping plot from the relation

$$\frac{V+\Omega R'}{\omega_\alpha c'} = \frac{1}{k(1+\mu)(\omega_\alpha/\omega)} \ . \tag{68}$$

If flutter can exist then it will be found by decreasing the reduced frequency which is assumed in step (1) until the damping coefficient from step (4) goes to zero.

CHAPTER III

DISCUSSION OF RESULTS

This chapter begins with comparisons between results obtained here and in earlier works. Some of the major parameters effecting the flutter velocity were varied and the results are presented here.

Comparison of Lift Deficiency Functions

With a decay function of

$$f(y) = 1 - e^{-p/y^2}$$

an exact evaluation of the integrals given in the definitions for ΔF_1, ΔF_2, ΔF_4, and ΔF_5 is possible. Plots of this decay function for various decay rates are given in Figure 10. The method of solution of these integrals is given in Appendix D. A numerical method for evaluating the integrals is described in Appendix B. The numerical method allows for complete flexibility in the choice of the decay function. All of these integrals are functions of reduced frequency alone.

Agreement to five significant figures was achieved between the exact and numerical results for the reduced frequency in the range from 0.008 to 4.0. For k between 0.008 and 0.02 the numerical method was good to four significant figures for the imaginary part of ΔF_5. This accuracy is quite adequate for the determination of the modified lift deficiency function for helicopter flutter. If a decay function is found that better fits the motion of the system, it can be applied to this

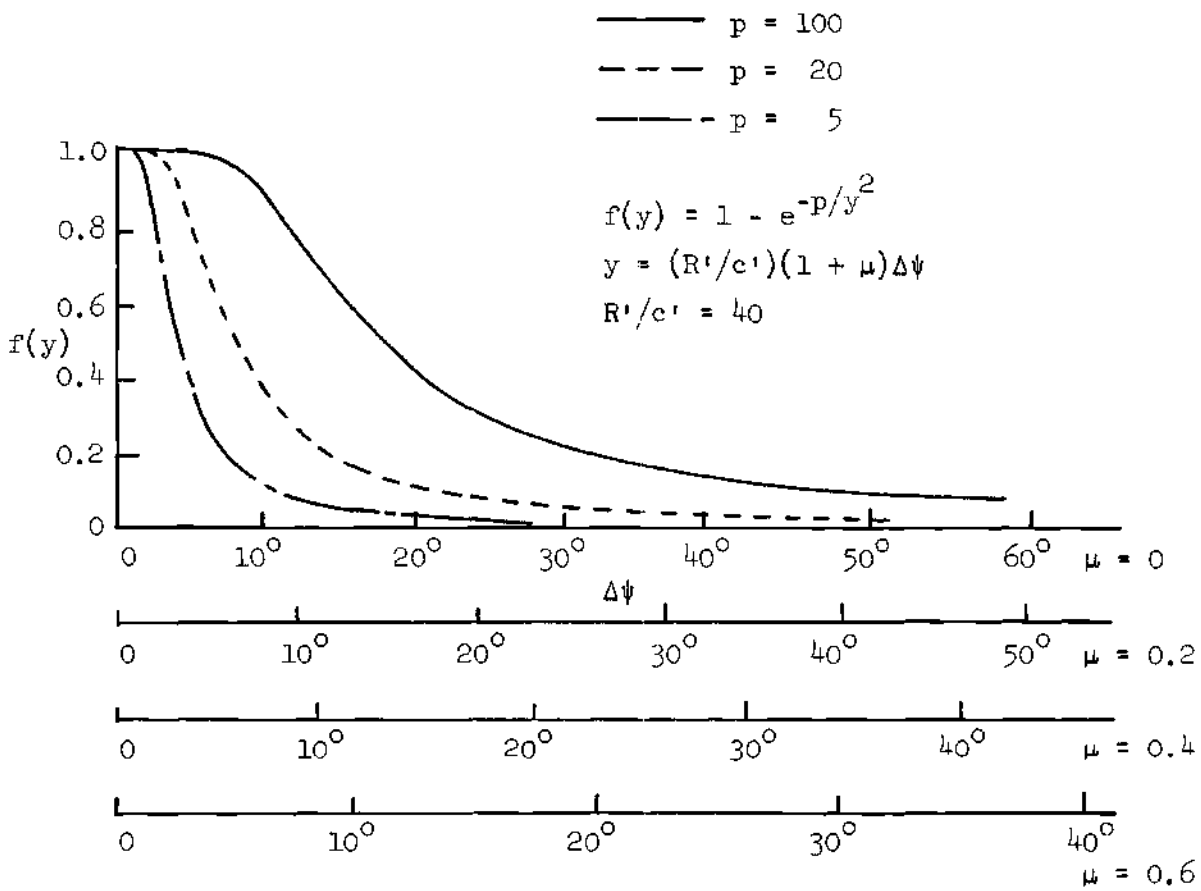

Figure 10. Decay Function for Various Decay Rates.

numerical method, and accurate results can be expected.

The calculations in the exact method for values of the reduced frequency greater than 4.0 lost precision when nine significant digits were carried. However, only values of k less than one are of interest in a lifting surface flutter analysis. This is evident from the fact that

$$k = \omega c'/\Omega R'(1+\mu) \ .$$

Thus, a high flutter speed requires small reduced frequency.

The effect of all of the previously shed wakes appears in the wake weighting function $W(k,s,h) + \Delta W$. This term is evaluated as shown in Appendix C. Each term in the relation for the modified lift deficiency function given in equation (35) can now be evaluated. Figure 11 shows a comparison between the lift deficiency functions obtained with and without decay. The decay rate was 4.0 so that

$$f(y) = 1 - e^{-4/y^2}$$

and the advance ratio was taken to be 0.1.

High and low inflow was considered. With $\lambda = 0.16$ for high inflow, the curves for the real and imaginary part of the lift deficiency function are fairly smooth since the previously shed wakes are too far away to have much effect. For a low inflow ratio of $\lambda = 0.02$ the wakes have a strong effect on the lift deficiency function if there is no decay. With decay, the wakes lose some of their effect and so the variation of the lift deficiency function with reduced frequency is smoother. The reason for this loss of effect becomes apparent by

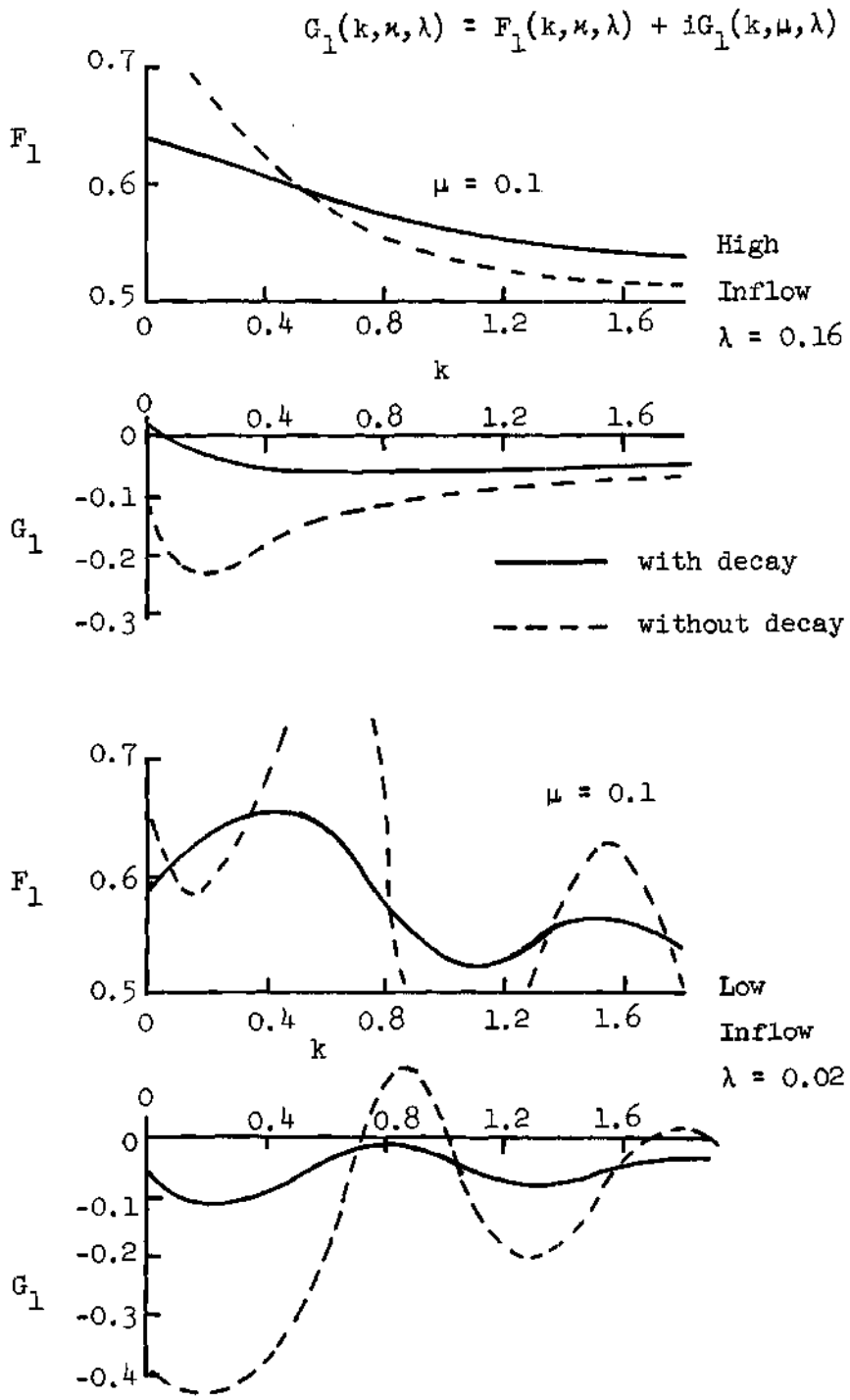

Figure 11. Lift Deficiency Function with and without Decay.

examining Figure 9 which shows that the wake sections that lie directly below the blade lose strength due to decay.

The wakes cause a lift loss and phase shift even at zero reduced frequency. With no decay it can be shown that

$$\lim_{k \to 0} C_1(k,\mu,\lambda) = \frac{h - is}{h - is + \pi} \tag{69}$$

where

$$s = \mu 2\pi R'/bc'$$

and

$$h = \lambda 2\pi R'/bc' \ .$$

In hover, $s = 0$ so that equation (69) reduces to the value found by Loewy (1) for zero k and integer frequency ratio, ω/Ω.

In Figure 12 it is evident that a significant difference exists between the lift deficiency functions found from fixed wing theory (Theodorsen) and the present theory. This difference is greatest at the low values of k where flutter would occur. This difference remains even with infinite wake spacing due to the decay in the reference wake.

The terms that appear due to decay are ΔF_1, ΔF_2, ΔF_4, ΔF_5, and ΔW. With the decay function

$$f(y) = 1 - e^{-p/y^2}$$

these terms will go to zero as p approaches infinity. Figures 13, 14, and 15 show plots of these functions versus reduced frequency for various decay rates.

Theodorsen: $C(k) = F(k) + iG(k)$

Present Theory: $C_1(k,\mu,\lambda) = F_1(k,\mu,\lambda) + iG_1(k,\mu,\lambda)$

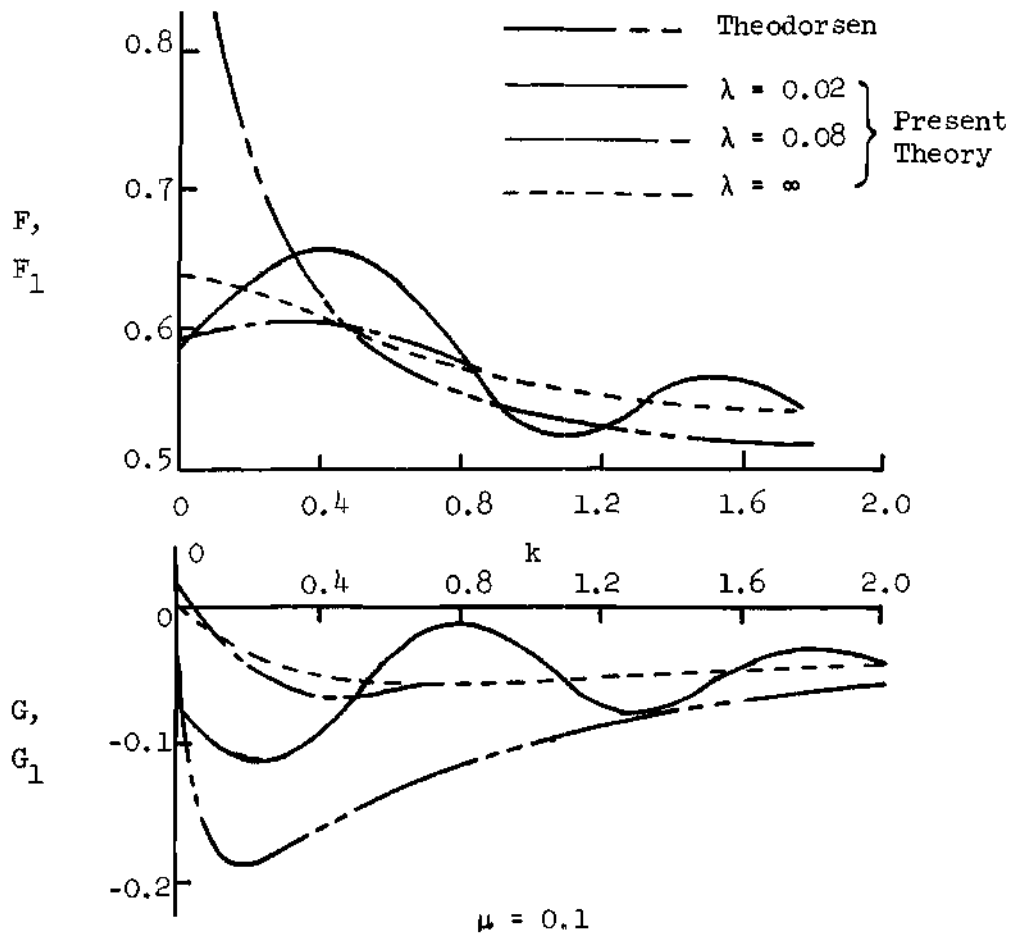

Figure 12. Comparison with Theodorsen.

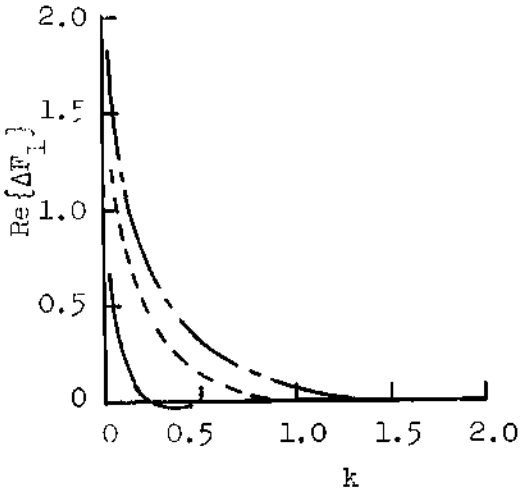

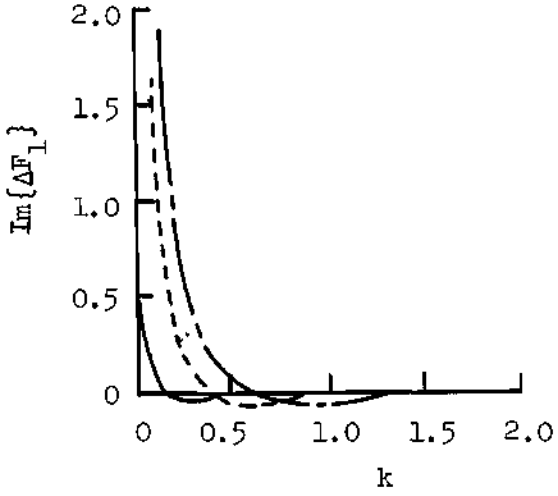

$f(y) = 1 - e^{-p/y^2}$

——— p = 5

– – – – – p = 10

——— p = 100

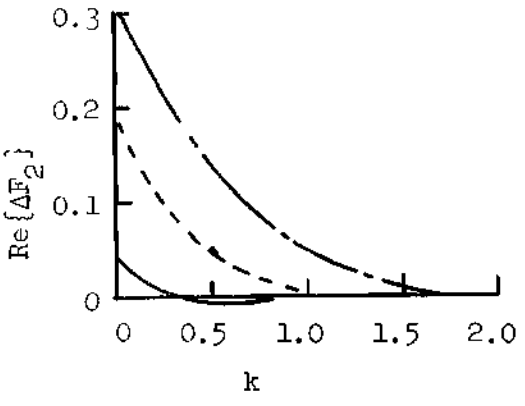

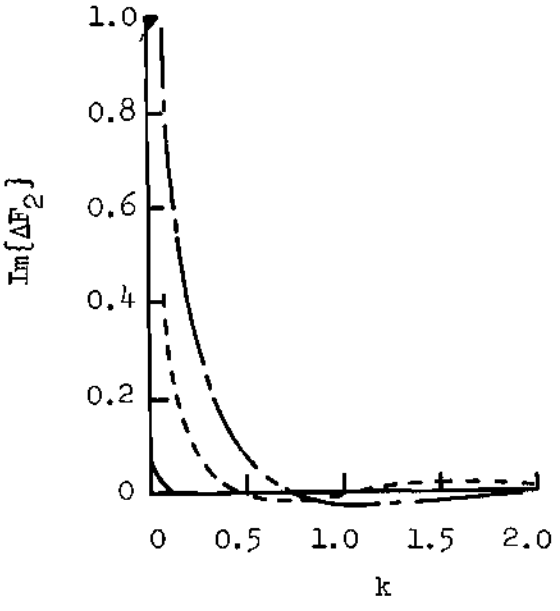

Figure 13. Change in Lift Terms Due to Decay for Various Decay Rates.

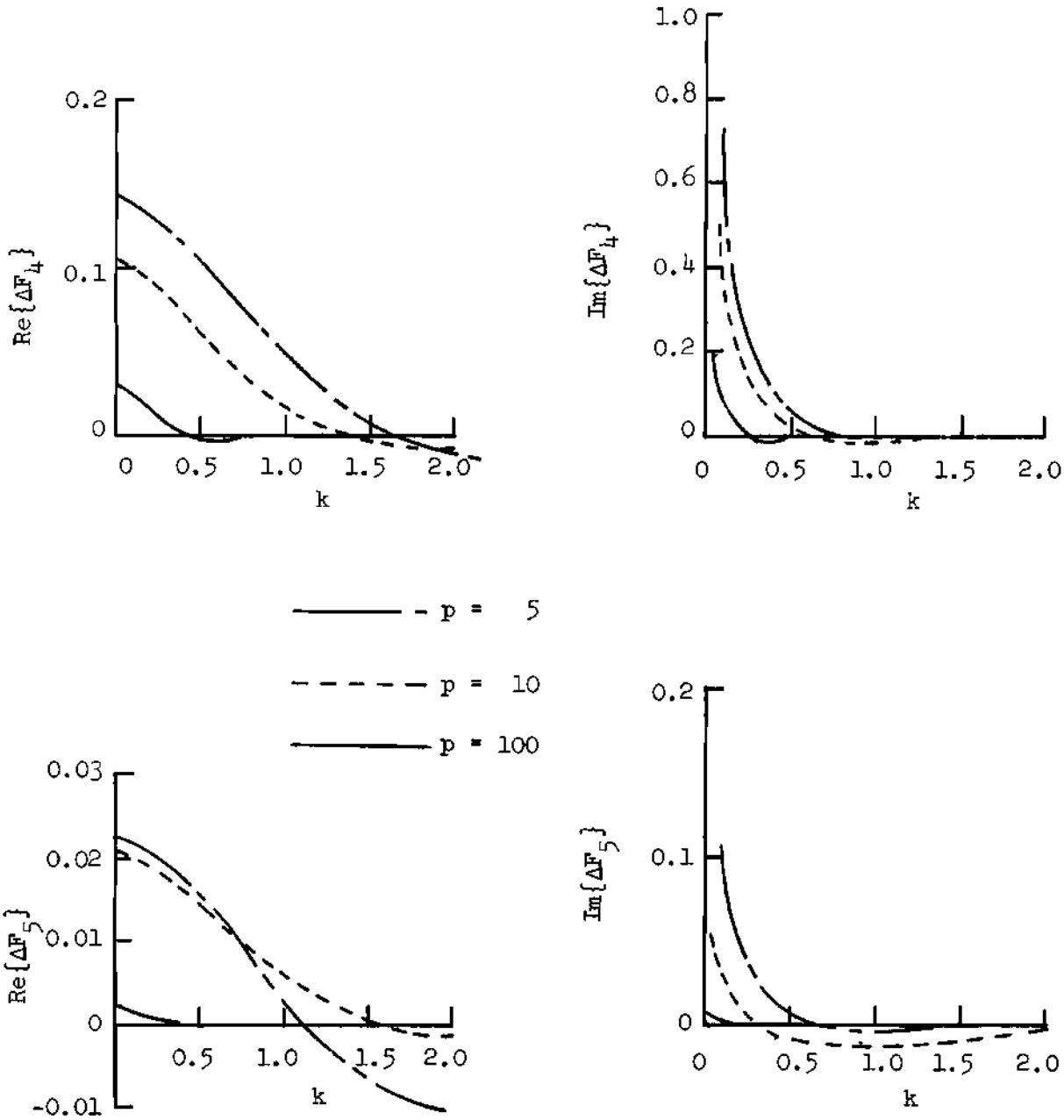

Figure 14. Change in Moment Terms due to Decay for Various Decay Rates.

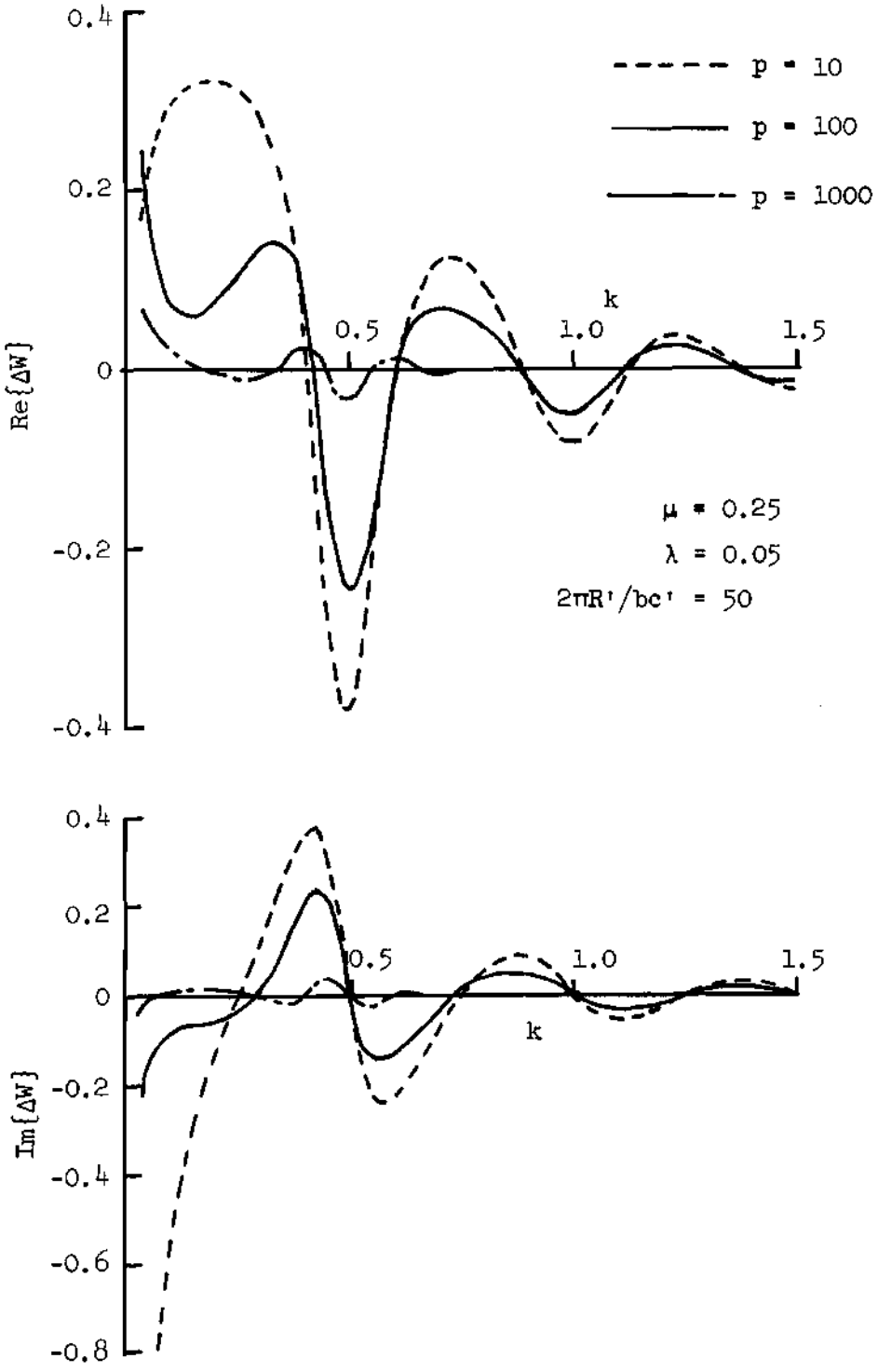

Figure 15. Change in Wake Weighting Function due to Decay for Various Decay Rates.

With no decay, the present lift deficiency function given in equation (35) reduces to

$$C_1(k,\mu,\lambda) = G(k,s,h)\{H_1^{(2)}(k)+2W(k,s,h)J_1(k)\} \tag{70}$$

where now equation (22) reduces to

$$G(k,s,h) = 1/\{H_1^{(2)}(k)+iH_o^{(2)}(k) + 2W(k,s,h)[J_1(k)+iJ_o(k)]\} .$$

By comparison with equation (3), it is evident that the present lift deficiency function yields the same results as Loewy's (1) lift deficiency function if

$$W(k,s,h) = \hat{W}(kh,m)$$

where m is the frequency ratio, ω/Ω. Since

$$W(k,s,h) = 1/(e^{kh}\, e^{-iks} - 1)$$

and

$$\hat{W}(kh,m) = 1/(e^{kh}\, e^{i2\pi m} - 1)$$

for an equivalent single bladed rotor, it is clear that equality will exist between the two wake weighting functions if

$$e^{-iks} = e^{i2\pi m} .$$

Since

$$k = \omega c'/\Omega R'(1+\mu)$$

and

$$s = \mu 2\pi R'/c'$$

for b = 1, this condition can be expressed as

$$\mu/(1+\mu) = N/m - 1 \qquad (71)$$

where N is an integer. In hover, equation (71) requires that the frequency ratio in Loewy's (1) model be an integer. This is to be expected since an integral ratio would make the blade behave in the same way each time it passes $\psi = 90^{\circ}$, as has been assumed here. Equation (71) shows equality for particular non-integral frequency ratios in forward flight. Forward flight in the present model effectively shifts the wakes downstream. The result is a phase difference between wakes that is similar to Loewy's (1) model with non-integral frequency ratio.

If there is no decay and the wake spacing is infinite, then $W(k,s,\infty) = 0$ and, as is evident by comparing equations (70) and (2),

$$C_1(k,s,\infty) = C(k)$$

so that the present lift deficiency function reduces to Theodorsen's (4).

Sample Flutter Analyses

The characteristics of the blade considered in the following cases are given in Table 1 below.

Trends Observed

The velocity-damping plot obtained for a helicopter moving with an advance ratio of 0.3 is shown in Figure 16. This velocity-damping plot is the result of the two-dimensional flutter analysis described in Chapter II applied to the blade segment at the tip of the blade. The damping (g) required for neutral stability is plotted versus total

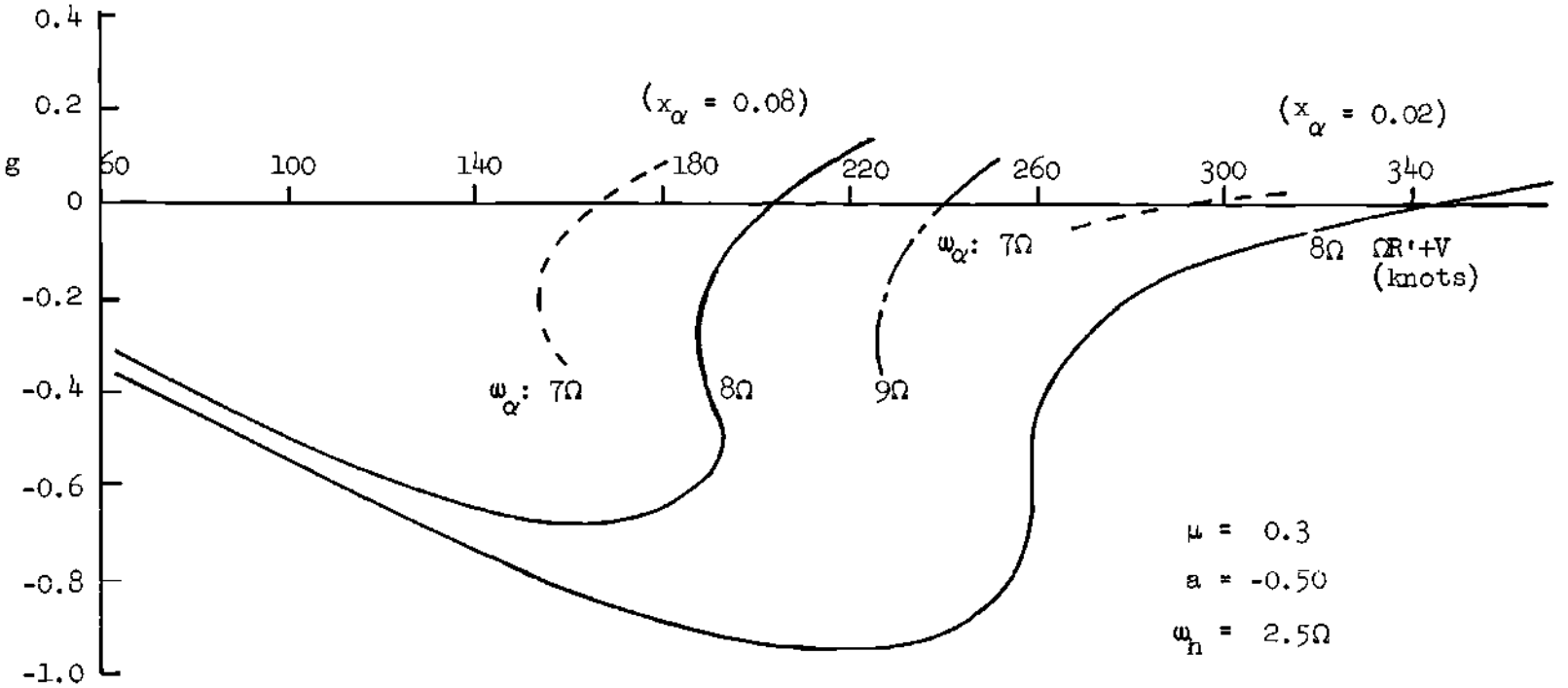

Figure 16. Velocity-Damping Plot.

Table 1. Characteristics of Sample Blade

Parameter	Value
μ	0.016
r_α^2	0.051
a	- 0.50
x_α	0.02, 0.04, 0.08
ω_h/ω_α	0.312
b	5
$2\pi R'/bc'$	51.4

airspeed ($\Omega R'+V$). Plots are shown for the unstable mode for two c.g. locations. As would be expected, the flutter speed decreases as the c.g. is moved aft.

Figure 16 also shows the influence of torsional stiffness. If the torsional frequency was changed due to stiffness so that ω_h/ω_α was 0.357 or 0.278, then a new family of curves would result. Indicated on Figure 16 are portions of these curves where they cross the flutter boundary. It can be seen that the flutter speed increases as the frequency ratio increases.

Figure 17 depicts the influence on flutter speed of the build-up and decay of shed vorticity for several c.g. positions. The influence of advance ratio on the flutter speed decreases as the advance ratio gets larger because the distance between the blade and the center of strength for each shed wake increases with advance ratio. This increased

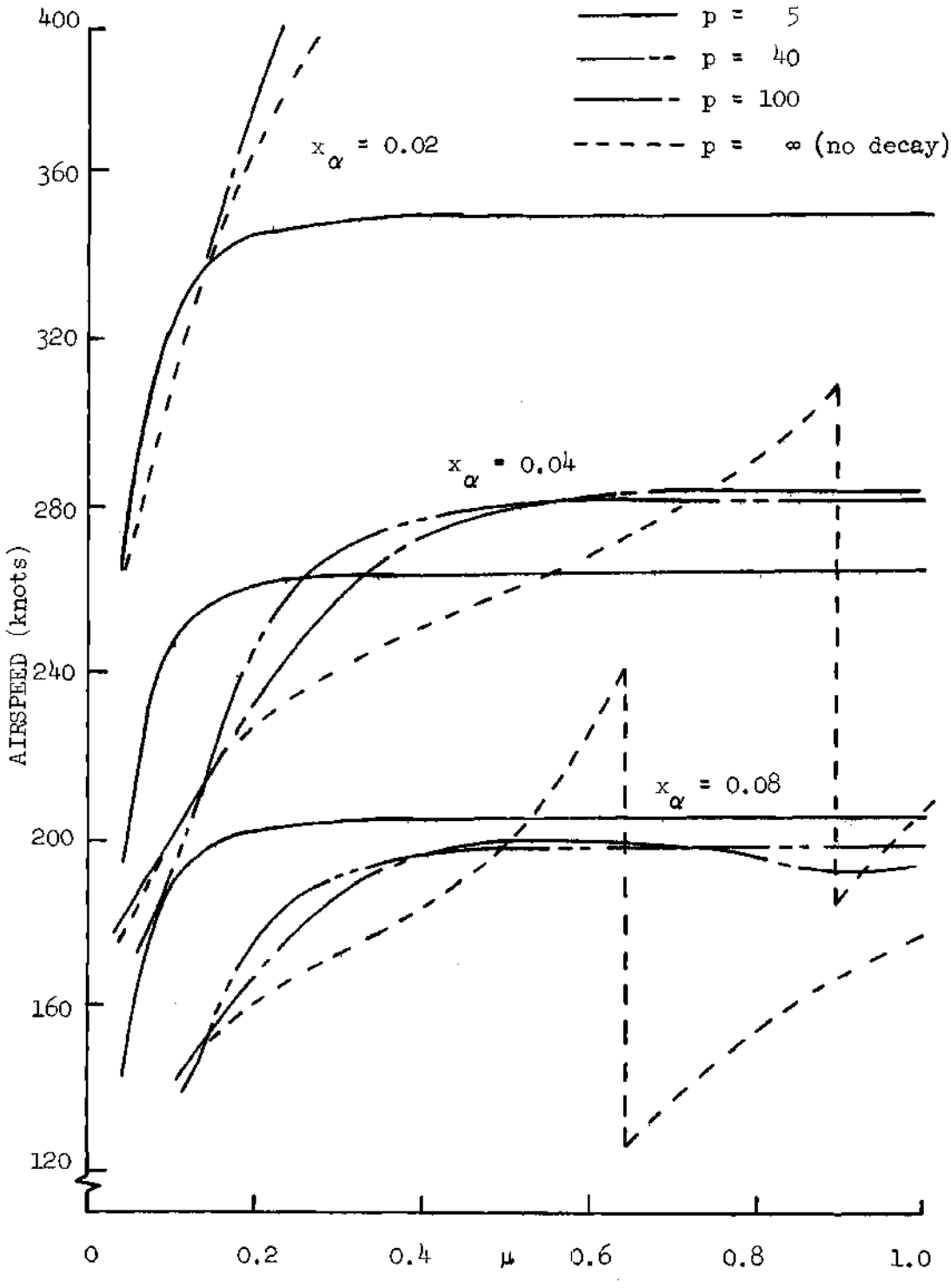

Figure 17. Variation of Flutter Speed with Advance Ratio.

separation can be seen from Figure 9, and it reduces the effect that the wakes have on the flutter speed. With build-up and decay, changes in flutter speed due to advance ratio disappear for advance ratios in excess of 0.3.

Also plotted in Figure 17 is the case where no build-up or decay is introduced. Since the wakes, without this effect, extend infinitely forward and behind the rotor, the vorticity near the rotor will remain at full strength even at very high advance ratios. Thus the advance ratio will only affect phase, and so the flutter speed continues to change with advance ratio.

From the families of curves shown in Figure 17, it can be seen that the flutter is most sensitive to the distance between the elastic axis and the center of gravity. For a given center of gravity location the flutter velocity varies with decay rate as well as advance ratio. The most conservative decay rates will be those that yield the lowest flutter velocity at various advance ratios.

Inflow Variation

If fuselage drag and/or auxiliary lift is included for an analysis of a helicopter then the inflow will vary with advance ratio. The fuselage drag may be given as

$$D = \frac{1}{2} \rho \Omega^2 R'^2 \mu^2 C_D S'_F$$

where S'_F is the frontal area of the fuselage and C_D is its drag coefficient. The auxiliary lift may be given as

$$L = \frac{1}{2} \rho \Omega^2 R'^2 \mu^2 C_L S'$$

where S' is the area of the lifting surface. Both lift and drag will now vary with advance ratio. The amount of tilt necessary from the rotor to overcome drag is given by α_T where

$$\alpha_T = \tan^{-1} \frac{D - T_{aux}}{W - L} \tag{72}$$

where T_{aux} is any auxiliary thrust applied to attain high forward speeds and W is the weight of the aircraft. No auxiliary thrust was considered here, but this thrust would be necessary in order to keep the rotor tilt within bounds when drag increases and the lift approaches the weight of the aircraft as forward speed is increased.

The thrust that is required from the rotor is

$$T = (W - L)/\cos \alpha_T \ .$$

Wheatley (20) showed that the inflow through the rotor can be found from the relation

$$\lambda = \mu \sin \alpha_T + \frac{C_T/2}{(\lambda^2 + \mu^2)^{1/2}} \tag{73}$$

where the thrust coefficient is given by

$$C_T = T/\pi\rho\Omega^2 R'^4 \ .$$

If a weight coefficient is defined as

$$C_W = W/\pi\rho\Omega^2 R'^4$$

and no auxiliary thrust is applied, then the tilt of the tip path plane,

from equation (72), will be

$$\alpha_T = \tan^{-1} \frac{C_D S_F \mu^2}{2C_W - C_L S \mu^2}$$

where

$$S_F = S'_F/\pi R'^2$$

and

$$S = S'/\pi R'^2 .$$

Figure 18 shows the variation of the inflow ratio with advance ratio as obtained from equation (73) for several values of the weight coefficient and no auxiliary lifting surface. A plot of flutter speed versus advance ratio, allowing inflow to vary with forward speed and omitting auxiliary lift, is given in Figure 19.

When auxiliary lift is included the thrust required from the rotor at higher speeds will be decreased. This means that the inflow may decrease with larger advance ratios. This decrease will bring the wakes closer to the rotor vertically while increased forward flight puts their centers of strength further to the rear and the net effect is unpredictable. Without decay no alleviation of the effect of closer wake spacing will occur so that sharp differences will exist between results gained with and without decay. A sample variation of flutter speed with advance ratio with and without decay when drag and auxiliary lift are included is shown in Figure 20. For a given lift coefficient the lift supplied by the auxiliary surfaces could exceed the weight of the aircraft at high advance ratios. The auxiliary lift for Figure 20 was kept below 80% of

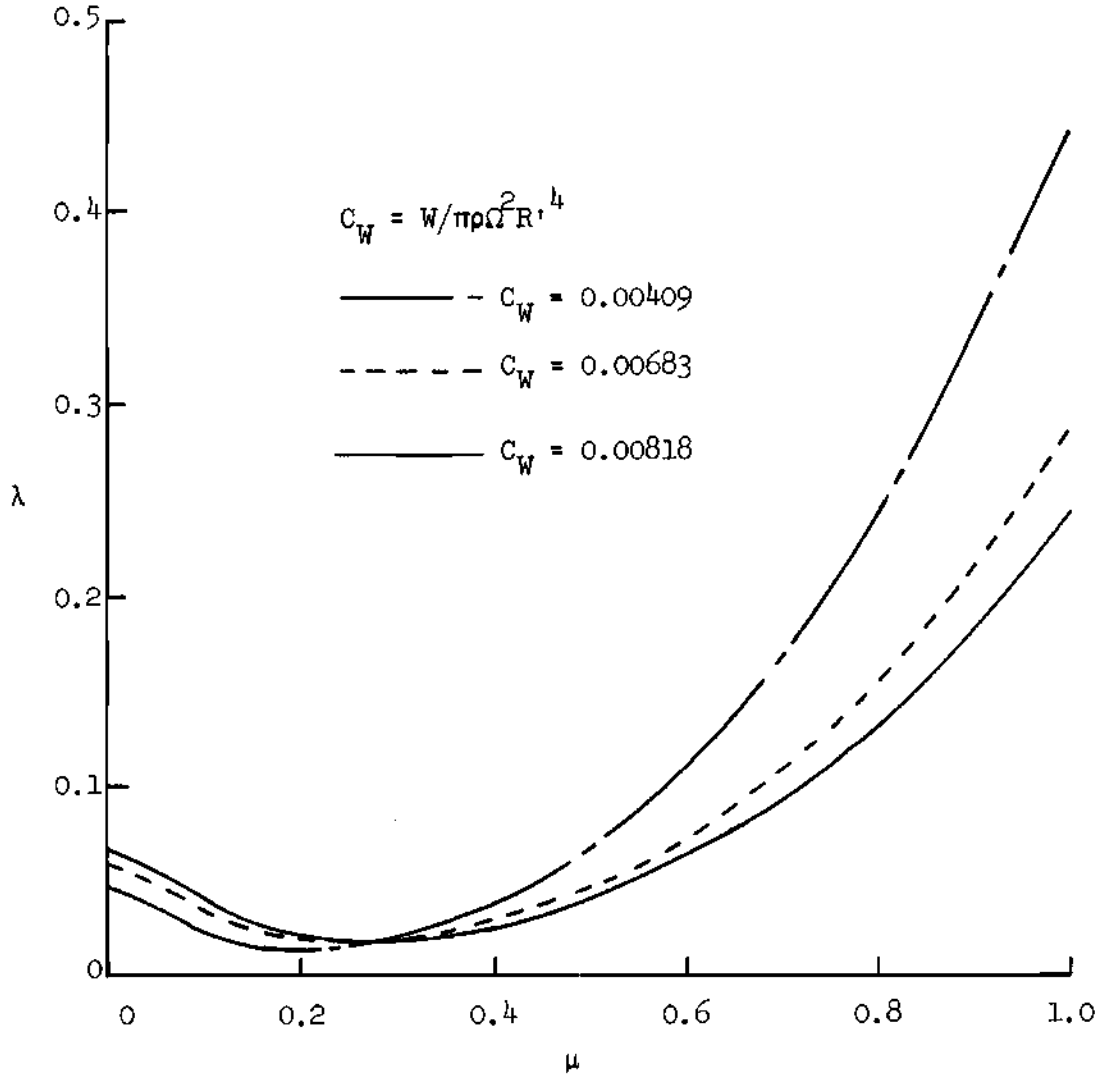

Figure 18. Variation of Inflow with Forward Speed.

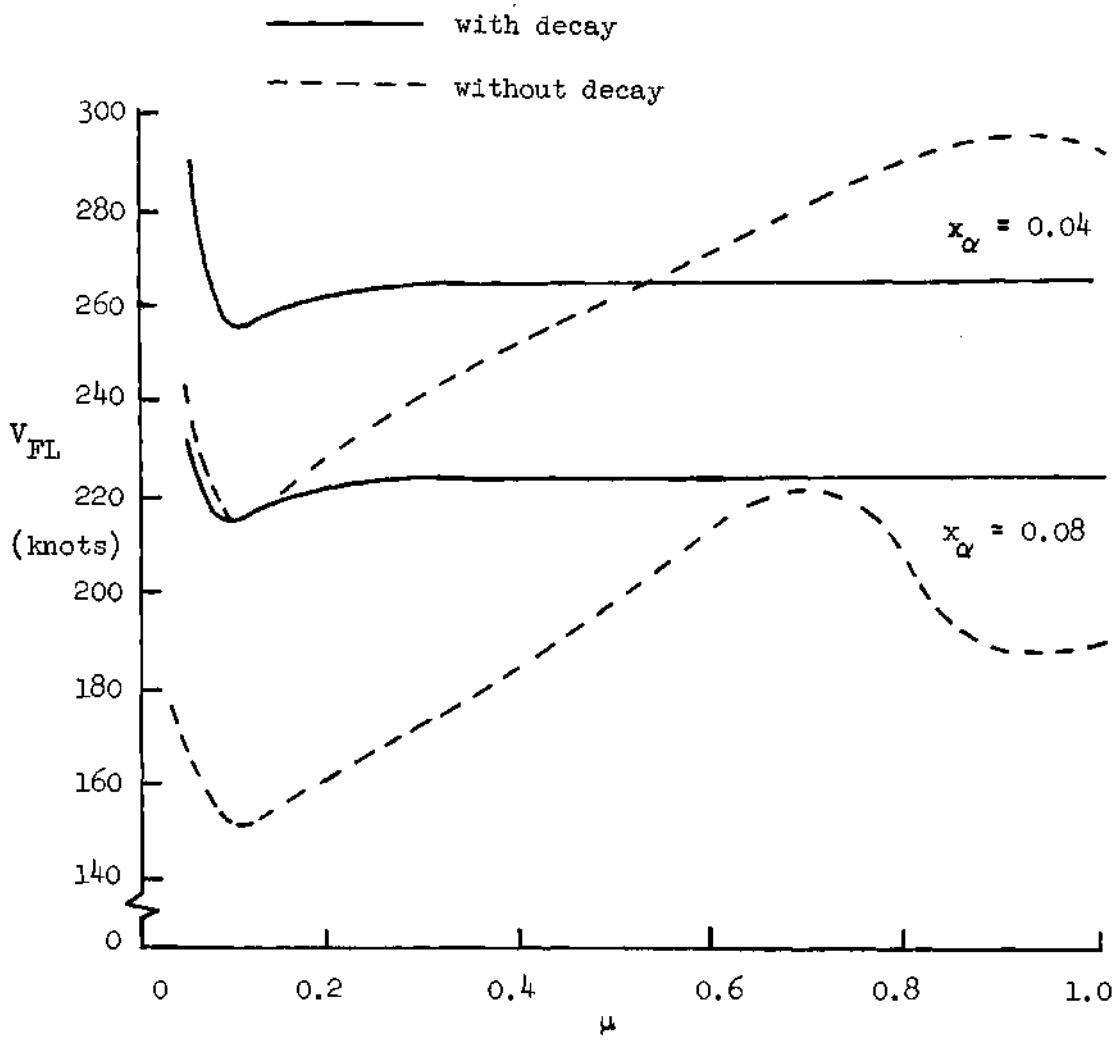

Figure 19. Flutter Speed Variation when Inflow Varies with Advance Ratio -- No Auxiliary Lift.

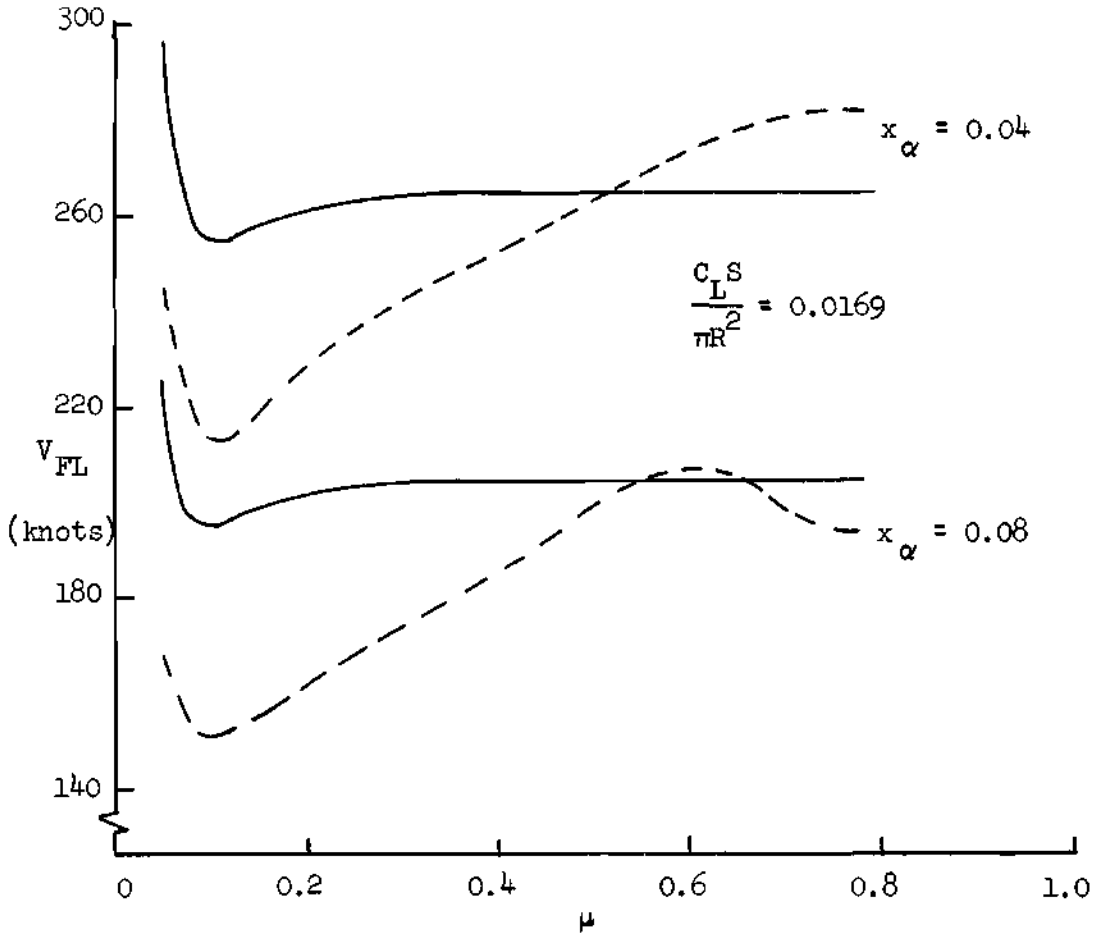

Figure 20. Flutter Speed Variation with Auxiliary Lift.

the weight of the aircraft. Actually, design criteria would produce an upper bound for advance ratio.

Effect of c.g. Location

The relationship of (1) the present theory with build-up and decay of vorticity; (2) the present theory without this effect; and (3) fixed-wing unsteady aerodynamic theory is shown in Figure 21. Plotted is blade segment c.g. position versus flutter speed ($\Omega R' + V$) for a design advance ratio, $\mu = 0.3$. For the case shown there is a crossover of the curves. When the blade c.g. is sufficiently removed from the elastic axis, the case with no decay gives the most conservative results, whereas when the c.g. is near the quarter-chord the most conservative results are those given by the present theory.

If the elastic axis and center of gravity are coincident then $x_\alpha = 0$, and the bending and torsion modes are decoupled. When the elastic axis is at the quarter chord, the bending and torsion terms of the aerodynamic lift and moment coefficients, as shown by equations (52), (61), and (62), are uncoupled. For these conditions flutter does not occur when decay of vorticity is neglected and the elastic axis and c.g. are at the quarter-chord. However, the introduction of the decay function will yield flutter for this case, as shown by Figure 22. It should be noted, however, that with the blade characteristics given in Table 1 and $x_\alpha = 0$, the flutter speed obtained is too high to be of significance in practice. Incompressible potential flow has been used here and so any flutter speeds that exceed a Mach number of about 0.6 should be regarded with caution since Hammond (21) and Jones and Rao (22) found significant differences between compressible and incompressible theory

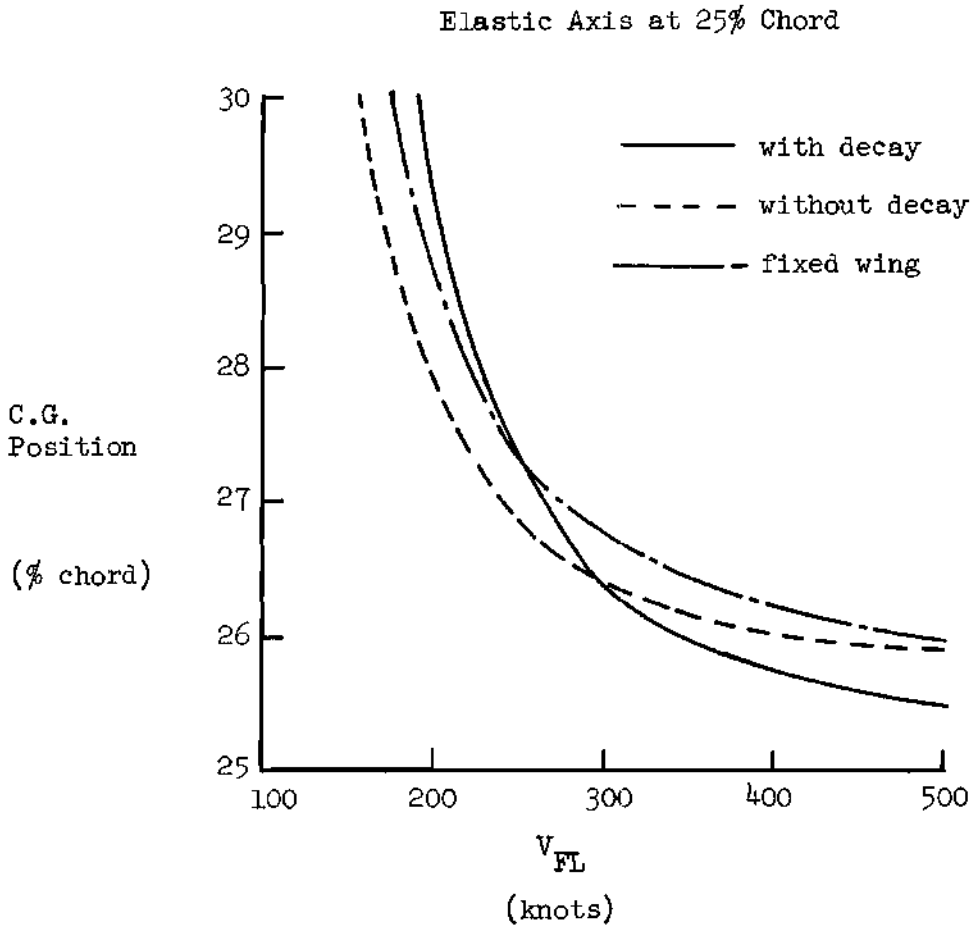

Figure 21. Influence of c.g. Position on Flutter Speed.

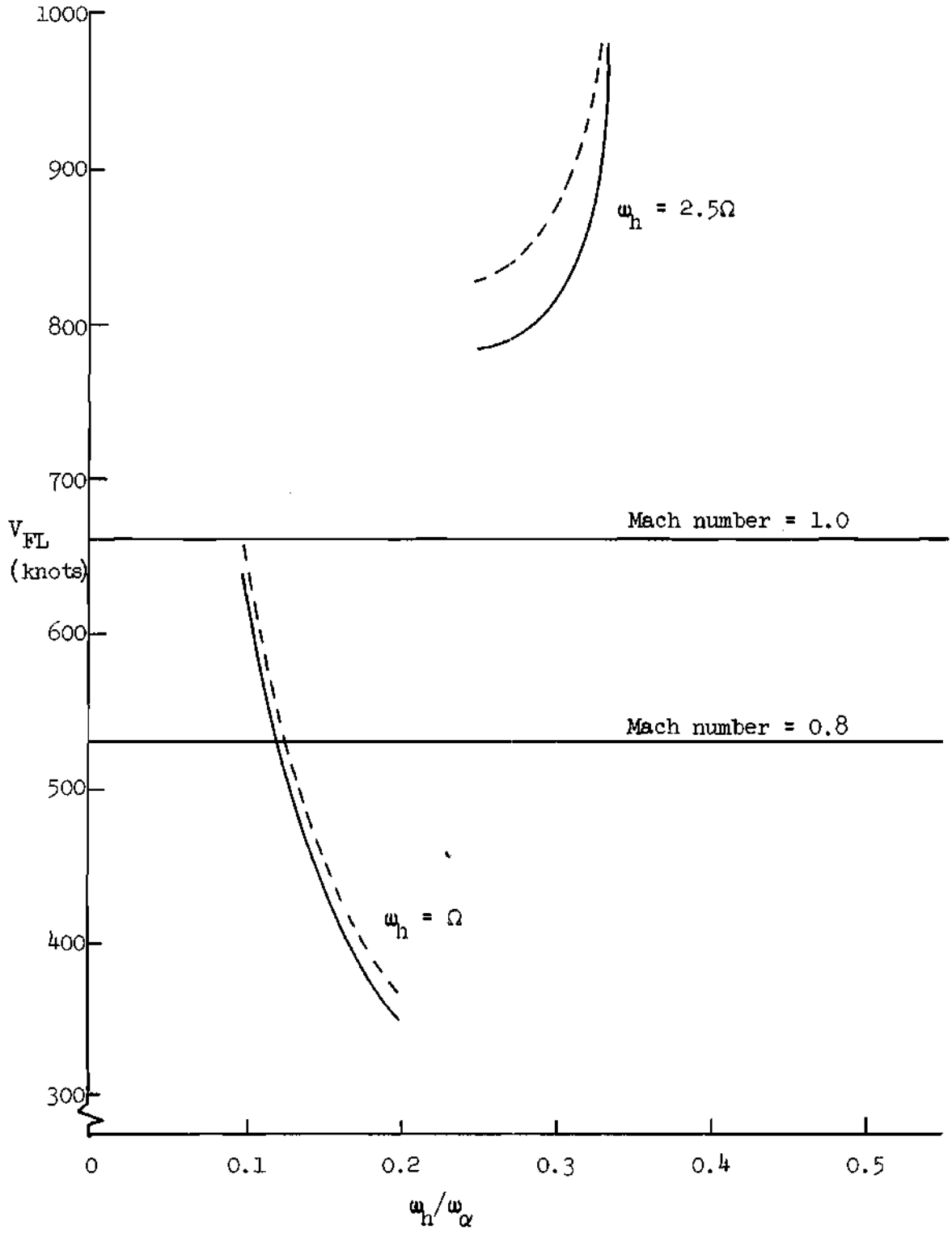

Figure 22. Variation of Flutter Speed with Stiffnes with c.g. and Elastic Axis at the Quarter Chord.

at these higher Mach numbers.

Application to Design

Results of a forward flight flutter analysis can be summarized in a design chart such as given by Figure 23. Plotted is the airspeed of the aircraft versus percent rotor speed.

Figure 23 is constructed by first drawing in the lines of constant advance ratio. Then, with the flutter speed determined for a given advance ratio, the rotor speed which puts the tip at flutter speed is found from

$$V_{FL} = \Omega_{FL} R'(1 + \mu) .$$

The percent rotor speed for flutter is computed from

$$\frac{\Omega_{FL}}{\Omega} = \frac{V_{FL}}{\Omega R'(1 + \mu)} .$$

The point for this percent rotor speed is now marked on the appropriate advance ratio line, and connecting these points for various advance ratios defines the flutter boundary.

For a compound helicopter in which rotor load and rotor speeds can be reduced at higher advance ratios, the tip speed can be kept below the flutter speed by decreasing rotor speed as airspeed increases. The chart shows the safe operating region for the helicopter. With such a chart the pilot can readily determine what the maximum allowable rotor speed is for a given airspeed, or what airspeed can be attained with a given rotor speed.

The lower part of the flutter boundary curves in Figure 23

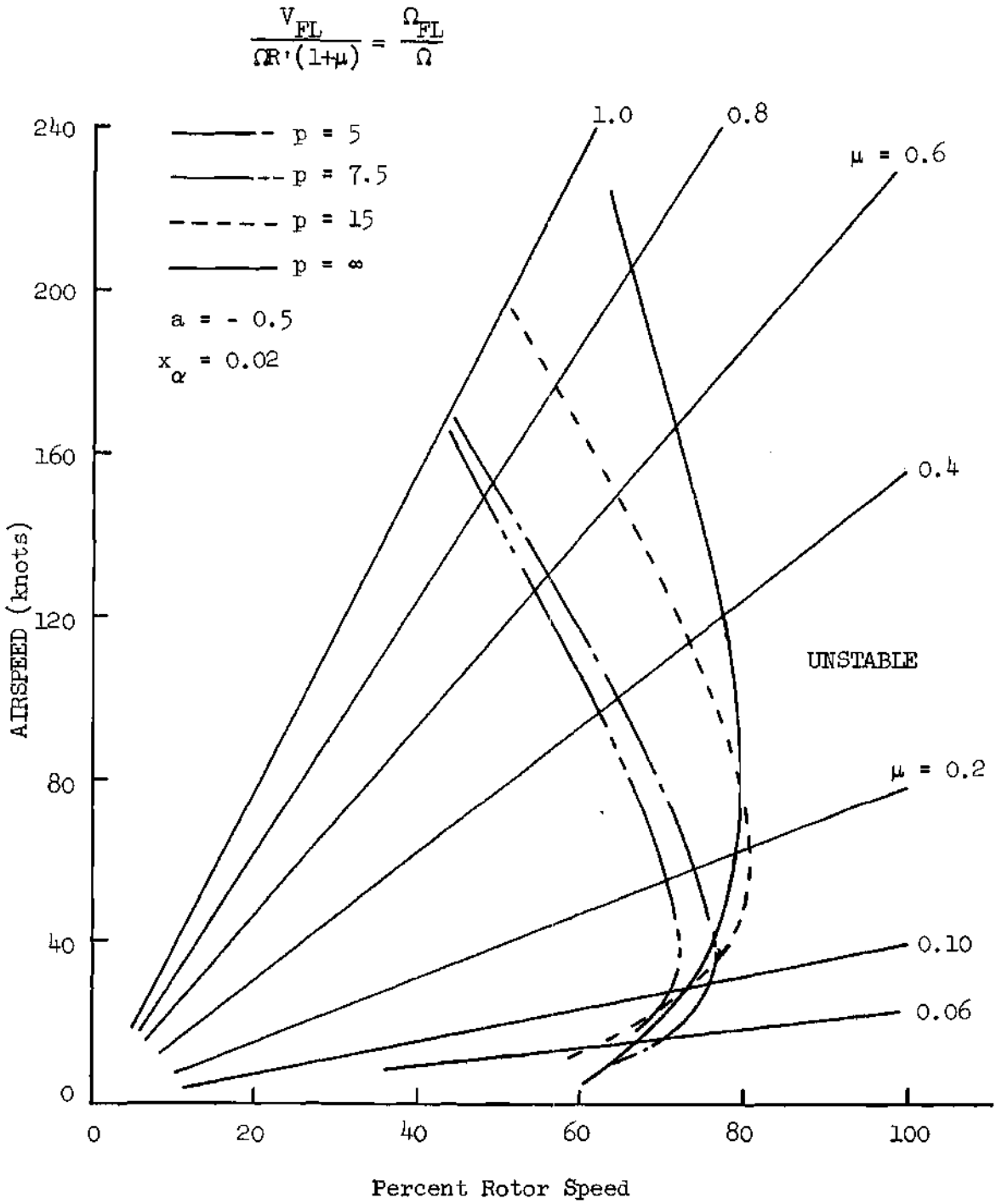

Figure 23. Flutter Boundary for Various Decay Rates.

indicates that a reduction in rotor speed is required for the sample problem at low advance ratios. This is due to the grouping of rotor wakes at these low speeds. Within this region there would be a transition between the forward flight theory presented here and that of Loewy (1). The decay rate will be low for low advance ratios and so various decay rates might be applied to the lower portion of Figure 23 in order to more accurately fit it to the true physical case. However, this concept can not be extended too far since very low advance ratios will produce a decay rate that does not make the motion completely die out during a blade revolution. In this case each blade will not necessarily behave the same each time it passes $\psi = 90^{\circ}$ and this contradicts a basic assumption of the present theory. The present theory puts all of the wakes in phase with each other in hover and the resulting low flutter speed would be misleading in general. For the particular cases where the flutter frequency is an integral or half integral multiple of the rotor speed the wakes will indeed be in phase. In this case, the aerodynamic damping does drop sharply near integral frequency ratios as shown by Loewy's (1) work and at half integral ratios by experiments run by Daughaday, DuWaldt, and Gates (11).

CHAPTER IV

CONCLUSIONS AND RECOMMENDATIONS

A method for determining rotor blade flutter in forward flight has been developed. Two-dimensional incompressible unsteady aerodynamic theory is used and the shed vorticity both in and below the plane of the rotor is accounted for. The influence of wake build-up and decay, wake spacing, and chordwise location of the blade center of gravity on the flutter speed were investigated. Finally, a possible application to helicopter design has been presented.

Conclusions

From the results obtained in this study, it can be concluded that:

1. A flutter analysis has been developed which is valid for any decay function that satisfies the conditions

$$f(0) = 1 \qquad f'(0) = 0$$

$$f(1) = 1 - \delta \qquad f'(1) = \epsilon$$

$$f(\infty) = 0 \qquad f'(\infty) = 0$$

where δ and ϵ are small. The approximate technique for evaluating the integrals over the reference wake must be used for decay functions in general. Comparison with exact results using the decay function

$$f(y) = 1 - e^{-p/y^2}$$

showed the approximate technique to be good to five decimal places except

for very low values of reduced frequency in the case of ΔF_5.

2. The wakes and decay function significantly alter the lift deficiency function, especially at low values for the reduced frequency where flutter occurs. The flutter speed is lowered by inclusion of both wakes and the decay function.

3. As is typical in flutter in general, the flutter speed dropped when the center of gravity was moved aft.

4. The variation of flutter speed with advance ratio and inflow ratio followed trends that are consistent with the variation of the wake geometry with μ and λ. With build-up and decay the wakes that were shed previously became too far removed from the blade to effect the flutter speed when the advance ratio increased beyond about 0.3.

Recommendations

It is recommended that

1. Wind tunnel tests on a model that consists of a nonlifting rotating beam with an airfoil panel at the tip could be run. The center of gravity for this panel should be adjustable so that the flutter speed can be reduced to values that are attainable by the model and tunnel. Information might be gained from such tests that would show the azimuth region in which flutter occurred.

2. Other decay functions should be applied to the theoretical analysis so that meaningful comparisons could be made between theory and any experimental results that become available.

3. In order to account for the entire rotor blade, this analysis should be expanded to three dimensions by applying the two dimensional

aerodynamics given here to radial strips along the rotor blade and using blade modes for vibration analysis.

APPENDIX A

EVALUATION OF PRESSURE IN TERMS OF DOWNWASH

The pressure in terms of the local bound vorticity is given in equation (24) as

$$-\frac{\Delta\bar{p}(x^*)}{\rho U c'} = \bar{\gamma}_a(x^*) + ik\int_{-1}^{x^*}\bar{\gamma}_a(x)\,dx\ . \tag{A-1}$$

Equation (20) gives the local bound vorticity in terms of the downwash along the chord. Thus, substituting equation (20) into equation (A-1) will yield the pressure in terms of the downwash. Integrating the vorticity equation (20) from -1 to x^* and then changing the order of integration yields

$$\frac{\pi}{2}\int_{-1}^{x^*}\bar{\gamma}_a(x)\,dx = \int_{-1}^{1}\sqrt{\frac{1+\xi}{1-\xi}}\,\bar{v}_a(\xi)\int_{-1}^{x^*}\sqrt{\frac{1-x}{1+x}}\,\frac{dx}{x-\xi}\,d\xi$$

$$+\frac{ik\bar{\Gamma}_a}{2\pi}\int_{1}^{\infty}\left[f(y) - \frac{1}{ik}\frac{df}{dy}\right]e^{-iky}\int_{-1}^{x^*}\sqrt{\frac{1-x}{1+x}}\int_{-1}^{1}\sqrt{\frac{1+\xi}{1-\xi}}\,\frac{d\xi\,dx\,dy}{(x-\xi)(y-\xi)}$$

$$+\frac{k\bar{\Gamma}_a}{2}(W+\Delta W)\int_{-1}^{1}\sqrt{\frac{1+\xi}{1-\xi}}\ e^{-ik\xi}\int_{-1}^{x^*}\sqrt{\frac{1-x}{1+x}}\,\frac{1}{x-\xi}\,dx\,d\xi\ . \tag{A-2}$$

The first and third terms of equation (A-2) can be evaluated by using the following relation:

$$\int_{-1}^{x^*} \sqrt{\frac{1-x}{1+x}}\,\frac{dx}{x-\xi} = -\left[\frac{\pi}{2} + \sin^{-1} x^* + \sqrt{\frac{1-\xi}{1+\xi}}\,\Omega_1(x^*,\xi)\right]$$

where $\Omega_1(x^*,\xi)$ is given by equation (29).

For the second term note that

$$\frac{1}{x-\xi}\,\frac{1}{y-\xi} = \frac{1}{y-x}\left[\frac{1}{x-\xi} - \frac{1}{y-\xi}\right] .$$

Thus,

$$\int_{-1}^{1} \sqrt{\frac{1+\xi}{1-\xi}}\,\frac{d\xi}{(x-\xi)(y-\xi)} = \frac{\pi}{x-y}\sqrt{\frac{y+1}{y-1}} .$$

Finally, the second term of equation (A-2) becomes

$$\int_{-1}^{x^*} \sqrt{\frac{1-x}{1+x}} \int_{-1}^{1} \sqrt{\frac{1+\xi}{1-\xi}}\,\frac{d\xi}{(x-\xi)(y-\xi)}$$

$$= -\pi\sqrt{\frac{y-1}{y+1}}\left[\frac{\pi}{2} + \sin^{-1} x^* + \sqrt{\frac{y-1}{y+1}}\,\Omega_2(x^*,y)\right]$$

where $\Omega_2(x^*,y)$ is given by equation (27).

Putting these relations into equation (A-2) yields

$$\frac{\pi}{2}\int_{-1}^{x^*} \bar{\gamma}_a(x)dx = -\int_{-1}^{1}\left[\sqrt{\frac{1+\xi}{1-\xi}}\left(\frac{\pi}{2} + \sin^{-1}x^*\right) + \Omega_1(x^*,\xi)\right]\bar{v}_a(\xi)d\xi$$

$$-\frac{ik\bar{\Gamma}_a}{2}\int_{1}^{\infty}\left[f(y) - \frac{1}{ik}\frac{df}{dy}\right]\left[\sqrt{\frac{y+1}{y-1}}\left(\frac{\pi}{2} + \sin^{-1}x^*\right)\right.$$

$$\left. + \Omega_2(x^*,y)\right]e^{-iky}\,dy - \frac{k\bar{\Gamma}_a}{2}(W + \Delta W)\int_{-1}^{1} e^{-ik\xi}\left[\sqrt{\frac{1+\xi}{1-\xi}}\left(\frac{\pi}{2}\right.\right.$$

$$+ \sin^{-1}x^*\Big) + \Omega_1(x^*,\xi)\Big]d\xi \ . \qquad \text{(A-3)}$$

Now, note that $\Omega_1(1,\xi) = 0$ and that $\Omega_2(1,y) = -\pi$. Thus, by making $x^* = 1$ in equation (A-3), it is immediately obvious that

$$\frac{1}{2}\bar{\Gamma}_a e^{-ik} = -\int_{-1}^{1}\sqrt{\frac{1+\xi}{1-\xi}}\,\bar{v}_a(\xi)d\xi$$

$$-\frac{ik\bar{\Gamma}_a}{2}\int_1^\infty\left[f(y) - \frac{1}{ik}\frac{df}{dy}\right]\left[\sqrt{\frac{y+1}{y-1}} - 1\right]e^{-iky}\,dy$$

$$-\frac{k\bar{\Gamma}_a}{2}(W + \Delta W)\int_{-1}^{1} e^{-ik\xi}\sqrt{\frac{1+\xi}{1-\xi}}\,d\xi \ . \qquad \text{(A-4)}$$

So, subtracting $\left(\frac{\pi}{2} + \sin^{-1}x^*\right)$ times equation (A-4) from equation (A-3) yields

$$\frac{\pi}{2}\int_{-1}^{x^*}\bar{\gamma}_a(x)dx = \frac{1}{2}\bar{\Gamma}_a e^{-ik\left(\frac{\pi}{2} + \sin^{-1}x^*\right)} - \int_{-1}^{1}\Omega_1(x^*,\xi)\bar{v}_a(\xi)d\xi$$

$$-\frac{ik\bar{\Gamma}_a}{2}\int_1^\infty\left[f(y) - \frac{1}{ik}\frac{df}{dy}\right]\left[\Omega_2(x^*,y) + \frac{\pi}{2} + \sin^{-1}x^*\right]e^{-iky}\,dy$$

$$-\frac{k\bar{\Gamma}_a}{2}(W + \Delta W)\int_{-1}^{1} e^{-ik\xi}\,\Omega_1(x^*,\xi)d\xi \ . \qquad \text{(A-5)}$$

Finally, substituting the vorticity relation shown in equations (20) and (A-5) into the pressure equation (A-1) and combining terms yields

$$-\frac{\Delta\bar{p}(x^*)}{\rho U c'}\frac{\pi}{2} = \int_{-1}^{1}\left[\sqrt{\frac{1-x^*}{1+x^*}}\sqrt{\frac{1+\xi}{1-\xi}}\frac{1}{x^*-\xi} - ik\,\Omega_1(x^*,\xi)\right]\bar{v}_a(\xi)d\xi$$

$$+\frac{ik\bar{\Gamma}_a}{2}\sqrt{\frac{1-x^*}{1+x^*}}\int_1^\infty (f-f'/ik)e^{-iky}\left[\sqrt{\frac{y+1}{y-1}}\frac{1}{x^*-y} - ik\sqrt{\frac{1+x^*}{1-x^*}}\left(\Omega_2(x^*,y)\right.\right.$$

$$\left.\left.+\frac{\pi}{2}+\sin^{-1}x^*\right)\right]dy + \frac{k\bar{\Gamma}_a}{2}(W+\Delta W)\sqrt{\frac{1-x^*}{1+x^*}}\int_{-1}^{1} e^{-ik\xi}\left[\sqrt{\frac{1+\xi}{1-\xi}}\frac{1}{x^*-\xi}\right.$$

$$\left.- ik\sqrt{\frac{1+x^*}{1-x^*}}\,\Omega_1(x^*,\xi)\right]d\xi + \frac{1}{2}ik\bar{\Gamma}_a\, e^{-ik}\left(\frac{\pi}{2}+\sin^{-1}x^*\right) . \qquad \text{(A-6)}$$

The second integral and final term of equation (A-6) can be combined if a function $F(k,x^*)$ is defined to be

$$F(k,x^*) = -\frac{2}{\pi}\int_1^\infty (f - f'/ik)e^{-iky}\left[\sqrt{\frac{y+1}{y-1}}\frac{1}{x^*-y}\right.$$

$$\left.- ik\sqrt{\frac{1+x^*}{1-x^*}}\left(\Omega_2(x^*,y)+\frac{\pi}{2}+\sin^{-1}x^*\right)\right]dy$$

$$-\frac{2}{\pi}\sqrt{\frac{1+x^*}{1-x^*}}\,e^{-ik}\left(\frac{\pi}{2}+\sin^{-1}x^*\right) . \qquad \text{(A-7)}$$

Equation (A-7) can be simplified by integrating two pieces of it by parts. Since the decay function and its first derivative are zero at infinity, the last term of equation (A-7) cancels with the $\left(\frac{\pi}{2}+\sin^{-1}x^*\right)$ term in the integrand after integration by parts. Since $\Omega_2(x^*,1) = 0$ and

$$\frac{\partial\Omega_2(x^*,y)}{\partial y} = \sqrt{\frac{1-x^*}{1+x^*}}\left[\frac{1}{\sqrt{y^2-1}}+\sqrt{\frac{y+1}{y-1}}\frac{1}{x^*-y}\right]$$

equation (A-7) reduces to

$$F(k,x^*) = iH_0^{(2)}(k) + \Delta F_1(k) + \sqrt{\frac{1+x^*}{1-x^*}}\, F_1(k,x^*) \qquad \text{(A-8)}$$

where $F_1(k,x^*)$ and $\Delta F_1(k)$ are given by equations (26) and (28) respectively.

The third integral of the pressure equation (A-6) can be evaluated by integrating by parts. Since

$$\frac{\partial \Omega_1(x^*,\xi)}{\partial \xi} = \sqrt{\frac{1-x^*}{1+x^*}}\sqrt{\frac{1+\xi}{1-\xi}}\left(\frac{1}{1+\xi} + \frac{1}{x^*-\xi}\right),$$

the terms involving the $1/(x^*-\xi)$ factor in this third integral cancel, leaving

$$-\int_{-1}^{1} e^{-ik}\sqrt{\frac{1+\xi}{1-\xi}}\,\frac{1}{1+\xi}\,d\xi = -\int_0^{\pi} e^{-ik\cos\varphi}\,d\varphi$$

$$= -\pi J_0(k) \quad . \qquad \text{(A-9)}$$

Applying equations (A-7) and (A-9) as evaluations of all of the terms of equation (A-6) except the first integral simplifies equation (A-6) to

$$-\frac{\Delta\bar{p}(x^*)}{\rho U c'}\,\frac{\pi}{2} = \int_{-1}^{1}\left[\sqrt{\frac{1-x^*}{1+x^*}}\sqrt{\frac{1+\xi}{1-\xi}}\,\frac{1}{x^*-\xi} - ik\Omega_1(x^*,\xi)\right]\bar{v}_a(\xi)\,d\xi$$

$$+\frac{1}{2}\,\pi\, ik\bar{\Gamma}_a\sqrt{\frac{1-x^*}{1+x^*}}\left[\frac{1}{2}\,F(k,x^*) + i\,J_0(k)(W+\Delta W)\right]$$

which is the pressure equation in terms of the downwash.

Substituting equation (21) as the relation for the total bound vorticity and equation (A-8) into this last equation yields the final form for the equation for the pressure difference across the airfoil:

$$-\frac{\Delta\bar{p}(x^*)}{\rho U c'}\frac{\pi}{2} = \int_{-1}^{1}\left[\sqrt{\frac{1-x^*}{1+x^*}}\sqrt{\frac{1+\xi}{1-\xi}}\frac{1}{x^*-\xi} - ik\Omega_1(x^*,\xi)\right]\bar{v}_a(\xi)d\xi$$

$$+ G(k,s,h)\left\{\left[iH_0^{(2)}(k) + \Delta F_1(k) + 2i(W+\Delta W)J_0(k)\right]\sqrt{\frac{1-x^*}{1+x^*}}\right.$$

$$\left. + F_1(k,x^*)\right\}\int_{-1}^{1}\sqrt{\frac{1+\xi}{1-\xi}}\,\bar{v}_a(\xi)d\xi\ .$$

APPENDIX B

NUMERICAL INTEGRATION

The integrals which comprise the effect of the decay function on the lift deficiency function are given by equations (28), (23), (32), and (38). Each of these integrals are combinations of the integrals

$$\begin{Bmatrix} I_1 \\ I_2 \end{Bmatrix} = \int_1^\infty (f - f'/ik) \frac{e^{-iky}}{\sqrt{y^2-1}} \begin{Bmatrix} 1 \\ y \end{Bmatrix} dy \tag{B-1}$$

and

$$\begin{Bmatrix} I_3 \\ I_4 \end{Bmatrix} = \int_1^\infty (f' - f''/ik)\ (y - \sqrt{y^2-1})e^{-iky} \begin{Bmatrix} 1 \\ y \end{Bmatrix} dy\ . \tag{B-2}$$

These integrals are easily seen to be of the form

$$I_5 = \int_1^\infty \frac{f(y)}{\sqrt{y^2-1}} \sin ky\ dy \tag{B-3}$$

and

$$I_6 = \int_1^\infty \frac{df(y)}{dy}\ (y - \sqrt{y^2-1}) \sin ky\ dy\ . \tag{B-4}$$

Integrals I_5 and I_6 will now be examined in order to study the approach used in obtaining the approximate value of integrals I_1, I_2, I_3, and I_4.

For a decay function of $f(y) = 1 - e^{-5/y^2}$, the integrand of I_5, and its amplitude, is plotted in Figure 24-a and the integrand of I_6 appears in Figure 24-b. The reduced frequency is 0.5 in these figures. In order to consider integrals of the form I_5 and I_6, the more general integral

$$\int_1^\infty A(y) \sin ky \, dy$$

will be discussed. It is convenient at this point to assume that k is less than $\pi/2$ so that $\pi/2k$ will be greater than 1. In this case the infinite integrals can be split up into cycles such that

$$\int_1^\infty A(y) \sin ky \, dy = \int_1^{\pi/2k} A(y) \sin ky \, dy + \int_{\pi/2k}^{2\pi/k} A(y) \sin ky \, dy$$

$$+ \sum_{N=1}^{M-1} \int_{2N\pi/k}^{2(N+1)\pi/k} A(y) \sin ky \, dy + \int_{2M\pi/k}^{\infty} A(y) \sin ky \, dy \quad \text{(B-5)}$$

where the integer M is such that $2M\pi$ is large enough so that an accurate estimate of the last integral may be obtained by means of asymptotic series. The first integral on the right side of equation (B-5) will be handled by a transformation and application of Simpson's rule to the transformed integral. The second integral, which represents the unfinished portion of the first cycle, and all of the cycles appearing in the summation will be handled by Simpson's rule using judicious choices for the points at which the integrand is evaluated.

Initial Integration

The term $\sqrt{y^2-1}$ appears in each of the integrands for I_1, I_2, I_3,

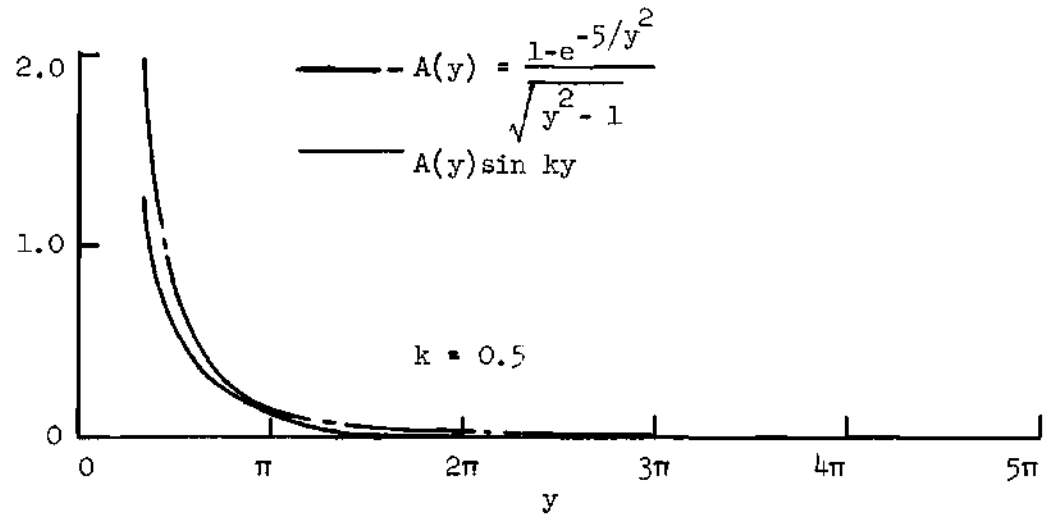

Figure 24a. Integrand for Integral I_5.

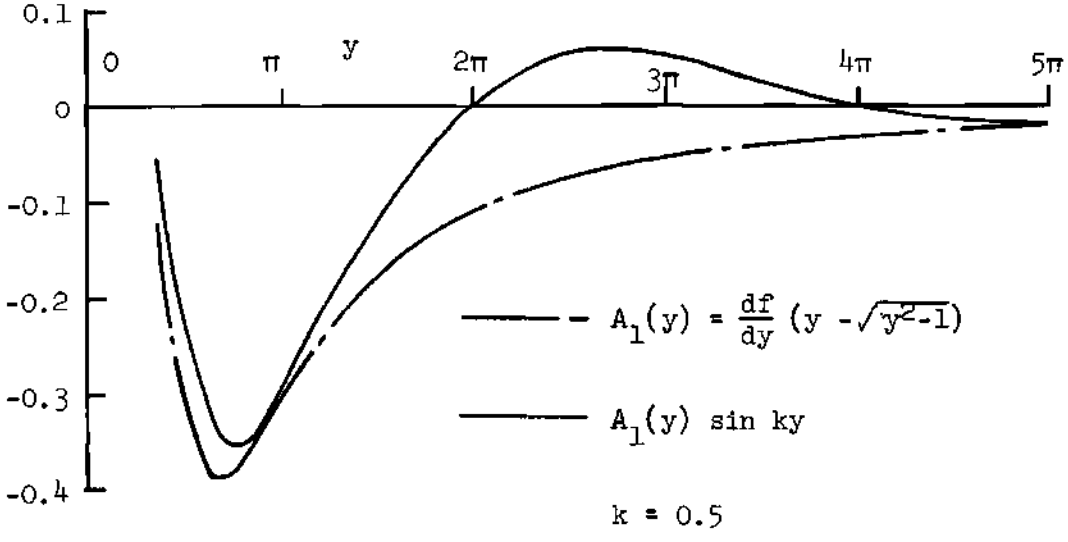

Figure 24b. Integrand for Integral I_6.

and I_4 and this term suggests the transformation $\cosh \varphi = y$. For the integral in Equation (B-3) the first integral on the right hand side of Equation (B-5), with this transformation, will be

$$\int_1^{\pi/2k} \frac{f(y)}{\sqrt{y^2-1}} \sin ky \, dy$$

$$= \int_0^{\cosh^{-1}(\pi/2k)} f(\cosh \varphi) \sin (k \cosh \varphi) d\varphi \qquad \text{(B-6)}$$

and for Equation (B-6) it will be

$$\int_1^{\pi/2k} \frac{df(y)}{dy} (y - \sqrt{y^2-1}) \sin ky \, dy$$

$$= \int_0^{\cosh^{-1}(\pi/2k)} \frac{df(\cosh \varphi)}{d(\cosh \varphi)} \frac{1}{2}(1-e^{-2\varphi}) \sin(k \cosh \varphi) d\varphi. \qquad \text{(B-7)}$$

For I_5 the transformation $y = \cosh \varphi$ as given in Equation (B-6) was necessary in order to obtain an integrand with no singularity. This same transformation produces no advantage that is immediately apparent from equation (B-7), but it did produce markedly better results in the computation of integrals I_3 and I_4. This improvement over the values obtained using the integrand on the left side of equation (B-7) is due to the fact that with $y = \cosh \varphi$,

$$dy = \sinh \varphi \, d\varphi \, .$$

Thus, with $d\varphi$ constant (as required by Simpson's rule) the step size which is taken, in effect, on y is reduced near $y=1$ (i.e. $\varphi=0$). This

reduced step size is shown in Figure 25 and it is clear from these figures that in the region where the integrands are the largest and change the most quickly, the integration points are spaced the closest.

The singularity at y = 1 that exists in Equation (B-3) could have been eliminated by writing

$$\frac{f(y)}{\sqrt{y^2-1}} = \frac{f(y) - f(1)}{\sqrt{y^2-1}} + \frac{f(1)}{\sqrt{y^2-1}} \quad . \tag{B-8}$$

The first term on the right hand side of Equation (B-8) is finite when y is near 1 and is in fact zero when y = 1. Integration of the second term can be done directly. This method actually eliminates singularities rather than covering them up as was done by transforming the variable of integration.

Integration Over Cycles

The third phase in the evaluation of the infinite integral in equation (B-5) is the evaluation of a series of the finite integrals

$$\int_{2N\pi/k}^{2(N+1)\pi/k} A(y) \sin ky \, dy$$

which represent integration over a cycle for sin(ky). From Figure 26 it may be seen how this cycle can be divided for integration by Simpson's rule. This procedure involves fitting a parabola to the three points in a subdivision of the cycle. These subdivisions are the areas between the solid vertical lines in Figure 26. It might be noted here that attempts to fit higher order polynomials to the curve to be integrated can lead

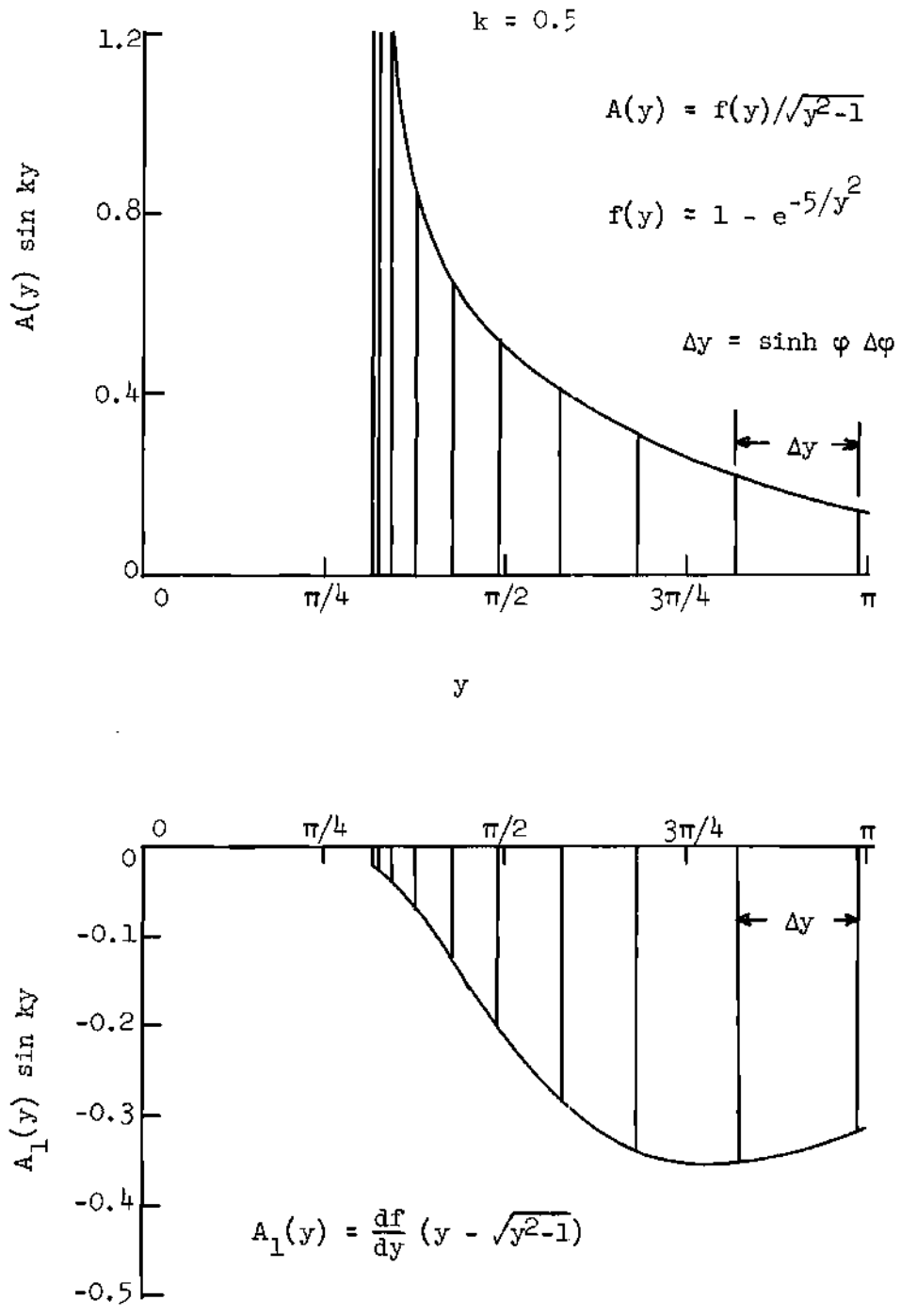

Figure 25. Initial Integration Points.

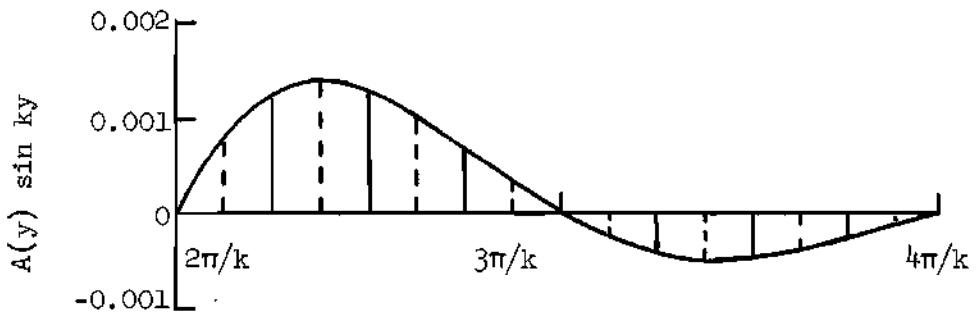

Figure 26. Single Cycle for Integration by Simpson's Rule.

to large errors in the value for the integral. These errors are due to the extreme divergence from the curve, between the points at which the polynomial is fitted, that may occur with higher order polynomials.

If a quarter cycle is split up into an even number of subdivisions, then the values for e^{-iky} can be computed at these points and stored. These values do not need to be calculated for successive cycles since

$$e^{-iky(y+2n\pi/k)} = e^{-iky} \qquad n = 1,2,3,\ldots .$$

Furthermore, the values for e^{-iky} in the other quarter cycles are obtained simply from the relation

$$e^{-ik(w+n\pi/2k)} = (-i)^n e^{-ikw} \qquad n = 1,2,3 .$$

If k is less than $\pi/2$ then the starting point for integration over quarter cycles will be $\pi/2k$, which is the start of the second quarter cycle. Integration over quarter cycles 2, 3, and 4 then will take care of the second phase of integration for equation (B-5). The third phase, which was just described, is then reached and it represents integration over several complete cycles.

If k is greater than $\pi/2$ then more than one quarter cycle is lost due to the fact that integration begins at one instead of zero. The number of quarter cycles that are lost must be known in order to figure the starting point for integration over quarter cycles (phase 2) and how many quarter cycles remain before reaching the series of complete cycles (phase 3). If L is the number of quarter cycles lost, then L can easily be computed from the requirement that

$$L\ \pi/2k > 1$$

or

$$L = \mathrm{Int}(2k/\pi) + 1$$

where Int(x) is the integer part of x. The number of quarter cycles between $L\pi/2k$ and the first complete cycle is

$$\bar{L} = 4 + \mathrm{Int}(L/4) - L\ .$$

It is important to know when the first complete cycle is reached since consistent accuracy through each phase requires closer spacing over this first broken cycle than that which is required further out in the complete cycles. This difference is evident from Figure 24a.

Asymptotic Expansion

The final phase in the integration of equation (B-5) is the evaluation of

$$\int_{2M\pi/k}^{\infty} A(y)e^{-iky}\,dy = \frac{2\pi M}{k}\int_{1}^{\infty} A(2\pi Mt/k)e^{-i2\pi Mt}\,dt$$

by asymptotic series. In general terms if (a,b) is a real interval then the asymptotic expansion of the Fourier integral

$$\int_{a}^{b} e^{ixt}\,\varphi(t)\,dt$$

is accomplished by successive integration by parts. Erdelyi (23) states the following theorem:

If $\varphi(t)$ is N times continuously differentiable for $a \le t \le b$ then

$$\int_a^b e^{ixt}\,\varphi(t)\,dt = B_N(x) - A_N(x) + O(x^{-N}) \text{ as } x \to \infty$$

where

$$A_N(x) = \sum_{n=0}^{N-1} i^{n-1}\varphi^{(n)}(a)x^{-n-1}e^{ixa}$$

and

$$B_N(x) = \sum_{n=0}^{N-1} i^{n-1}\varphi^{(n)}(b)x^{-n-1}e^{ixb}$$

and where $\varphi^{(n)}$ is the nth derivative of φ.

Thus, by asymptotic expansion,

$$\frac{2\pi M}{k}\int_1^\infty A(2\pi Mt/k)e^{-i2\pi Mt}\,dt$$

$$= \sum_{n=0}^{N-1} (-i/k)^{n+1}\,A^{(n)}(2\pi M/k) \quad . \qquad \text{(B-9)}$$

The term $B_N(x)$ in equation (B-9) will be zero in this case since the upper limit is infinity and the amplitude function and at least its first N derivatives are zero at infinity.

The integrals which were to be evaluated are given in equations (B-1) and (B-2). From equations (B-1) and (B-2) it can be seen that the amplitude function will be

$$A(y) = u(y)\,v(y)$$

where

$$u(y) = \begin{cases} f(y) - f'(y)/ik & \text{for Eqn. (B-1)} \\ f'(y) - f''(y)/ik & \text{for Eqn. (B-2)} \end{cases}$$

and

$$v(y) = \begin{cases} 1/(y^2-1)^{1/2} \\ y/(y^2-1)^{1/2} & \text{for Eqn. (B-1)} \\ y - (y^2-1)^{1/2} \\ y^2 - y(y^2-1)^{1/2} & \text{for Eqn. (B-2)} \end{cases} .$$

With this separation, equation (B-9) becomes

$$\int_{2M\pi/k}^{\infty} u(y)\, v(y) e^{-iky}\, dy$$

$$= \frac{2\pi M}{ik} \sum_{n=0}^{N-1} (-i/k)^n \sum_{m=0}^{n} \frac{n!}{m!(n-m)!} u^{(m)}(2\pi M/k) v^{(n-m)}(2\pi M/k) . \quad \text{(B-10)}$$

The purpose of the separation into functions of the decay function $u(y)$ and the functions $v(y)$ may be understood by examining equation (B-10). The functions $v(y)$ will not vary due to various choices made for the decay function. Thus, when other decay functions are considered, the higher derivatives of the amplitude function that are required for equation (B-9) can be obtained by supplying in equation (B-10) just the decay function and (N-1) of its derivatives.

The decay function chosen here was

$$f(y) = 1 - e^{-p/y^2}$$

in order to make an exact evaluation of the integrals possible. This exact method is described in Appendix D. Seven derivatives are required

for a five term asymptotic expansion due to the fact that u(y) involves a second derivative of the decay function. The coefficients for the first seven derivatives of

$$f(y) = 1 - e^{-p/y^2}$$

are given in Table B-1 where

$$f^{(n)}(y) = e^{-p/y^2} \sum_{m=1}^{n} a_m p^m / y^{2m+n} \quad .$$

Table B-1. Coefficients for the Derivatives of $f(y) = 1 - \exp(-p/y^2)$

n							
1	-2						
2	6	-4					
3	-24	36	-8				
4	120	-300	144	-16			
5	-720	2640	-2040	480	-32		
6	5040	-25200	27720	-10320	1440	-64	
7	-40320	262080	-383040	-43680	-199920	4032	-128
m=	1	2	3	4	5	6	7

The first five derivatives of each possibility for v(y) are given in Table B-2. In order to avoid round off errors for the large values of y at which the derivatives will be calculated, the numerator and

Table B-2. Derivatives for v(y).

n	$v^{(n)}(y)$
0	$(y^2-1)^{-1/2}$
1	$-y(y^2-1)^{-3/2}$
2	$(2y^2+1)(y^2-1)^{-5/2}$
3	$-3y(2y^2+3)(y^2-1)^{-7/2}$
4	$3(8y^4+24y^2+3)(y^2-1)^{-9/2}$
5	$-15y(8y^4+40y^2+15)(y^2-1)^{-11/2}$
0	$y(y^2-1)^{-1/2}$
1	$-(y^2-1)^{-3/2}$
2	$3y(y^2-1)^{-5/2}$
3	$-3(4y^2+1)(y^2-1)^{-7/2}$
4	$15y(4y^2+1)(y^2-1)^{-9/2}$
5	$-45(8y^4+12y^2+1)(y^2-1)^{-11/2}$
0	$y - (y^2-1)^{1/2}$
1	$1 - y(y^2-1)^{-1/2}$
2	$(y^2-1)^{-3/2}$
3	$-3y(y^2-1)^{-5/2}$
4	$3(4y^2+1)(y^2-1)^{-7/2}$
5	$-15y(4y^2+3)(y^2-1)^{-9/2}$

(Continued)

Table B-2. Derivatives for v(y). (Continued)

0	$y^2-y(y^2-1)^{1/2}$
1	$2y - (2y^2-1)(y^2-1)^{-1/2}$
2	$2 + y(-2y^2+3)(y^2-1)^{-3/2}$
3	$-3(y^2-1)^{-5/2}$
4	$15y(y^2-1)^{-7/2}$
5	$-15(6y^2+1)(y^2-1)^{-9/2}$

denominator of any fraction were divided through by the power of y necessary to make all of their terms of order one or less. For example,

$$-45(8y^4+12y^2+1)(y^2-1)^{-11/2} = (-45/y^7)(8+12/y^2+1/y^4)(1-1/y^2)^{-11/2} \quad .$$

The evaluations of v(y) and v'(y) for

$$v(y) = y - (y^2-1)^{1/2}$$

and the evaluations of v(y), v'(y), and v"(y) for

$$v(y) = y^2 - y(y^2-1)^{1/2}$$

were done by binomial expansion so that the terms on the order of one could be cancelled analytically. For each form for v(y), this type of cancellation eliminated the need for taking differences to get the value of v(y) and its derivatives.

APPENDIX C

EVALUATION OF INTEGRALS FOR PREVIOUSLY SHED WAKES

The effect of all of the previously shed wakes is given by equation (17) which states that

$$-i\pi[W(k,s,h) + \Delta W]$$

$$= \sum_{n=1}^{\infty} e^{ikns} \int_{-\infty}^{\infty} \left[f(nhy-ns) - \frac{1}{ik} \frac{df}{dy} \right] \cdot \frac{y\, e^{-iknhy}}{y^2 + 1}\, dy \ . \quad \text{(C-1)}$$

If there is no decay then $f(z) = 1$ and, as can be seen by equation (18), $\Delta W = 0$. Thus, with no decay,

$$-i\pi W(k,s,h) = \sum_{n=1}^{\infty} e^{+ikns} \int_{-\infty}^{\infty} \frac{y\, e^{-iknhy}}{y^2 + 1}\, dy \ . \quad \text{(C-2)}$$

By use of equation (11) in Table 103 from Bierens (24), equation (C-2) becomes

$$W(k,s,h) = \sum_{n=1}^{\infty} e^{-knh}\, e^{ikns} \ .$$

But,

$$\sum_{n=1}^{\infty} z^n = z \sum_{n=0}^{\infty} z^n = z/(1-z) \ . \qquad |z| < 1$$

Thus,

$$W(k,s,h) = 1/(e^{kh}\, e^{-iks} - 1) \ . \qquad (C\text{-}3)$$

When decay does exist, equation (C-1) will have to be evaluated using the residues of the integrand. For a contour integral around quadrants III and IV of the complex plane,

$$-\int_{-\infty}^{\infty} \frac{p(z)}{q(z)} = 2\pi i \sum_{j=1}^{k} p(z_j)/q'(z_j) \qquad (C\text{-}4)$$

where z_j is a simple pole of $q(z)$ in quadrants III and IV so that

$$q(z_j) = 0 \text{ and } q'(z_j) \neq 0 \qquad j = 1,2,\ldots,k$$

and k is the number of poles for $q(z)$.

For example, in equation (C-2),

$$p(z) = z\, e^{-iknhz}$$

and

$$q(z) = z^2 + 1 \ .$$

Thus, the two poles for $q(z)$ are

$$z = \pm i$$

and so in the lower half of the z plane one pole exists at $z = -i$. Now, equation (C-4) yields

$$-\int_{-\infty}^{\infty} \frac{ze^{-iknhz}}{z^2+1}\,dz = i\pi e^{-knh} .$$

If the decay function has no poles in the lower half of the z plane then equation (C-1) becomes

$$W + \Delta W = \sum_{n=1}^{\infty} e^{ikns}\, e^{-knh}\left[f(-ns-inh) - \frac{1}{ik}f'(-ns-inh)\right]. \qquad (C\text{-}5)$$

With

$$f(y) = 1 - e^{-p/y^2}$$

the wake effects due to decay are

$$\Delta W = -\sum_{n=1}^{\infty} e^{-knh}\, e^{ikns}\, e^{-p/(s+ih)^2 n^2}\left[1 + i\,\frac{2p}{kn^3(s+ih)^3}\right]. \qquad (C\text{-}6)$$

If the terms in the series in equation (C-6) are represented by q_n so that

$$W = -\sum_{n=1}^{\infty} q_n$$

then the ratio test shows that

$$\lim_{n\to\infty} |q_{n+1}|/|q_n| = e^{-kh} .$$

Thus the series in equation (C-6) is convergent if $kh > 0$.

Since

$$s = \mu 2\pi R'/bc'$$

$$h = \lambda 2\pi R'/bc'$$

and $2\pi R'/bc'$ will be on the order of 50 for most helicopter rotors, care must be taken to avoid round off error in equation (C-6), especially when using complex arithmetic.

Other Choices for the Decay Function

Two other decay functions were considered. The first one was

$$f(y) = 1/(1 + p^2 y^2)$$

and the second was

$$f(y) = 1/\cosh(py) \ .$$

Each of these satisfy the conditions

$$f(0) = 1$$

$$f'(0) = 0$$

$$f^{(n)}(\infty) = 0 \qquad n \geq 0 \ .$$

Only the first seven derivatives are required to be zero at infinity for the fifth order asymptotic expansion used here. Other assumptions made on the decay function in the theoretical development were that

$$f(1) \cong 1$$

and

$$f'(1) \cong 0$$

and these conditions are satisfied by putting the necessary limitations on the rate of decay, p.

If the decay function does not have a pole at z = -i, then equation (C-5) will give the portion of the wake effects that is due to the pole for the $1/(1+y^2)$ term of the integrand in equation (C-1). The effect due to the pole(s) of the decay function must be added to equation (C-5) to get the value of $W(k,s,h) + \Delta W$.

The first derivative of the decay function treated here does have second order poles. However, since

$$f'(y) = \frac{df(nhz-ns)}{d(nhz)}$$

it is easily shown by integrating by parts that equation (C-1) becomes

$$W + \Delta W = \sum_{n=1}^{\infty} \frac{e^{ikns}}{\pi\, knh} \int_{-\infty}^{\infty} \frac{f(nhz-ns)(1-z^2)e^{-iknhz}}{(z^2+1)^2}\, dz \qquad (C-7)$$

thus eliminating the second order pole of the derivative for the decay function. But this produces a second order pole at z = -i. Thus, the approach used was to treat the pole at z = -i by equation (C-5) and to treat the poles of the decay function by equation (C-7).

For the decay function given by

$$f(y) = 1/(1 + p^2y^2)$$

the first derivative is

$$f'(y) = -\,2p^2y\, f(y)/(1 + p^2y^2)\ .$$

Thus, with y = nhz-ns, the residue at z = -i is [see equation (C-5)]

$$K_1 = -\frac{1}{2} e^{-knh} \left(\frac{1}{1 + p^2 n^2 (s+ih)^2} \right) \left[1 - \frac{2p^2}{ik} \frac{n(s+ih)}{1 + p^2 n^2 (s+ih)^2} \right] .$$

The poles for a given value of n for f(nhz-ns) will be at

$$0 = 1 + p^2 n^2 (hz_o - s)^2 .$$

Thus the poles in the lower half of the complex plane are at

$$z_o = s/h - i/nph .$$

With this decay function, the integrand for equation (C-7) can be put in the form p(z)/q(z) where

$$p(z) = (1 - z^2) e^{-iknhz}$$

and

$$q(z) = [1 + p^2 n^2 (hz-s)^2](z^2 + 1)^2 .$$

Thus, the residue is

$$K_2 = \frac{(1 - z_o^2) e^{-ikns} e^{-x/p}}{(z_o^2 + 1)^2 (-2inph)}$$

where

$$z_o = s/h - i/nph .$$

Finally, putting the residue K_1 into equation (C-5) and the residue K_2 into equation (C-7) and summing over all of the wakes yields

$$W(k,s,h) + \Delta W = \sum_{n=1}^{\infty} \frac{e^{-knh}\, e^{iks}}{1 + p^2 n^2 (s+ih)^2} \left[1 - \frac{2p^2}{ik} \frac{n(s+ih)}{1+p^2 n^2 (s+ih)^2}\right]$$

$$+ \frac{e^{-k/p}}{kph^2} \sum_{n=1}^{\infty} \frac{1 - z_o^2}{n^2 (z_o^2 + 1)^2} \qquad \text{(C-8)}$$

where

$$z_o = s/h - i/nph$$

for the decay function

$$f(y) = 1/(1 + p^2 y^2) \ .$$

The evaluation of the wake weighting function is more involved for the decay function

$$f(y) = 1/\cosh(py)$$

since this function has an infinite number of poles when the imaginary part of z is negative and thus yields a double sum which must be evaluated. The first derivative for f(y) in this case is

$$f'(y) = - \sinh(py)\ f(y)/\cosh(py) \ .$$

The residue at z = -i in this case is

$$K_1 = \frac{- e^{-knh}}{2 \cosh(ns - inh)} \left[1 - \frac{1}{ik} \tanh(ns + inh)\right] .$$

The poles in the negative z plane for

$$f(nhz-ns) = 1/\cosh(nhz-ns)$$

are

$$z_m = \frac{s}{h} - i\,\frac{(2m+1)\pi}{2nph} \qquad m = 0,1,2, \ldots .$$

The residues at these poles for equation (C-7) are

$$K_m = \frac{-(1 - z_m^2)\, e^{-ikns}\, e^{-k\pi(2m+1)/2p}}{pnh\,(z_m^2 + 1)^2\, i\,(-1)^{m+1}} .$$

Finally, applying K_1 to equation (C-1) and K_m to equation (C-7) yields

$$W(k,s,h) + \Delta W = \sum_{n=1}^{\infty} \frac{e^{-knh}\, e^{ikns}}{k\cosh(ns+inh)}\,[k + i\tanh(ns+inh)]$$

$$+ \frac{2}{kph^2} \sum_{n=1}^{\infty} \frac{1}{n^2} \sum_{m=0}^{\infty} \frac{(-1)^m(1 - z_m^2)\, e^{-k\pi(2m+1)/2p}}{(1 + z_m^2)^2} \qquad \text{(C-9)}$$

where

$$z_m = \frac{s}{h} - i\,\frac{(2m+1)}{2nph} .$$

In summary then, the wake weighting function, $W(k,s,h) + \Delta W$, for a decay function of

$$f(y) = 1 - e^{-p/y^2}$$

is given by equation (C-3) for $W(k,s,h)$ and equation (C-6) for ΔW. The effect of the previously shed wakes for a decay function of

$$f(y) = 1/(1 + p^2y^2)$$

is given in equation (C-8) and the effect for

$$f(y) = 1/\cosh(py)$$

is given in equation (C-9).

Other decay functions can be treated by using equation (C-5) for the pole at $z = -i$ and adding to this the result found by evaluating equation (C-7) at the pole(s) of the decay function. Some other choices that might be considered for the decay function are given in Table C-1. These might also be linearly combined as

$$f(y) = a_1 f_1(y) + a_2 f_2(y) + \ldots + a_m f_m(y)$$

so long as

$$\sum_{n=1}^{m} a_n = 1$$

so that $f(0) = 1$. The decay rates p and r in the elementary functions listed may also be changed for superposition so that the decay function may be modified in some range of the space variable y without modifying it too much in other ranges.

Table C-1. Some Possible Decay Functions

1	$\operatorname{sech}^r(py)$	$r > 0$
2	$(1 + p^2y^2)^{-r}$	$r > 0$
3	$1 - \left[\frac{2}{\pi} \tan^{-1}(py)\right]^{2m}$	$m = 1,2,3,\ldots$

APPENDIX D

EXACT INTEGRATION

The integrals that must be evaluated were given in Appendix B as

$$\begin{Bmatrix} I_1 \\ I_2 \end{Bmatrix} = \int_1^\infty (f - f'/ik) \frac{e^{-iky}}{\sqrt{y^2 - 1}} \begin{Bmatrix} 1 \\ y \end{Bmatrix} dy \qquad \text{(D-1)}$$

and

$$\begin{Bmatrix} I_3 \\ I_4 \end{Bmatrix} = \int_1^\infty (f'-f''/ik)(y - \sqrt{y^2-1})e^{-iky} \begin{Bmatrix} 1 \\ y \end{Bmatrix} dy \quad . \qquad \text{(D-2)}$$

These integrals can be evaluated exactly if their integrands, excluding the factor e^{-iky}, can be expanded as a power series in y. The values for I_1 through I_4 are then obtained through term by term integration of the series. For reasons of convergence, which will be clarified later, it is convenient to split up the infinite integrals into a segment going from 1 to β and a segment from β to infinity. The value taken for β is arbitrary, but it should be near 2 in order to get acceptable convergence for both the upper and lower segments.

Integration from β to Infinity

In order to illustrate the method used in evaluating the infinite integrals exactly, the integrals

$$I_7 = \int_\beta^\infty f(y)(y^2-1)^{-1/2} e^{-iky} dy \qquad \text{(D-3)}$$

and $\beta > 1$

$$I_8 = \int_{\beta}^{\infty} f'(y)(y - \sqrt{y^2-1})e^{-iky}\, dy \tag{D-4}$$

will be treated in detail.

By the binomial theorem,

$$(y^2-1)^{-1/2} = \frac{1}{y} \sum_{m=0}^{\infty} a_m/y^{2m} \tag{D-5}$$

where the coefficients a_m are given by

$$a_m = \frac{(2m)!}{(2^m\, m!)^2} \tag{D-6}$$

or

$$a_m = a_{m-1}\,(1 - 1/2m)\ ;\ a_0 = 1\ .$$

If the decay function can be expressed as

$$f(y) = \sum_{n=0}^{\infty} b_n/y^{2n} \tag{D-7}$$

then, multiplying equation (D-5) by equation (D-7) makes equation (D-3) become

$$I_7 = \sum_{m=0}^{\infty} c_m \int_{\beta}^{\infty} \frac{e^{-iky}}{y^{2m+1}}\, dy \tag{D-8}$$

where

$$c_m = \sum_{n=0}^{m} b_{m-n}\, a_m = \sum_{n=0}^{m} b_n\, a_{m-n} \quad . \tag{D-9}$$

For a given value of m in equation (D-8), integration by parts yields

$$\int_{\beta}^{\infty} \frac{e^{-iky}}{y^{m+1}}\, dy = \frac{e^{-ikb}}{m\beta^m} - \frac{ik}{m} \int_{\beta}^{\infty} \frac{e^{-iky}}{y^m}\, dy$$

or

$$\hat{E}_{m+1} = \frac{e^{-ikb}}{m\beta^m} - \frac{ik}{m}\, \hat{E}_m \tag{D-10}$$

where $\hat{E}_m$ is defined to be

$$\hat{E}_m = \int_{\beta}^{\infty} \frac{e^{-iky}}{y^m}\, dy \quad .$$

With this definition, equation (D-8) becomes

$$I_7 = \sum_{m=0}^{\infty} c_m\, \hat{E}_{2m+1} \quad . \tag{D-11}$$

Since the coefficients c_m in Equation (D-11) remain on the order of 1 for all m, the rate of convergence of the series will depend upon $\hat{E}_m$. From Equation (D-10) it is apparent that $\hat{E}_m$ will be of the order β^{-m}/m. Thus, β should be greater than one in order to gain acceptable convergence from Equation (D-11).

Once the value for $\hat{E}_1$ is known, the values of $\hat{E}_m$ can be found

from the recurrence relation given in equation (D-10). These are the values that will be put into equation (D-11) in order to evaluate I_7 and similar integrals.

The integral $\hat{E}_1$ is obtained from the exponential integral

$$E_1(z) = \int_z^\infty \frac{e^{-t}}{t}\, dt \qquad |\arg z| < \pi$$

as given by Equation 5.1.1 of Abramowitz and Stegun (25). By making $t = iky$, it is apparent that

$$E_1(i\beta k) = \hat{E}_1 \quad .$$

Sine and Cosine Integrals

This section covers the steps required in the calculation of $\hat{E}_1$. Separating $\hat{E}_1$ into its real and imaginary parts gives

$$\hat{E}_1 = \int_\beta^\infty \frac{\cos ky}{y}\, dy - i \int_\beta^\infty \frac{\sin ky}{y}\, dy$$

$$= -Ci(\beta k) + i[Si(\beta k) - \pi/2] \quad . \qquad \text{(D-12)}$$

The series expansions for $Si(z)$ and $Ci(z)$ are given by

$$Si(z) = \sum_{n=0}^{\infty} \frac{(-1)^n z^{2n+1}}{(2n+1)(2n+1)!}$$

and

$$Ci(z) = \sum_{n=1}^{\infty} \frac{(-1)^n z^{2n}}{2n\,(2n)!} + \gamma + \ln z$$

where $\gamma = 0.57721$ is Euler's constant.

Solution for I_1 and I_2

From equation (D-7)

$$f'(y) = -2 \sum_{n=0}^{\infty} n\, b_n / y^{2n+1} \quad . \tag{D-13}$$

Following the same procedure as that used in obtaining the integral I_7 as given by equation (D-11) yields

$$I_1 = \sum_{m=0}^{\infty} \left(C_m \hat{E}_{2m+1} + \frac{1}{ik} d_m \hat{E}_{2m+2} \right) \tag{D-14}$$

where

$$d_m = \sum_{n=0}^{m} n\, b_n\, a_{m-n} \tag{D-15}$$

and where c_m is given by equation (D-9) and the binomial coefficients a_m are given by equation (D-6).

The integrand for I_2 is simply y times the integrand for I_1 and so

$$I_2 = \sum_{m=0}^{\infty} \left(c_m \hat{E}_{2m} + \frac{1}{ik} d_m \hat{E}_{2m+1} \right) \tag{D-16}$$

where $\hat{E}_1$ is given by equation (D-12), $\hat{E}_m$ for $m = 2,3,4,\ldots$ are found from the recurrence relation in equation (D-10), c_m is found from equation (D-9), d_m is given by equation (D-15), and a_m is given by equation (D-6). The coefficients b_n for the decay function are found from the series

expansion of the decay function. With

$$f(y) = 1 - e^{-p/y^2}$$

these coefficients are

$$b_0 = 0 \; ; \quad b_n = (-1)^{n+1} \, p^n/n! \quad n = 1,2,3, \ldots .$$

Solution for I_3 and I_4

The series for the first derivative of the decay function is given by equation (D-13). The second derivative will be

$$f''(y) = 2 \sum_{n=0}^{\infty} (2n+1)n \, b_n/y^{2n+2} . \qquad \text{(D-17)}$$

The other portion of the integrand in equation (D-2) is given by the binomial theorem as

$$y[1 - (1 - 1/y^2)^{1/2}] = \frac{1}{2y} \sum_{m=0}^{\infty} g_m/y^{2m} \qquad \text{(D-18)}$$

where

$$g_m = \frac{(2m)!}{2^{2m} \, m! \, (m+1)!} \qquad \text{(D-19)}$$

or

$$g_m = g_{m-1} \, (2m-1)/(2m+2) \; ; \quad g_0 = 1 .$$

Multiplying equation (D-18) by equation (D-13) for f'(y) and equation (D-17) for f''(y) and substituting the result into equation (D-2)

yields

$$I_3 = - \sum_{m=0}^{\infty} \left(h_m \hat{E}_{2m+2} + \frac{r_m}{ik} \hat{E}_{2m+3} \right) \qquad \text{(D-20)}$$

where

$$h_m = \sum_{n=0}^{m} n\, b_n\, g_{m-n}$$

and

$$r_m = \sum_{n=0}^{m} n\,(2n+1) b_n\, g_{m-n} \,.$$

Since the integrand for I_4 is y times the integrand for I_3, equation (D-20) immediately yields

$$I_4 = - \sum_{m=0}^{\infty} \left(h_m \hat{E}_{2m+1} + \frac{1}{ik} r_m \hat{E}_{2m+2} \right) \qquad \text{(D-21)}$$

as the upper portion for the integral for I_4.

Integration of Lower Segment

Integrals I_1 and I_2

With a decay function

$$f(y) = 1 - e^{-p/y^2}$$

the lower segment of the integral in Equation (D-1) can be transformed to

$$\int_1^\beta \frac{f-f'/ik}{\sqrt{y^2-1}}\, e^{-iky} dy = \int_1^\beta \frac{e^{-iky}}{\sqrt{y^2-1}}\, dy - \int_0^{\sec^{-1}\beta} e^{-p\cos^2\varphi}\, e^{-ik\sec\varphi}\, \sec\varphi\, d\varphi$$

$$+ \frac{2g}{ik} \int_0^{\sec^{-1}\beta} e^{-p\cos^2\varphi}\, e^{-ik\sec\varphi}\, \cos^2\varphi d\varphi \qquad \text{(D-22)}$$

where $y = \sec\varphi$ has been substituted for the second and third integrals. Similarly, the initial integral for I_2 becomes

$$\int_1^\beta (f - f'/ik) \frac{y}{\sqrt{y^2-1}}\, e^{-iky}\, dy = \int_1^\beta \frac{ye^{-iky}}{\sqrt{y^2-1}}\, dy$$

$$- \int_0^{\sec^{-1}\beta} e^{-p\cos^2\varphi}\, e^{-ik\sec\varphi}\, \sec^2\varphi\, d\varphi$$

$$+ \frac{2g}{ik} \int_0^{\sec^{-1}\beta} e^{-p\cos^2\varphi}\, e^{-ik\sec\varphi}\, \cos\varphi\, d\varphi\,. \qquad \text{(D-23)}$$

The Cauchy product for infinite series yields

$$e^{-p\cos^2\varphi} \cos(k\sec\varphi) = \sum_{n=0}^{\infty} c_n \cos^{2n}\varphi + \sum_{n=1}^{\infty} d_n \sec^{2n}\varphi \qquad \text{(D-24)}$$

where

$$c_n = \frac{(-1)^n p^n}{n!} \sum_{m=0}^{\infty} \frac{n!}{(n+m)!} \frac{p^m k^{2m}}{(2m)!}$$

and

$$d_n = \frac{(-1)^n k^{2n}}{(2n)!} \sum_{m=0}^{\infty} \frac{p^m}{m!} \frac{k^{2m}(2n)!}{[2(n+m)]!}\,.$$

Similarly, it can be shown that

$$e^{-p\cos^2\varphi}\sin(k\sec\varphi) = \sum_{n=1}^{\infty} f_n \cos^{2n-1}\varphi + \sum_{n=0}^{\infty} h_n \sec^{2n+1}\varphi \qquad \text{(D-25)}$$

where

$$f_n = \frac{(-p)^n}{n!} \sum_{m=0}^{\infty} \frac{p^m\, n!}{(n+m)!} \frac{k^{2m+1}}{(2m+1)!}$$

and

$$h_n = \frac{(-1)^n k^{2n+1}}{(2n+1)!} \sum_{m=0}^{\infty} \frac{p^m}{m!} \frac{k^{2m}\,(2m+1)!}{(2n+2m+1)!} .$$

Combining equations (D-24) and (D-25) immediately yields

$$\int_0^{\sec^{-1}\beta} e^{-p\cos^2\varphi}\, e^{-ik\sec\varphi}\, d\varphi = c_0 C_0 + \sum_{n=1}^{\infty} (c_n C_{2n} + d_n S_{2n}) - ik\, h_0 S_1 - i \sum_{n=1}^{\infty} (f_n C_{2n-1} + h_n S_{2n+1}) \qquad \text{(D-26)}$$

with the definitions

$$C_n \triangleq \int_0^{\sec^{-1}\beta} \cos^n\varphi d\varphi = \frac{(\beta^2-1)^{1/2}}{n\,\beta^n} + \frac{n-1}{n} C_{n-2} \qquad \text{(D-27)}$$

and

$$S_n \triangleq \int_0^{\sec^{-1}\beta} \sec^n\varphi d\varphi = \frac{\beta^{n-2}(\beta^2-1)^{1/2}}{n-1} + \frac{n-2}{n-1} S_{n-2} \quad . \tag{D-28}$$

The initial integrals are

$$C_0 = S_0 = \tan^{-1} (\beta^2-1)^{1/2}$$

$$C_1 = (\beta-1)^{1/2}/\beta$$

and

$$S_1 = \ln (\beta + \sqrt{\beta^2-1}) \quad .$$

Higher order integrals are obtained from the recurrence relations shown in equations (D-27) and (D-28).

The integrals needed for equations (D-22) and (D-23) are obtained by simply shifting the subscripts for C_n and S_n in equation (D-26) by an appropriate amount. For example,

$$\int_0^{\sec^{-1}\beta} e^{-p \cos^2\varphi} e^{-ik \sec\varphi} \sec\varphi d\varphi = c_0 S_1$$

$$+ \sum_{n=1}^{\infty} (c_n C_{2n-1} + d_n S_{2n+1}) - i h_o S_2$$

$$- i \sum_{n=1}^{\infty} (f_n C_{2n-2} + h_n S_{2n}) \tag{D-29}$$

and

$$\int_0^{\sec^{-1}\beta} e^{-p\cos^2\varphi}\, e^{-ik\sec\varphi}\cos^2\varphi\, d\varphi$$

$$= c_o C_2 + \sum_{n=1}^{\infty} (c_n C_{2n+2} + d_n S_{2n-2}) - i\, h_o C_1$$

$$- i \sum_{n=1}^{\infty} (f_n C_{2n+1} + h_n S_{2n-1}) \qquad \text{(D-30)}$$

are the relations needed for equation (D-22). The relations needed for equation (D-23) are very similar.

By making the transformation $y = w+1$ the last two integrals involved in equations (D-22) and (D-23) become

$$\int_1^{\beta} \frac{e^{-iky}}{\sqrt{y^2-1}}\, dy = \frac{e^{-ik}}{\sqrt{2}} \int_0^{\beta-1} e^{-ikw}\, w^{-1/2}(1+w/2)^{-1/2} dw \qquad \text{(D-31)}$$

and

$$\int_1^{\beta} \frac{y\, e^{-iky}}{\sqrt{y^2-1}}\, dy = \frac{e^{-ik}}{\sqrt{2}} \int_0^{\beta-1} e^{-ikw}(w^{-\frac{1}{2}} + w^{\frac{1}{2}})(1+w/2)^{-\frac{1}{2}}\, dw\ . \qquad \text{(D-32)}$$

But

$$e^{-ikw}(1+w/2)^{-1/2} = \sum_{n=0}^{\infty} (-1)^n D_n w^n$$

where

$$D_n = \sum_{m=0}^{n} \frac{(ik)}{(n-m)!} \frac{(2m)!}{8^m\, (m!)^2} \qquad \text{(D-33)}$$

and so

$$\int_0^{\beta-1} w^{-\frac{1}{2}} e^{-ikw} (1+w/2)^{-\frac{1}{2}} dw = (\beta-1)^{\frac{1}{2}} \sum_{n=0}^{\infty} \frac{(-1)^n D_n (\beta-1)^n}{n + 1/2} \qquad (D-34)$$

and

$$\int_0^{\beta-1} w^{\frac{1}{2}} e^{-ikw} (1+w/2)^{-\frac{1}{2}} dw = (\beta-1)^{3/2} \sum_{n=0}^{\infty} \frac{(-1)^n D_n (\beta-1)^n}{n + 3/2} . \qquad (D-35)$$

Finally, the first part of the initial integral for I_1 is evaluated by using the series in equation (D-34) for the evaluation of the integral in equation (D-31), where the coefficients D_n are given by equation (D-33). This integral in equation (D-31) is the first integral shown in equation (D-22) for I_1. The second integral in equation (D-22) is given by equation (D-29) and the third integral is given by equation (D-30).

The first part of the integral I_2, as given by equation (D-23) is shown in equation (D-32). Equation (D-32) is evaluated through application of equations (D-34) and (D-35). The last two integrals in equation (D-23) are found by use of equation (D-26) with the proper subscript changes for the integrals C_n and S_n.

Integrals I_3 and I_4.

The initial portions of I_3 and I_4 are

$$\int_1^{\beta} (f' - f''/ik) (y - \sqrt{y^2-1}) e^{-iky} dy$$

and

$$\int_1^\beta (f' - f''/ik)\,(y^2 - y\sqrt{y^2-1})\epsilon^{-iky}\,dy\ .$$

Integration by parts gives

$$-ik\int_1^\beta (f' - f''/ik)\,v(y)e^{-iky}\,dy$$

$$= f'(\beta)v(\beta)e^{-ik\beta} - f'(1)\,v(1)\,e^{-ik} - \int_1^\beta f'(y)\,v(y)\,e^{-iky}\,dy.$$

Since $f'(y) = -\frac{2p}{y^3}\,e^{-p/y^2}$, the substitution $y = \sec\varphi$ yields

$$\frac{ik}{2p}\int_1^\beta (f'-f''/ik)(y - \sqrt{y^2-1})e^{-iky}\,dy$$

$$= e^{-ik\beta}\,e^{-p/\beta^2}\,(\beta-\sqrt{\beta^2-1})/\beta^3 - e^{-ik}\,e^{-p} - \int_1^\beta \frac{e^{-p/y^2}}{y^3}\,e^{-iky}\,dy$$

$$+ \int_0^{\sec^{-1}\beta} e^{-p\cos^2\varphi}\,e^{-ik\sec\varphi}\cos\varphi\,d\varphi \qquad \text{(D-36)}$$

and

$$\frac{ik}{2p}\int_1^\beta (f'-f''/ik)(y^2-y\sqrt{y^2-1})e^{-iky}\,dy$$

$$= e^{-ik\beta}\,e^{-p/\beta^2}\,(\beta-\sqrt{\beta^2-1})/\beta^2 - e^{-ik}e^{-p}$$

$$- 2\int_1^\beta \frac{e^{-p/y^2}}{y^3}\,e^{-iky}\,dy$$

$$+ \int_1^{\sec^{-1}\beta} e^{-p\cos^2\varphi}\,e^{-ik\sec\varphi}\,(2 - \cos^2\varphi)\,d\varphi\ . \qquad \text{(D-37)}$$

The last integral in equations (D-36) and (D-37) are found from equation (D-26) with proper subscript changes.

The other integral is computed from the series

$$\int_1^\beta \frac{e^{-p/y^2}}{y^m} e^{-iky}\, dy = \sum_{n=0}^{\infty} \frac{(-p)^n}{n!} H_{m+2n} \qquad \text{(D-38)}$$

with the definition

$$H_n = \int_1^\beta e^{-iky}\, y^{-n}\, dy \ .$$

Integration by parts yields the recurrence relation

$$H_{n+1} = (e^{-ik} - e^{-ik\beta}/\beta^n - ik\, H_n)/n \qquad \text{(D-39)}$$

where

$$H_1 = \ln \beta + \sum_{n=1}^{\infty} \frac{(-ik)^n}{n(n!)} (\beta^n - 1) \ . \qquad \text{(D-40)}$$

Calculation of the first finite exponential integral by equation (D-40) makes possible the evaluation of each term in equation (D-38) through the recurrence relation given in equation (D-39).

Finally, applying equation (D-38) and (D-26) to equations (D-36) and (D-37) yields the lower portions of I_3 and I_4 respectively.

LITERATURE CITED

1. Loewy, R. G., "A Two Dimensional Approach to the Unsteady Aerodynamics of Rotary Wings," Journal of the Aerospace Sciences, Vol. 24, 1957, pp. 82-98.

2. Jones, J. P., "Influence of the Wake on the Flutter and Vibration of Rotor Blades," Oscillation Sub-Committee Aeronautical Research Council Report #18, Jan. 1956.

3. Hammond, C. E., "A Parametric Study of Helicopter Rotor Blade Flutter Under Low Inflow Conditions, Using Incompressible Aerodynamics," Georgia Institute of Technology, School of Aerospace Engineering, Student Special Problem, June 1968.

4. Theodorsen, T., "General Theory of Aerodynamic Instability and the Mechanism of Flutter," NACA Report 496, 1935.

5. Miller, R. H., "Rotor Blade Harmonic Air Loading," American Institute of Aeronautics and Astronautics Journal, Vol. 2, No. 7, July 1964, pp. 1254-1269.

6. Ichakawa, Teruo, "Linear Aerodynamic Theory of Rotor Blades," J. of Aircraft, Vol. 4, No. 3, May-June 1967, pp. 210-218.

7. Drees, Jan M., "Aeroelastic Rotor Phenomena and Nonsteady Rotor Aerodynamics," New York Academy of Sciences, Annals, Vol. 154, Nov. 22, 1968, pp. 481-505.

8. Brooks, George W. and Sylvester, Maurice A., "The Effect of Control Stiffness and Forward Speed on the Flutter of a 1/10 Scale Dynamic Model of a Two-Blade Jet-Driven Helicopter Rotor," NACA TN 3376, April 1955.

9. Gates, C. A., Piziali, R. A., and DuWaldt, F. A., "Comparison of Theoretical and Experimental Flutter Characteristics for a Model Rotor in Translational Flight," Institute of Aeronautical Sciences Annual Meeting, New York, New York, Jan. 21-23, 1963, Paper 63-91.

10. Leone, P. F., "Theoretical and Experimental Study of the Coupled Flap Bending and Torsion Aero-Elastic Vibrations of a Helicopter Rotor Blade," American Helicopter Society 13th Annual Forum, Washington, D.C., May 8-11, 1957.

11. Daughaday, H., DuWaldt, F. and Gates, C., "Investigation of Helicopter Blade Flutter and Load Amplification Problems," Journal of American Helicopter Society, July 1957, p. 27.

12. Stammers, C. W., "The Flapping Torsion Flutter of a Helicopter Blade in Forward Flight," Institute of Sound and Vibration Research Technical Report 3, Feb. 1968.

13. Stammers, C. W., "The Bending Torsion Flutter of a Hingeless Rotor Blade," ISVR-TR-9, October 1968.

14. Niebanck, C. F., "A Comparison of Dynamically Scaled Model Rotor Test Data with Discrete Azimuth Aeroelastic Stability Theory," presented at the American Helicopter Society 25th National Forum, May 1969.

15. Garrick, I.E., "Bending-Torsion Flutter Calculations Modified by Subsonic Compressibility Corrections," NACA TN 1034, 1946.

16. Schwarz, L., "Berechnung der Druckverteilung einer harmonisch sich Verformenden Tragflache in ebener Strömung," Luftfahrtforschung, Band 17, Nr. 11 and 12, 1940.

17. Söhngen, H., "Die Lösungen der Integralgleichung und deren Anwendung in der Tragflugeltheorie," Mathimatische Zeitschrift, Band 45, 1939, pp. 245-264.

18. Jones, W. P., "Aerodynamic Forces on Wings in Non-Uniform Motion," British Aeronautical Research Council, Reports and Memoranda No. 2117, 1945.

19. Carleman, Torsten, "Sur la résolution de certaines équations intégrales," Arkiv För Matematik, Astronomi och Fysik, Band 16, No. 26, 1922.

20. Wheatley, John B., "An Aerodynamic Analysis of the Autogyro Rotor with a Comparison between Calculated and Experimental Results," NACA Report 487, 1934.

21. Hammond, C. E., "Compressibility Effects in Helicopter Rotor Blade Flutter," Ph.D. Thesis, Georgia Institute of Technology, Dec. 1969.

22. Jones, W. P. and Rao, B. M., "Compressibility Effects on Oscillating Rotor Blades in Hovering Flight," Volume of Technical Papers on Structural Dynamics and Aeroelasticity Specialist Conference, New Orleans, La., April 16-17, 1969.

23. Erdelyi, A., Asymptotic Expansions, Dover, 1956.

24. Bierens De Haan, Nouvelles Tables d'integrals defienies, Stechart and Co., 1939.

25. Abramowitz, Milton and Stegun, Irene A. (eds.) Handbook of Mathematical Functions, National Bureau of Standards, U.S. Gov. Printing Office, 1964.

OTHER REFERENCES USED

1. Bisplinghoff, R. L., Ashley, H. and Halfman, R. L., Aeroelasticity, Addison Wesley, Reading, Mass., 1955.

2. Churchill, Ruel V., Complex Variables and Applications, McGraw-Hill Inc., 1960.

3. Fung, Y. C., The Theory of Aeroelasticity, John Wiley and Sons, New York, 1955.

4. Loewy, R. G., "A Two Dimensional Approximation to the Unsteady Aerodynamics of Rotary Wings," Cornell Aeronautical Laboratory Report No. 75, October 1955.

5. Scanlan, R. H. and Rosenbaum, R., Introduction to the Study of Aircraft Vibration and Flutter, The MacMillan Co., New York, 1951.

VITA

Keith Waldo Shipman was born on April 5, 1943 in Fresno, California as the son of Mark K. and Elaine A. Shipman. He graduated from Grand Junction High School in Grand Junction, Colorado in June, 1961. After completing basic engineering courses at the Colorado School of Mines he transferred to the Georgia Institute of Technology in September, 1963 where he received the degree of Bachelor of Aerospace Engineering in June, 1965.

Beginning graduate studies in September, 1965 he was awarded the degree Master of Science in Aerospace Engineering in June, 1967 and continued to study for the doctoral degree.

During the summer of 1969 he worked on V/STOL dynamics problems for the Boeing-Vertol Co. in Ridley Park, Pennsylvania.

He is married to the former Rogene Bertrand of Grand Junction, Colorado and they have two daughters, Rebecca Anne and Barbara Lynn.